

OPTIMAL SPACE-TIME TRANSMIT SIGNAL DESIGN

FOR MULTI-STATIC RADAR

by

ATULYA TEJA DEEKONDA

B.E., Electronics and Communications Engineering

Chaitanya Bharathi Institute of Technology, Osmania University

Hyderabad, India – 2002

Submitted to the Department of Electrical Engineering and Computer Science and the Faculty of the Graduate School of the University of Kansas in partial fulfillment of the requirements for the degree of Master of Science.

Thesis Committee:

Prof. James Stiles: Chairperson

Prof. Glenn Prescott

Prof. Muhammed Dawood

Date of Defense January 31, 2005

*To my grandfather,
who taught us that hard work
inspires and leads to success.*

Acknowledgements

I would like to thank my advisor Prof. James Stiles for giving me an opportunity to work under him and for helping and encouraging me all through out my studies at The University of Kansas. I also would like to thank Prof. Glenn Prescott and Prof. Muhammad Dawood for accepting to be on my committee.

I thank my parents D.E. Ramchander and D.Anuradha, my brother D. Aditya for encouraging me and supporting me at every step of my studies and with whose help I could reach to this stage. I thank my grandparents D. Pentaiah and D. Anasuya for their love and support.

I thank my friend Vishal Sinha for helping me with my research and I would like to thank all my friends and well wishers without whose support, this work would not have been possible.

In the end I thank GOD ALMIGHTY for making his presence felt in my ups and downs.

Table of Contents

Abstract.....	xi
1. Introduction.....	1
1.1 Synthetic Aperture Radar	1
1.2 Multi Element Synthetic Aperture Radar	2
1.3. Motivation:.....	4
1.4 Outline of the Thesis.....	5
2. Processing and Analysis of Multi-static Radar System.	8
2.1 Description and Analysis	8
2.2 Estimators:.....	11
2.2.1 Matched filter.....	12
2.2.2 Maximum Likelihood Estimator:	13
2.2.3 Minimum Mean Square Error Estimator	14
3. The Optimization Criterion	16
3.1 Analysis of the optimization criteria χ	16
3.3 Relation between the correlation coefficient ξ and χ	22
3.3 Inverse of the B matrix	23
4. Description and Evaluation of Algorithm-1 and Algorithm-2 ..	25
4.1 Algorithm 1(Collective Projection Algorithm)	25
4.2 Performance of Algorithm-1	29
4.3 Algorithm-2(Individual Projection Algorithm).....	32
4.4 Performance of Algorithm-2	35
4.5 Analysis of the optimization criterion χ using numerically generated input values.	40

4.6 Comparison of Algorithm-1 to Algorithm-2.....	41
4.7 H matrices generated from Gaussian distributions with different Means and different Standard Deviations	49
4.7.1 Case – 1: ($M=3000$; $N=4$; $T=10$).....	51
4.6.2 Case – 2: ($M=1000$; $N=8$; $T=10$).....	52
4.6.3 Case – 12: ($M=100$; $N=40$; $T=10$).....	53
4.8 Comparison of Algorithm-2 solution with Genetic Algorithm Solution and Randomly Generated Solutions	57
4.8.1 Genetic Algorithm:.....	57
4.8.3 Randomly Generated Codes	59
4.8.3 Algorithm -2:	60
4.8.3 Comparison with Random Codes:	61
5. Simulation of a Radar Model	67
5.1 Transmit Signal Model	67
5.2 Target Model.....	77
5.3 Receiver Measurements	77
5.4 Model Equations.....	80
5.5 Default values used in the Radar Model.....	83
5.6 Numerical Values for the Model	89
6. Analysis of Algorithm-2 using the Radar Model.....	92
6.1 Performance Analysis of Algorithm-2 with the Radar Model.....	92
6.1.1 Case-1($P=1$; $Q=1$; $J=1$):	94
6.1.2 Case 2 ($P=3$; $Q=3$; $J=1$):	96
6.1.3 Case 3 ($P=5$; $Q=5$; $J=1$):	97
6.1.4 Case 4 ($P=7$; $Q=7$; $J=1$):	99
6.1.5 Case 5 ($P=9$; $Q=9$; $J=1$):	101
6.1.6 Case 6 ($P=11$; $Q=11$; $J=1$):	102
6.2 Analysis of the Algorithm with 2 Transmit Elements ($J = 2$).....	105
6.2.1 Case 1 ($P=1$; $Q=1$; $J=2$):	106
6.2.2 Case 2 ($P=3$; $Q=3$; $J=2$):	107
6.2.3 Case 3 ($P=5$; $Q=5$; $J=2$):	109
6.2.4 Case 4 ($P=7$; $Q=7$; $J=2$):	110
6.2.5 Case 5 ($P=9$; $Q=9$; $J=2$):	112
6.2.6 Case 6 ($P=11$; $Q=11$; $J=2$):	113

6.3 Comparison of P=11; Q=11 and J=2 case with Standard Code (P=1; Q=1) and Three random codes.	116
6.3.1 Standard Code (P=1; Q=1)	116
6.3.2 Random Code-1	117
6.3.3 Random Code-2	117
6.3.4 Random Code - 3	118
6.3.5 Transmit Code given by the Algorithm	118
6.4 Analysis of the Optimization Criterion χ with inputs from the Radar model.	119
6.5 Energy in the Response vector for J=2; P=11; Q=11 case	120
6.6 Comparison of Convergence of χ bound for J=1; J=2 and different values of P and Q.....	121
6.7 Comparison of Maximum Correlation Coefficient values for J=1; J=2 with respect to total Iteration Number.....	123
6.8 Relation between Rank of C matrix (R_c) and the number of Transmit Elements (J).....	124
7.1 Conclusions.....	126
7.2 Suggested Future Work.....	128
References.....	130

Table of Figures

Fig 2.1: A multi-static radar system with ‘ t ’ number of targets and their reflections... 9	9
Fig 4.1: Flow Chart of Algorithm-1	28
Fig 4.2: Eigen spectrum before orthogonal projection.....	29
Fig 4.3: Eigen spectrum after the orthogonal projection.....	30
Fig 4.4: χ - value spectrum obtained using the transmit code given by Algorithm-1.	31
Fig 4.5: Flow chart of Algorithm-2.....	34
Fig 4.6: Eigen spectrum before the start of iterations.	35
Fig 4.7: Eigen Spectrum after the first iteration.....	36
Fig 4.8: Eigen spectrum after Iteration=27.....	37
Fig 4.9: Eigen spectrum after Iteration=40.....	37
Fig 4.10: Plot showing convergence of the χ bound with respect to iteration number.	38
Fig 4.11: Plot showing the correlation coefficient curve and $ 1 - \chi $ curve.....	40
Fig 4.12: Different cases that Algorithm-1 and Algorithm -2 have been compared in.	42
Fig 4.13: Comparison of Histograms of χ and maximum Correlation coefficient values, for Alg-1 and Alg-2 for case1.....	43
Fig 4.14: Comparison of Histograms of χ and Correlation for Alg-1 and Alg-2 for case-6	45
Fig 4.15: Comparison of Histograms of χ and Correlation for Alg-1 and Alg-2 for.	46
Fig 4.16: Plots of standard deviation of χ with respect to the transmit signal dimension for Alg-1 and Alg-2.	47
Fig 4.17: Plot showing the mean of max correlation with respect to the transmit signal dimension for Alg-1 and Alg-2.	48
Fig 4.18: Four blocks of the “Varying H-matrices” with different mean and different standard deviations.	49

Fig 4.19: Comparison of Histograms of χ and Correlation for Alg-1 and Alg-2 for case-1	51
Fig 4.20: Comparison of Histograms of χ and Correlation for Alg-1 and Alg-2 for case-6	52
Fig 4.21: Comparison of Histograms of χ and Correlation for Alg-1 and Alg-2 for case-12	53
Fig 4:22: Plots of standard deviation of χ with respect to the transmit signal dimension for Alg-1 and Alg-2.	54
Fig 4:23: Plot showing the mean of max correlation with respect to the transmit signal dimension for Alg-1 and Alg-2.	55
Fig 4.24: Comparison of Histograms of χ and Correlation for Alg-1 and Alg-2 for case1.....	63
Fig 4.25: Comparison of Histograms of χ and Correlation for Alg-1 and Alg-2 for case 6.....	64
Fig 4.26: Comparison of Histograms of χ and Correlation for Random Code and Alg-2 for case1	65
Fig 5.1: Multistatic Synthetic Aperture Radar System.....	83
Fig 6.1: Spatial, Total and Temporal Ambiguity plot along the Cross Track axis for $P=1; Q=1$	94
Fig 6.2: A 2-D plot of the correlation of the target of interest and all the targets in the grid (2-D ambiguity plot) for $P=1; Q=1$	95
Fig 6.4: A 2-D plot of the correlation of the target of interest and all the targets in the grid (2-D ambiguity plot) for $P=3; Q=3$	97
Fig 6.5: Spatial, Total and Temporal Ambiguity plot along the Cross Track axis for $P=5; Q=5$	98
Fig 6.6: A 2-D plot of the correlation of the target of interest and all the targets in the grid (2-D ambiguity plot) for $P=5; Q=5$	98
Fig 6.7: Spatial, Total and Temporal Ambiguity plot along the Cross Track axis for $P=7; Q=7$	99

Fig 6.8: A 2-D plot of the correlation of the target of interest and all the targets in the grid (2-D ambiguity plot) for $P=7; Q=7$	100
Fig 6.9: Spatial, Total and Temporal Ambiguity plot along the Cross Track axis for $P=9; Q=9$	101
Fig 6.10: A 2-D plot of the correlation of the target of interest and all the targets in the grid (2-D ambiguity plot) for $P=9; Q=9$	102
Fig 6.11: Spatial, Total and Temporal Ambiguity plot along the Cross Track axis for $P=11; Q=11$	103
Fig 6.12: A 2-D plot of the correlation of the target of interest and all the targets in the grid (2-D ambiguity plot) for $P=11; Q=11$	103
Fig 6.13: Total Ambiguity plot along the Cross Track axis for $P=1; Q=1$	106
Fig 6.14: A 2-D plot of the correlation of the target of interest and all the targets in the grid (2-D ambiguity plot) for $P=1; Q=1$	107
Fig 6.15: Total Ambiguity plot along the Cross Track axis for $P=3; Q=3$	108
Fig 6.16: A 2-D plot of the correlation of the target of interest and all the targets in the grid (2-D ambiguity plot) for $P=3; Q=3$	108
Fig 6.17: Total Ambiguity plot along the Cross Track axis for $P=5; Q=5$	109
Fig 6.18: A 2-D plot of the correlation of the target of interest and all the targets in the grid (2-D ambiguity plot) for $P=5; Q=5$	110
Fig 6.19: Total Ambiguity plot along the Cross Track axis for $P=7; Q=7$	111
Fig 6.20: A 2-D plot of the correlation of the target of interest and all the targets in the grid (2-D ambiguity plot) for $P=7; Q=7$	111
Fig 6.21: Total Ambiguity plot along the Cross Track axis for $P=9; Q=9$	112
Fig 6.22: A 2-D plot of the correlation of the target of interest and all the targets in the grid (2-D ambiguity plot) for $P=9; Q=9$	113
Fig 6.23: Total Ambiguity plot along the Cross Track axis for $P=11; Q=11$	114
Fig 6.24: A 2-D plot of the correlation of the target of interest and all the targets in the grid (2-D ambiguity plot) for $P=11; Q=11$	115
Fig 6.25: Total Ambiguity plot along the Cross Track axis for $P=1; Q=1$	116

Fig 6.26: Total Ambiguity plot along the Cross Track using random code-1.	117
Fig 6.27: Total Ambiguity plot along the Cross Track using random code-2.	117
Fig 6.28: Total Ambiguity plot along the Cross Track using random code-2.	118
Fig 6.29: Total Ambiguity plot along the Cross Track using best transmit code.	118
Fig 6.30: Plot showing the correlation coefficient curve and $ 1 - \chi $ curve.....	119
Fig 6.31: The energy in the response vector for every single target in the target grid shown in dB scale.	120
Fig 6.32: Plot showing the convergence of χ with for one and two transmit elements respectively.....	121
Fig 6.33: Plot showing the improvement of maximum correlation with increase in total number of basis functions.	123

Abstract

One of the main characteristics of any radar system in general, is the system's transmit signal. An ideal transmit signal has two main functions to perform. First, it should be designed in such a way that most of the energy falls on the targets of interest and not on the clutter or the targets that we are not concerned, and the second function is to produce responses from dissimilar targets to be totally uncorrelated. The main objective of this study was to devise an optimal space-time transmit waveform that would produce responses from dissimilar targets to be as uncorrelated as possible. In this effort, an Algorithm has been developed in such a way that it comes up with a space-time transmit signal based on a given scenario of the radar system. This transmit signal tries to minimize the maximum correlation between any two targets in a target area. Having developed the Algorithm, its performance was analyzed numerically by generating its inputs randomly from a Gaussian distribution. A radar model was designed and the performance was also analyzed by giving inputs to the Algorithm from the model. From the analysis, it was learnt that the performance of the Algorithm largely depends on the given scenario of the radar system. It has also been found that, as the dimensions of the transmit signal subspace is increased, more flexibility was provided to the Algorithm to come up with the best code possible. Hence, higher the total number of dimensions better is the ability of the Algorithm to come up with the best code.

Therefore, in this thesis it has been proved that it is possible to develop a space-time transmit signal, which aims to minimize the maximum correlation

between dissimilar targets in a target grid by the virtue of its spatial and temporal properties.

CHAPTER - 1

1. Introduction

In general, the transmit signal is a very important factor of any radar system. Hence, in order to have a very good estimate of the scattering coefficients of the targets, the transmit signal has been used as a design parameter. In this study, Algorithms that come up with a space-time transmit signal are developed for multi-static radar systems. This transmit signal tries to make the responses from dissimilar targets, as orthogonal as possible. Although the Algorithms can be used for any kind of radar, in this study, they have been used for multi-static synthetic aperture radar systems. Hence, in this chapter, firstly, we will look into the characteristics of Single aperture radar and then will discuss Multi aperture Synthetic aperture radar system.

1.1 Synthetic Aperture Radar

Synthetic Aperture Radar is the most effective form of radar used in remote sensing for imagery. It utilizes complex data processing techniques in order to achieve a narrow beam. It forms its images in 2-Dimensions. One, Range direction, which is also called the cross-track direction, is in the direction perpendicular to the direction of propagation of the radar. Two, Azimuth direction also called the Along-Track direction, is along the direction of the propagation of the radar. The range resolution depends on the width of the pulse that is transmitted or in other words it depends on the bandwidth of the radar. This is true for both, SAR radars as well as any other kind of radars. The azimuth resolution depends on the beamwidth of the radar. Synthetic

aperture radar has much better azimuth resolution compared to other radars. This is because, for a fine azimuth resolution, a radar needs to have a very big antenna and for normal radars to have such a big antenna is physically impractical. As the synthetic aperture radar synthesizes a large antenna it achieves a very narrow beamwidth, hence a very fine azimuth resolution.

Single element synthetic aperture radar, as the name indicates, contains only one aperture and functions by synthesizing a big radar antenna. It functions by moving from one point to another either in air or space, and collects data all along its journey. It processes the entire data collected as though there were a virtual antenna whose length was equal to the distance of its journey. This feature of SAR helps in achieving a very narrow beamwidth or a very fine azimuth resolution with comparatively small antenna mounted on an aircraft or a satellite. A single aperture synthetic aperture radar can either have a fine azimuth resolution or wider coverage area. This is because, the single aperture radar can collect only BT number of independent samples, where B being the bandwidth and T being the observation time of the radar. In other words, it can only illuminate an area of BT target pixels. This problem can be addressed by employing a multi-aperture radar.

1.2 Multi Element Synthetic Aperture Radar

A Multi-Aperture radar is a constellation of coherent receivers working as a single radar system. In this system, we make use of spatial diversity technique by using multiple transmit and multiple receive elements. Each element in this system is

located spatially at a different location thus receiving data at different angles of arrival. Therefore, there are new spatial dimensions which are utilized to adequately resolve the targets in the azimuth direction while covering a wider area. This gives a possibility of having a cluster of coherent elements moving in the space coordinating with each other acting as a single radar system.

The main advantage of a Multi-Aperture (Multi-Element) Synthetic Aperture Radar over a Single Synthetic Aperture Radar system is that it enables a radar to have fine azimuth resolution simultaneously with a wider coverage area. If there are a total of N number of apertures in the radar system, then the multi-element radar system collects a total of NBT number of independent samples, hence there is an increase of N times in the total number of independent samples received compared to single aperture radar. This additional information is used to achieve wider coverage area and finer azimuth resolution.

Another important point to note is that the energy in the ambiguity function of a single aperture synthetic aperture radar is constant, that is, energy cannot be removed from the ambiguity function. However, for a space-time transmit signal, the ambiguity function is not invariant. Thus, by proper design of the space-time transmit signals; it is possible to minimize the energy in the ambiguity function, that is, minimize the maximum correlation between any two targets in a target grid.

1.3. Motivation:

Having received the response signal from the targets, the received signal needs to be processed in order to estimate the scattering characteristics of the targets. The most common estimator used to process the received signal is the matched filter. For a multi-aperture radar, the matched filter gives a very good estimate of the scattering characteristics if the apertures are arranged in a well defined contiguous pattern, but the estimate is not very good if the arrangement of the apertures is in a distributed fashion. As the arrangement of a physical multi-aperture radar resembles a distributed arrangement, a solution needs to be found out in order to have a good estimate of the scattering characteristics using a distributed aperture array.

It will be shown in the future chapters that a good estimate can be achieved by an estimator if the correlation between any two targets in a target grid is zero. As it is impossible to achieve zero correlation between any two targets responses, efforts can be made to minimize the correlation. The main aim of this study is to design algorithms that come up with optimal space-time transmit signals, that when transmitted would produce the response signals from different targets to be as orthogonal as possible.

The key idea behind coming up with such a code is to minimize the maximum correlation present between dissimilar targets. We call this approach as the Mini-Max solution. In this effort, an optimization criterion has been developed which acts as a yard stick that measures the performance of our algorithms. The bound of the values this criterion can assume, is a very important factor. Tighter the bound, lower is the

correlation between two targets. The derivation and analysis of the optimization criterion is discussed in future chapters.

1.4 Outline of the Thesis

Having found the motivation and the reason for this study, several questions were encountered in due course of the study. In the beginning, after developing the optimization criteria, we wanted to know if there was any direct relation between the criteria and the correlation coefficient. As the correlation coefficient is being minimized by tightening the bound of the criterion, it is very important to realize the relation between the criterion and the correlation coefficient. It was found that, by tightening the bound of the criterion we are actually reducing the real part of the complex correlation, thereby reducing the magnitude of the correlation. Hence, a direct relation exists between the criterion and the correlation coefficient, only if the imaginary part of the complex correlation becomes zero.

Having developed the algorithms, we wanted to see their performance initially using numerical data. In course of this numerical analysis, we tried to study the performance by varying the total number of independent measurements taken and dimensions of the transmit signal. It was found that the performance of the algorithms improved as we increased the total number of measurements and the dimensions of the transmit signal. We also found that, apart from the total number of measurements and the dimension of the transmit signal, the performance of the algorithms were also depended on the given radar scenario. Another important question that arose was how

good the result is given by the algorithms, in general. That is, we needed a yard stick to compare the performance of the transmit signal given by the algorithms. Thus, in order to get an idea of the efficacy of the algorithms, we compared the results with a randomly generated code and a code given by the Genetic Algorithm. Comparing the performance of the transmit signal given by the algorithm to that of a randomly generated code, we found that the transmit signal given by the algorithm performed much better in terms of lowering the maximum correlation. The plots of this comparison are shown in the subsequent chapters. When compared with the genetic algorithm, the code given by the genetic algorithm performed slightly better than the algorithm developed in this study. This shows that the algorithm may not come up with the best possible code in all radar system scenarios.

After analyzing the performance of the algorithm using numerical inputs, we then wanted to see how the algorithm would perform in conditions simulating real radar scenario. In order to answer this question, a radar model was designed in which the transmit signal was designed as a superposition of orthogonal basis functions. The performance of the algorithms was analyzed using the inputs of the algorithm from the radar model. It was found that as we increased the total number of basis functions, more flexibility was provided to the algorithm to come up with a better code. The limit on number of basis functions that can be used has also been derived in this study.

All the above experiments were performed using one transmit element. We then wanted to see the performance by increasing the total number of transmit

elements to 2, that is, including spatial dimensions to the transmit signal. It was found that the transmit signal obtained for this scenario performed better than one transmit element scenario in terms of reducing the maximum correlation between the targets. A disadvantage of using multiple transmit element is that, the ambiguity function for a multi transmit element space-time transmit signal does not remain invariant. Hence, for a case having multiple transmit elements, the algorithm needs to be modified such that it considers all the targets in the target grid to come up with a code.

CHAPTER – 2

2. Processing and Analysis of Multi-static Radar System.

In this chapter, a linear multi-static radar system is considered and its received signal is derived and processed. The derivation is based on the fact that for a linear radar system, the received signal is just a delayed form of transmit signal modified by the scattering coefficients of the targets. This chapter also explains the motivation behind this study. It discusses the processing of the received signal such that correct scattering estimates are obtained. It answers the question as to why we seek to have the responses from two dissimilar targets orthogonal to each other.

2.1 Description and Analysis

A linear, multistatic radar model was considered in order to analyze the response signal as shown in Fig 2.1. Let us assume there are a total of 'Y' apertures out of which one aperture is acting as both a transmitter and a receiver and all the other apertures act as only receivers. A total of ' m ' measurements are taken, assuming there are a total of ' t ' number of targets and we want to derive a transmit signal of dimension ' n ' which will minimize the maximum correlation between two dissimilar targets.

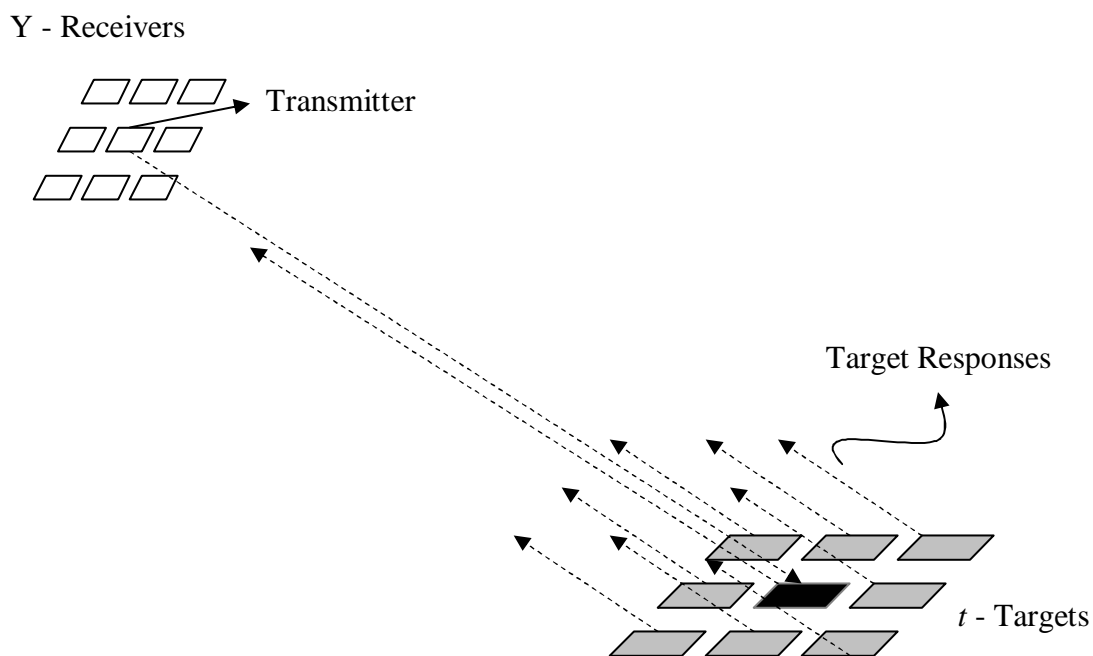


Fig 2.1: A multi-static radar system with ‘t’ number of targets and their reflections.

When a signal is transmitted by a radar, it travels through the propagation medium from the transmitter to the targets and gets scattered by the targets back to the receiver traveling through the same propagation medium. Thus, the received signal is just a delayed version of the transmit signal altered by the propagation medium and the scattering characteristics of the target. Therefore, the received signal over an illumination area of A can be represented in mathematical form as shown below [1].

$$\begin{aligned}
 r(t) &= \iint \gamma_o(\bar{x})h(\bar{x}, t, t')s(t')dt' dA + n(t) & (3.1) \\
 &= \int_A \gamma_o(\bar{x})\rho(\bar{x}, t)dA + n(t)
 \end{aligned}$$

Where,

$\bar{x} \rightarrow$ Represents the position vector of a target.

$s(t) \rightarrow$ Describes the complex transmit signal.

$\gamma_o(\bar{x}) \rightarrow$ Describes the complex scattering coefficient of the target surface.

$h(\bar{x}, t, t') \rightarrow$ Represents a complex time-varying impulse response describing the effects on the transmit signal when it travels from the transmitter to the receiver.

$n(t) \rightarrow$ Is the complex noise.

In general, any signal that is constrained in bandwidth and time can be approximated using its basis functions. Therefore, the transmit signal $s(t)$ can be written in terms of a finite set of N discrete samples as,

$$s(t) \approx \sum_{n=1}^N s(nT_s)g(t-nT_s) \quad (2.2)$$

Where, $s(nT_s)$ are the discrete samples of the continuous transmit signal $s(t)$ and $g(t)$ is the interpolation function that can be used to reconstruct the signal from its discrete values.

Similarly, the continuous received signal, the complex noise and the scattering coefficients can be described in to their respective discrete samples and are denoted as,

$$\begin{aligned} r_m &= r(mT_s) \\ \gamma_i &= \gamma_o(\bar{x}_i)\Delta A \\ H_{mm}^i &= \int h(\bar{x}_i, mT_s, t')g(t'-nT_s)dt' \quad (2.3) \\ s_n &= s(t_n) \\ n_m &= n(mT_s) \end{aligned}$$

Representing a continuous signal in terms of its discrete samples enables us to represent the received signal equation in linear algebra. Hence, substituting the equation (2.3), we can write (2.1) as [3],

$$\mathbf{r} = \sum_i \gamma_i \mathbf{H}_i \mathbf{s} + \mathbf{n} \quad (2.4)$$

$$= \sum_i \gamma_i \boldsymbol{\rho}_i + \mathbf{n} \quad (2.5)$$

$$\mathbf{r} = \mathbf{P}\boldsymbol{\gamma} + \mathbf{n} \quad (2.6)$$

Where,

$$\boldsymbol{\rho}_i = \mathbf{H}_i \mathbf{s} \quad (2.7)$$

$$\mathbf{P} = [\boldsymbol{\rho}_1; \boldsymbol{\rho}_2; \boldsymbol{\rho}_3; \dots; \boldsymbol{\rho}_T]$$

$$\mathbf{s} = [s_1, s_2, s_3, s_4, \dots, s_N]^T$$

$$\mathbf{r} = [r_1, r_2, r_3, r_4, \dots, r_M]^T$$

Therefore, in the equation (2.6), \mathbf{P} relates the scattering parameters $\boldsymbol{\gamma}$ to the measurement vector \mathbf{r} . It can also be viewed as, \mathbf{P} being a linear system through which $\boldsymbol{\gamma}$ passes, considering $\boldsymbol{\gamma}$ as a signal.

2.2 Estimators:

The received signal or the measurement vector needs to be processed so that the scattering characteristics of the targets can be estimated. There are different estimators that can be used to estimate the scattering characteristics of a target; one of the estimators called linear estimators will be discussed in this report.

Linear estimator provides the most simple and efficient way of estimating the scattering of a target. It estimates the scattering coefficient by taking

the dot product of the radar response and the estimate operator for each target. The general equation for the linear estimator is given by

$$\hat{\gamma}_i = \mathbf{W}_i' \mathbf{r} \quad (2.8)$$

The most common and simplest form of linear estimator is the correlation filter or the matched filter.

2.2.1 Matched filter

Any received radar signal contains signal, clutter and white noise. A matched filter is used to increase the signal to noise ratio (SNR) at its output. It achieves the maximum SNR by correlating the normalized response from a target with the response obtained from the received signal. The normalized response from a target pixel is given by,

$$\mathbf{W}_{\text{mf}} = \frac{\mathbf{p}_i}{|\mathbf{p}_i|^2} \quad (2.9)$$

Substituting the above equation into the linear estimator general equation (2.5) we

have,

$$\hat{\gamma}_i = \gamma_i + \sum_{j \neq i} \frac{\mathbf{p}_i' \mathbf{p}_j}{|\mathbf{p}_i|^2} + \frac{\mathbf{p}_i' \mathbf{n}}{|\mathbf{p}_i|^2} \quad (2.10)$$

In this expression, the first term represents an error less estimate of the scattering of the target, the second term represents the clutter energy which is the correlation between the target of interest and the other targets, and the third term is a noise term. It is obvious from the equation (2.10), that in order to get a close estimate of the scattering of the targets, we need to have the clutter energy and the noise as low as possible. Though, the matched filter minimizes the error due to noise, it is incapable

to remove the effect on the estimate due to the clutter. Hence, other estimators are considered to achieve a precise scattering estimate of the targets. We discuss about two other filters as follows.

2.2.2 Maximum Likelihood Estimator:

The maximum likelihood estimator can be found by first forming the maximum likelihood function of the equation (2.5). The maximum likelihood function is obtained by taking the natural log of the conditional probability density function of the measurement vector \mathbf{r} as [3],

$$\mathbf{L}(\mathbf{r}, \gamma) = \ln[\mathbf{P}(\mathbf{r} / \gamma)] = \ln \left[\frac{1}{\sqrt{|2\pi\mathbf{K}_n|}} \exp \left[-1/2(\mathbf{r} - \mathbf{P}\gamma)^H \mathbf{K}_n^{-1} (\mathbf{r} - \mathbf{P}\gamma) \right] \right] \quad (2.11)$$

Where, \mathbf{K}_n is the covariance matrix of the zero mean complex noise.

The value of γ which maximizes the maximum likelihood function $\mathbf{L}(\mathbf{r}, \gamma)$ can be found by taking the derivative of $\mathbf{L}(\mathbf{r}, \gamma)$ with respect to γ and equating it to zero. Hence, the value of γ which maximizes $\mathbf{L}(\mathbf{r}, \gamma)$ is the maximum likelihood estimate of γ denoted by $\hat{\gamma}_{\max_like}$

For more information about maximum likelihood estimator, please refer to reference [3]. The operator that performs the maximum likelihood estimation is given by,

$$\mathbf{w}_{\max_like} = \mathbf{P}^{-1} = [\mathbf{P}' \mathbf{P}]^{-1} \mathbf{P}' \quad (2.12)$$

and the estimated vector is give by,

$$\hat{\gamma}_{\max_like} = (\mathbf{w}_{\max_like}) \mathbf{r} \quad (2.13)$$

substituting (2.12) in (2.13), we get

$$\hat{\gamma}_{\max_like} = \gamma + [\mathbf{P}'\mathbf{P}]^{-1}\mathbf{P}'\mathbf{n} \quad (2.14)$$

Therefore, in the above equation, the second term is an error which is only due to noise. Therefore, the maximum likelihood estimator completely suppresses the error due to the clutter and performs very well in high SNR scenarios, but the performance of this filter deteriorates for low SNR cases.

2.2.3 Minimum Mean Square Error Estimator

A Minimum Mean Squared Error Estimator comes up with an estimate of a signal based on the minimum mean squared error criteria given by,

$$\mathbf{MMSE} = \frac{\partial E\{(\hat{\gamma} - \gamma)^2\}}{\partial \mathbf{W}_{\text{mmse}}} = 0 \quad (2.15)$$

It can also be visualized as stated in the orthogonality principle, which states that the error in estimation is orthogonal to each observation made. [3]

Again the derivation of the MMSE operator is beyond the scope of this thesis. For further details please refer to reference [3].

The Minimum Mean Squared Error Estimator is given by [3],

$$\mathbf{W}_{\text{mmse}} = \mathbf{K}_{\gamma}'\mathbf{P}'[\mathbf{P}\mathbf{K}_{\gamma}'\mathbf{P}'+\mathbf{K}_{\mathbf{n}}']^{-1} \quad (2.16)$$

Where, $\mathbf{K}_{\mathbf{n}}$ and \mathbf{K}_{γ} are noise covariance and scattering coefficient covariance respectively.

From the above equation, it is very clear that as the covariance of the noise tends to infinity, the magnitude of the minimum mean square error estimator approaches to zero. It tries to maximize the Signal to Interference ratio (SIR) where Interference is defined as sum of clutter and noise energy. Hence, in presence of high noise, it is best to use the MMSE filter to the other two estimators. Though it has been proved in the previous study that MMSE estimator performs much better than the matched filter, the MMSE filter processing algorithms are more complex and expensive to implement.

Another important point that is to be noted is that from all expressions of the operators W , it can be realized that all the estimators would give us the same result if the responses from different targets, i.e. the \mathbf{p}_i vectors were perfectly orthogonal to each other. In other words for all targets $i \neq j$, $\mathbf{p}_i' \mathbf{p}_j = 0$. Hence, as the MMSE estimator is complex and expensive to implement, we could use the Matched filter processing technique and still get good results if the responses from dissimilar targets are orthogonal to each other.

Therefore, in order to have an accurate estimate of the scattering coefficients of the targets from the received signal using a matched filter, we need the responses from dissimilar targets to be as orthogonal as possible. Thus, the entire effort of this study is to make the responses of dissimilar targets as orthogonal as possible to each other.

CHAPTER - 3

3. The Optimization Criterion

In order to develop the Algorithms that generate the space-time transmit signals which in turn make the responses from dissimilar targets as orthogonal as possible, a mathematical criterion is needed such that the solution that satisfies the criterion is the same solution that satisfies our requirements. In this chapter, the derivation and analysis of such an optimization criterion is discussed. As the bound of the criterion is being tightened in order to minimize the correlation coefficient between dissimilar targets, a very important question that needs to be answered is how closely the criterion relates to the correlation coefficient.

3.1 Analysis of the optimization criteria χ

As discussed in the last chapter, we seek to minimize the correlation between dissimilar targets such that the scattering coefficients of the targets are estimated correctly. Apart from making the responses from two different targets as orthogonal as possible, we also do not desire the energy in a target response to be zero. Hence, a criterion is needed whose solution when used as transmit signal, minimizes the correlation between dissimilar targets. Such a criteria is derived as follows,

The total energy in a radar response is given by,

$$\mathbf{E}_{\text{Total}} = \sum_i \boldsymbol{\rho}_i' \sum_i \boldsymbol{\rho}_i \quad (3.1)$$

Where, $\boldsymbol{\rho}_i$ is the response of the target 'i'.

Similarly, the sum of the energies of each target response is given as,

$$\mathbf{E}_{\text{sum}} = \sum_i \boldsymbol{\rho}_i' \boldsymbol{\rho}_i \quad (3.2)$$

When only two targets are considered, equation (3.1) and (3.2) can be written as,

$$\mathbf{E}_{\text{Total-2}} = (\boldsymbol{\rho}_i' + \boldsymbol{\rho}_j')(\boldsymbol{\rho}_i + \boldsymbol{\rho}_j) \quad (3.3)$$

$$= \boldsymbol{\rho}_i' \boldsymbol{\rho}_i + \boldsymbol{\rho}_j' \boldsymbol{\rho}_j + \boldsymbol{\rho}_i' \boldsymbol{\rho}_j + \boldsymbol{\rho}_j' \boldsymbol{\rho}_i \quad (3.4)$$

And
$$\mathbf{E}_{\text{sum-2}} = (\boldsymbol{\rho}_i' \boldsymbol{\rho}_i + \boldsymbol{\rho}_j' \boldsymbol{\rho}_j) \quad (3.5)$$

From equation (3.4) it can be seen that the first two terms give the energy in an individual target response, where as, the third and fourth terms give the correlation between two dissimilar targets.

Hence, our objective is to minimize the correlation between two targets (third and fourth terms in (3.4)) as much as possible. This requirement can be satisfied using a criterion formed by taking the ratio of equations (3.4) and (3.5). We call this criterion as the optimization criteria χ , given by,

$$\chi = \frac{(\boldsymbol{\rho}_i' + \boldsymbol{\rho}_j')(\boldsymbol{\rho}_i + \boldsymbol{\rho}_j)}{(\boldsymbol{\rho}_i' \boldsymbol{\rho}_i + \boldsymbol{\rho}_j' \boldsymbol{\rho}_j)} \quad (3.6)$$

From equation (2.7) we can write $\boldsymbol{\rho}_i$ as,

$$\boldsymbol{\rho}_i = \mathbf{H}_i \mathbf{s}$$

Substituting $\boldsymbol{\rho}_i$ in (3.6) we have,

$$\chi = \frac{\mathbf{s}'(\mathbf{H}_i + \mathbf{H}_j)'(\mathbf{H}_i + \mathbf{H}_j)\mathbf{s}}{\mathbf{s}'(\mathbf{H}_i' \mathbf{H}_i + \mathbf{H}_j' \mathbf{H}_j)\mathbf{s}} \quad (3.7)$$

Defining two matrices, A and B as,

$$\mathbf{A} = (\mathbf{H}_i + \mathbf{H}_j)'(\mathbf{H}_i + \mathbf{H}_j) \quad (3.8)$$

$$\mathbf{B} = (\mathbf{H}_i' \mathbf{H}_i + \mathbf{H}_j' \mathbf{H}_j) \quad (3.9)$$

Using the matrices \mathbf{A} and \mathbf{B} , (3.7) can also be written as,

$$\chi = \frac{\mathbf{s}' \mathbf{A} \mathbf{s}}{\mathbf{s}' \mathbf{B} \mathbf{s}} \quad (3.10)$$

Therefore, a solution \mathbf{s} to the equation (3.10) that makes the values of χ to be 1 is the same solution that ensures the responses from two dissimilar targets are totally uncorrelated. This can be proved mathematically as, when the responses from the targets i and j are totally uncorrelated, then,

$$\boldsymbol{\rho}_i' \boldsymbol{\rho}_j = 0 \quad (3.11)$$

Substituting (3.11) in (3.6), we get $\chi = 1$.

The main advantage of using this criterion is that the matrices \mathbf{A} and \mathbf{B} are positive definite matrices, which means eigen analysis can be used to derive a solution for χ .

Expanding (3.6) we get,

$$\chi = \frac{(\boldsymbol{\rho}_i' \boldsymbol{\rho}_i + \boldsymbol{\rho}_j' \boldsymbol{\rho}_j + \boldsymbol{\rho}_i' \boldsymbol{\rho}_j + \boldsymbol{\rho}_j' \boldsymbol{\rho}_i)}{(\boldsymbol{\rho}_i' \boldsymbol{\rho}_i + \boldsymbol{\rho}_j' \boldsymbol{\rho}_j)} \quad (3.12)$$

A limit for χ -values can be derived as follows.

If the target responses are normalized then,

$$\boldsymbol{\rho}_i' \boldsymbol{\rho}_i = \boldsymbol{\rho}_j' \boldsymbol{\rho}_j = 1 \quad (3.13)$$

Substituting (3.13) in (3.6) we have,

$$\chi = 1 + \text{Re}(\boldsymbol{\rho}_i' \boldsymbol{\rho}_j) \quad (3.14)$$

Hence, the term $\boldsymbol{\rho}_i' \boldsymbol{\rho}_j$ has a maximum value of 1 when the two response vectors are aligned in the same direction, and has a minimum value of -1, when the two vectors are aligned in the opposite direction. Substituting these maximum and minimum values of $\boldsymbol{\rho}_i' \boldsymbol{\rho}_j$ in (3.14), we get the limit for χ -values as,

$$0 \leq \chi \leq 2$$

Therefore, the values of χ lie between 0 and 2.

From the equation (3.10) we have,

$$\chi = \frac{\mathbf{s}' \mathbf{A} \mathbf{s}}{\mathbf{s}' \mathbf{B} \mathbf{s}}$$

From the definition of B matrix in equation (3.9), we can clearly say that the matrix B is a Hermitian Matrix. That is, complex conjugate transpose of B is itself.

$$\mathbf{B}' = \mathbf{B} \quad (3.15)$$

The B matrix can also be represented as,

$$\mathbf{B} = \mathbf{B}^{1/2} \mathbf{B}^{1/2} \quad (3.16)$$

Also,
$$\mathbf{B}^{1/2} \mathbf{B}^{-1/2} = \mathbf{I} \quad (3.17)$$

Multiplying the identity matrix with A in (3.10) we have,

$$\chi = \frac{\mathbf{s}' \mathbf{I} \mathbf{A} \mathbf{s}}{\mathbf{s}' \mathbf{B}^{1/2} \mathbf{B}^{1/2} \mathbf{s}} \quad (3.18)$$

Substituting (3.16) and (3.17) in (3.18) we have,

$$\chi = \frac{\mathbf{s}' \mathbf{B}^{1/2} \mathbf{B}^{-1/2} \mathbf{A} \mathbf{B}^{-1/2} \mathbf{B}^{1/2} \mathbf{s}}{\mathbf{s}' \mathbf{B}^{1/2} \mathbf{B}^{1/2} \mathbf{s}} \quad (3.19)$$

We then represent $\mathbf{s} \mathbf{B}^{1/2}$ as,

$$\tilde{\mathbf{s}} = \mathbf{B}^{1/2} \mathbf{s} \quad (3.20)$$

Also,
$$\tilde{\mathbf{s}}' = (\mathbf{B}^{1/2} \mathbf{s})' \quad (3.21)$$

$$\tilde{\mathbf{s}}' = \mathbf{s}' \mathbf{B}^{1/2} \quad (3.22)$$

as \mathbf{B} is Hermitian, $(\mathbf{B}^{1/2})' = \mathbf{B}^{1/2}$

Substituting $\tilde{\mathbf{s}}$ in equation (3.19) we have,

$$\chi = \frac{\tilde{\mathbf{s}}' \mathbf{B}^{-1/2} \mathbf{A} \mathbf{B}^{-1/2} \tilde{\mathbf{s}}}{\tilde{\mathbf{s}}' \tilde{\mathbf{s}}} \quad (3.23)$$

Normalizing $\tilde{\mathbf{s}}$ makes $\tilde{\mathbf{s}}' \tilde{\mathbf{s}} = 1$. Therefore, we are left with only the numerator of the equation (3.23).

$$\chi = \tilde{\mathbf{s}}' \mathbf{B}^{-1/2} \mathbf{A} \mathbf{B}^{-1/2} \tilde{\mathbf{s}} \quad (3.24)$$

Let us define a matrix \mathbf{C} which is given by,

$$\mathbf{C} = \mathbf{B}^{-1/2} \mathbf{A} \mathbf{B}^{-1/2} \quad (3.25)$$

Therefore substituting \mathbf{C} in (3.23) we have,

$$\chi = \frac{\tilde{\mathbf{s}}' \mathbf{C} \tilde{\mathbf{s}}}{\tilde{\mathbf{s}}' \tilde{\mathbf{s}}} \quad (3.26)$$

The \mathbf{C} matrix is the most important matrix used in the development of the Algorithms. It can be represented in terms of its Eigen values as well as Eigen vectors. The eigen values can be considered as the values that χ would assume when the corresponding eigen vectors are used as solutions to the criteria. The \mathbf{C} matrix can be represented in terms of its eigen values and eigen vectors as,

$$\mathbf{C} = \sum_{n=1}^N \lambda_n \hat{\mathbf{v}}_n \hat{\mathbf{v}}_n' \quad (3.27)$$

where, λ_n are the eigen values of the \mathbf{C} matrix,

$\hat{\mathbf{v}}_n$ are the eigen vectors of the \mathbf{C} matrix.

and n is the total number of dimensions in the \mathbf{C} matrix.

The eigen values of the \mathbf{C} matrix are a very important parameter. As was stated before, they are the values χ would assume when the corresponding eigen vectors are used as solutions to the χ criteria. The eigen values assume a value between 0 and 2.

$$\text{i.e.,} \quad 0 \leq \lambda_n \leq 2$$

The maximum and minimum values of λ_n (λ_{\max} and λ_{\min}) are considered to be a bound of the χ -values. The whole effort of Algorithms that have been developed will be to tighten this bound as far as possible. That is, bringing the values λ_{\max} and λ_{\min} as close to 1 as possible. A value of λ_n or χ equal to 1 has a solution which will make the responses from two targets perfectly uncorrelated. So, seeking all the λ_n values close to 1 would bring down the correlation proportionally.

There is a \mathbf{C} matrix for every pair of targets. If \mathbf{C} matrices are formed with a main target of interest and more than one other targets, one at a time, say we have a total of T targets including the target of interest, then there a total of $(T-1)$ number of \mathbf{C} matrices and a total of $N*(T-1)$ number of eigen values. Irrespective of the target pair the eigen values belong to, we seek to make the maximum value of λ_n as close to 1 as possible indirectly bringing down the maximum correlation.

A parameter that is used to decide the worst eigen values (i.e., λ_{\max} and λ_{\min}) is described as,

$$\theta = \left| 90 - \cos^{-1}(1 - \lambda_n) \right| \quad (3.28)$$

Where, $\theta = 90^\circ \rightarrow$ Responses from two targets are perfectly correlated. i.e., when the eigen value $\lambda_n = 0$ or 2.

$\theta = 0^\circ \rightarrow$ Responses from two targets are perfectly uncorrelated. i.e., when the eigen value $\lambda_n = 1$

Another parameter which gives us the correlation between two targets is given by,

$$\xi = \frac{|\mathbf{p}_i' \mathbf{p}_j|}{|\mathbf{p}_i| |\mathbf{p}_j|} \quad (3.29)$$

where ξ is the correlation coefficient between targets i and j.

\mathbf{p}_i and \mathbf{p}_j are the responses of targets i and j respectively, given by,

$$\mathbf{p}_i = \mathbf{H}_i \mathbf{s} \quad (3.30)$$

The angle between the two response vectors from the correlation coefficient can also be derived as,

$$\phi = \cos^{-1}(\xi).$$

Hence we seek to minimize θ or maximize ϕ , which indirectly means to tighten the eigen value bound.

3.3 Relation between the correlation coefficient ξ and χ

An important point that needs to be taken note of, is the relation between the correlation coefficient ξ and χ .

From the equation (3.6) the χ criteria can also be written as,

$$\chi = 1 - 2 \operatorname{Re} \left\{ \frac{\mathbf{p}_i' \mathbf{p}_j}{|\mathbf{p}_i|^2 + |\mathbf{p}_j|^2} \right\} \quad (3.31)$$

Where, $\mathbf{p}_i' \mathbf{p}_j$ gives us the complex correlation between target 'i' and target 'j'.

Hence, by seeking a χ value close to 1, we are actually minimizing the real part of the complex correlation term (second term in the equation (3.26)). However, if the imaginary part of the complex correlation is equal to 0, and $|\mathbf{p}_i| = |\mathbf{p}_j|$, then χ can be written as,

$$\chi = 1 - \left\{ \frac{|\mathbf{p}_i' \mathbf{p}_j|}{|\mathbf{p}_i| |\mathbf{p}_j|} \right\} = 1 - \xi \quad (3.32)$$

Therefore, a direct relation between χ and ξ exists only when the imaginary part of the complex correlation is zero and the responses from the two targets have equal energy. Plots that justify the usage of the optimization criteria χ to search for a better transmit code are shown in Chapter-4 and Chapter -6.

3.3 Inverse of the B matrix

As stated before, a positive definite square matrix can be written in terms of its eigen values and eigen vectors as,

$$\mathbf{B} = \sum_n \mu_n \hat{\mathbf{e}}_n \hat{\mathbf{e}}_n' \quad (3.33)$$

where, μ_n are the eigen values of the \mathbf{B} matrix,

$\hat{\mathbf{e}}_n$ are the eigen vectors of the \mathbf{B} matrix.

and n is the total number of dimensions in the \mathbf{B} matrix.

In the same way the inverse of this \mathbf{B} matrix can also be represented in terms of the eigen values and eigen vectors of the \mathbf{B} matrix as,

$$\mathbf{B}^{-1} = \sum_n \frac{1}{\mu_n} \hat{\mathbf{e}}_n \hat{\mathbf{e}}_n' \quad (3.34)$$

But, it is very important to note that, when the \mathbf{B} matrix is a non full-ranked matrix, only non-zero eigen values should be substituted in the above expression. This method of inversion is called pseudo inversion. Hence, for a non full ranked \mathbf{B} matrix, The inverse is taken as,

$$\mathbf{B}^{-1} = \sum_n \frac{1}{\mu_n} \hat{\mathbf{e}}_n \hat{\mathbf{e}}_n' \quad (\mu_n > 0) \quad (3.35)$$

Pseudo inversion of the \mathbf{B} matrix is used after the first iteration in Algorithm-2.

CHAPTER - 4

4. Description and Evaluation of Algorithm-1 and Algorithm-2

This chapter deals with the development, analysis and performance comparison of Algorithm-1 and Algorithm-2. In this chapter, the performance of the algorithms is evaluated based on randomly generated inputs. It addresses various concerns about how the algorithms would perform if the total number of measurements taken and the dimension of transmit signals are varied. It has also been shown based on various experiments that the performance of the algorithms largely depends on the radar scenario. Having, successfully developed the algorithm, a very important question that was to be answered was, how good is the result given by the Algorithm in general? This chapter answers the above question by comparing the algorithm result with a randomly generated result and a result generated by the Genetic Algorithm.

4.1 Algorithm 1(Collective Projection Algorithm)

Algorithm-1 is a basic Algorithm that was developed to achieve a transmit code that will minimize the maximum correlation between two dissimilar targets. The main idea behind this Algorithm is to tighten the bound of the eigen spectrum by projecting orthogonal to all the $(N-1)$ worst vectors present in the total subspace of all the \mathbf{C} matrices. In this Algorithm, eigen analysis is applied on the \mathbf{C} matrices.

From equation (3.26) we have,

$$\chi = \frac{\tilde{\mathbf{s}}' \mathbf{C} \tilde{\mathbf{s}}}{\tilde{\mathbf{s}}' \tilde{\mathbf{s}}} \quad (4.1)$$

Writing the \mathbf{C} matrix in terms of its eigen values and eigen vectors,

$$\mathbf{C} = \sum_{n=1}^N \lambda_n \hat{\mathbf{v}}_n \hat{\mathbf{v}}_n' \quad (4.2)$$

where, λ_n are the eigen values of the \mathbf{C} matrix,

$\hat{\mathbf{v}}_n$ are the eigen vectors of the \mathbf{C} matrix,

And, n is the total number of dimensions in the \mathbf{C} matrix.

A \mathbf{C} matrix with N dimensions can be represented in terms of N eigen values and N eigen vectors. As, a \mathbf{C} matrix is formed between the main target of interest and some other target in the grid, a total of $(T-1)$ number of \mathbf{C} matrices are formed, where T is the total number of targets present. Hence, a total of $N*(T-1)$ number of eigen vectors corresponding to $(T-1)$ number of \mathbf{C} matrices are present. Out of these $N*(T-1)$ eigen vectors, $(N-1)$ worst eigen vectors corresponding to the $(N-1)$ worst eigen values are chosen based on the value of θ . These eigen vectors are named as “worst vectors” for the reason that, if these eigen vectors were used as solutions to (4.1), a value close to 0 or 2 is obtained which indicates a high correlation between the targets. The $(N-1)$ worst vectors are eliminated by searching for a code in a subspace orthogonal to those vectors. As the solution for the equation (4.1) is in s-squiggle ($\tilde{\mathbf{s}}$) form, the $(N-1)$ worst vectors are initially converted into s-form, and then the orthogonal projection is performed on them. If \mathbf{s} is a vector that is orthogonal to $(N-1)$ worst vectors, then, it

is considered to be a better solution and gives us a χ -value which is better than those values obtained by using any of the $(N-1)$ vectors as solutions. Thus, using \mathbf{s} as a solution, a better maximum correlation is achieved. The next worst eigen vector which is the N th worst eigen vector that has not been eliminated will give the particular correlation coefficient value between two targets that can be considered as a bound. This indicates that, the solution (\mathbf{s} -vector) would not come up with a correlation value greater than that obtained by using the N th worst eigen vector. Hence we use the \mathbf{s} -vector as the transmit signal.

The Flow chart of this Algorithm is as shown in Fig 4.1.

Algorithm - 1

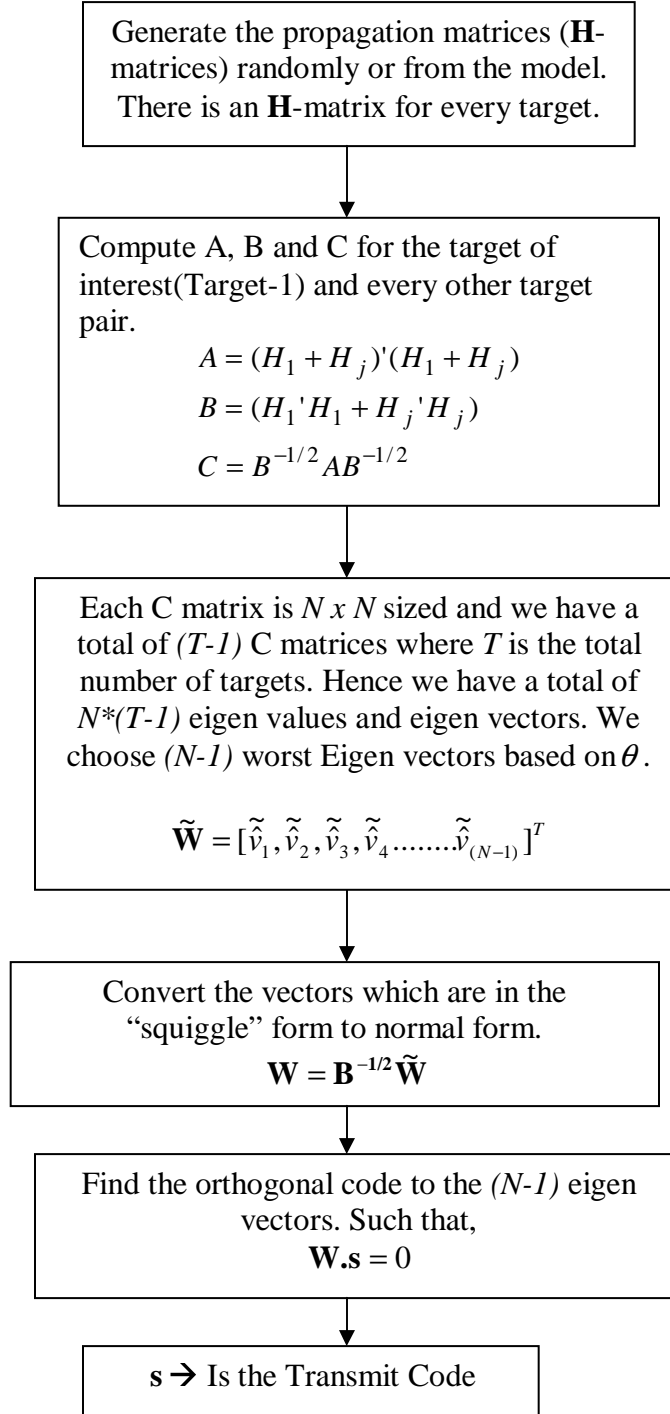


Fig 4.1: Flow Chart of Algorithm-1

4.2 Performance of Algorithm-1

In order to analyze the performance of Algorithm-1, the propagation matrices (\mathbf{H} -matrices) are generated randomly. Since the \mathbf{H} -matrices are complex matrices, both the real and the imaginary parts of every single element of the matrix are generated randomly from a Gaussian distribution with zero mean and variance one. The size of \mathbf{H} -matrices is $M \times N \times T$ where, M is the total number of measurements taken, N is the dimension of the transmit code and T is the total number of targets.

For analysis purpose we set $M=100$; $N = 40$ and $T=10$.

The results are as shown,

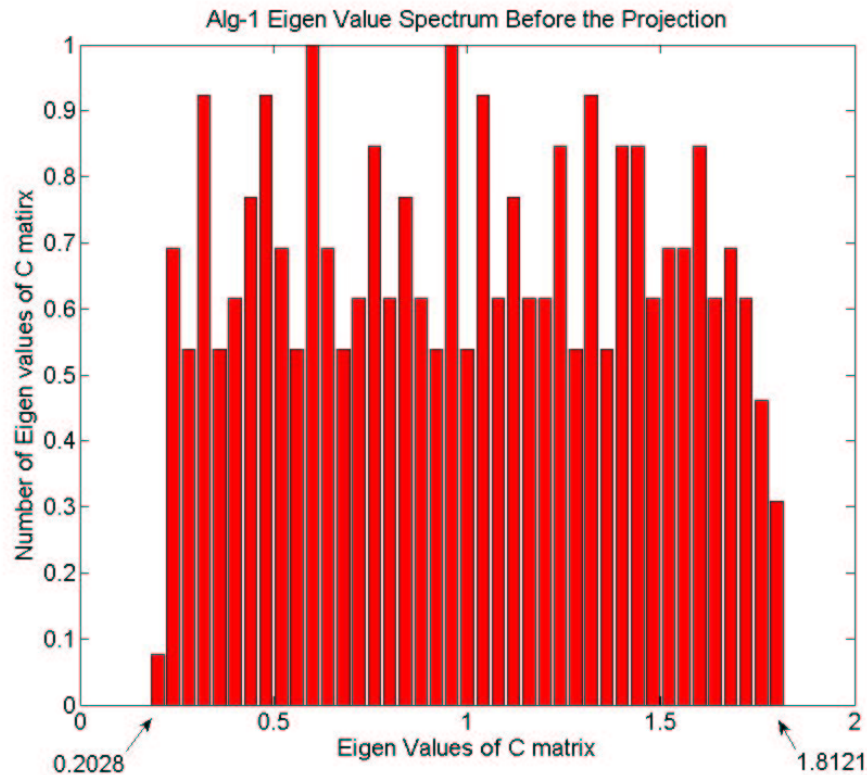


Fig 4.2: Eigen spectrum before orthogonal projection.

Fig 4.2 shows the spectrum of the eigen values of the \mathbf{C} matrix before the orthogonal projection in the subspace of $(N-1)$ worst vectors. It is observed from the Fig 4.2 that the eigen values are very loosely bound with a maximum value of 1.8121 and a minimum value of 0.2028. It can also be noticed that the eigen values are well within the values of 0 and 2.

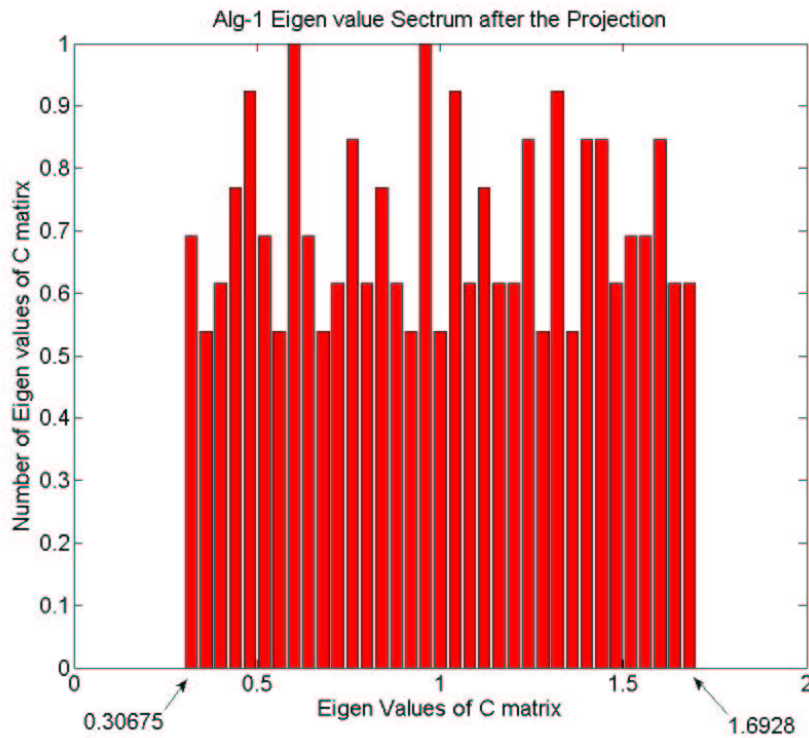


Fig 4.3: Eigen spectrum after the orthogonal projection.

Fig 4.3 shows the spectrum of the eigen values after the projection in the orthogonal subspace. As can be seen from Fig 4.3, the worst eigen values have been eliminated and the bound is tighter compared to the bound of the spectrum before the projection. The maximum value in this spectrum is 1.6928, corresponding to a $\theta = 43.85$ degrees

and the minimum value is 0.30675 corresponding to $\theta = 43.88$ degrees. Though the bound is not very tight, it is better than the bound before the projection. The N th worst eigen value that has not been eliminated is 0.30675. The corresponding eigen vector gives us a correlation coefficient value of 0.6707 ($\phi = 47.87$ degrees) which acts as a bound. Hence, any vector that is obtained by projecting orthogonal to the subspace of the $(N-1)$ number of worst vectors will give correlation values no greater than 0.6707. Fig 4.4 shows the spectrum of χ - values calculated using the transmit code \mathbf{s} given by the Algorithm. As we can see the χ values are very close to 1 with $\chi_{\max} = 1.0969$ and $\chi_{\min} = 0.8510$. The χ - values are well within the bound of 0.30675 set by the N th worst vector. The maximum correlation coefficient obtained with the transmit code is 0.1561.

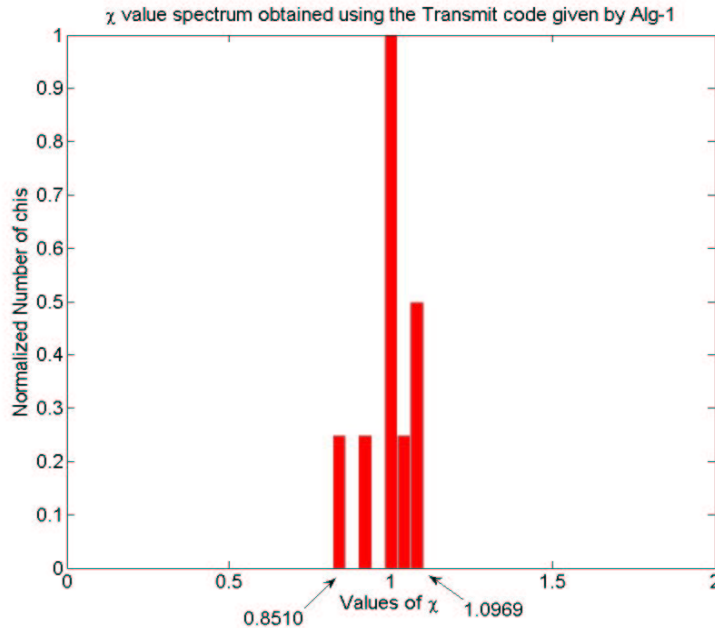


Fig 4.4: χ - value spectrum obtained using the transmit code given by Algorithm-1

A shortcoming of this Algorithm is that, it does not take into account the possibility of two or more of the $(N-1)$ worst eigen vectors being parallel to each other. The $(N-1)$ worst eigen vectors are picked and orthogonal projection performed on them collectively. There is a good possibility of the worst vectors being highly correlated to each other. Hence projecting orthogonal without taking into account the correlation between the vectors would not help much.

Therefore, the above reason gave us the motivation to develop a new Algorithm which takes into account the correlation between the worst vectors. The new Algorithm is called Algorithm-2 and it will be analyzed in the next chapters.

4.3 Algorithm-2(Individual Projection Algorithm)

This Algorithm takes into account the correlation between the worst eigen vectors of the \mathbf{C} matrices. In this Algorithm, instead of projecting orthogonal to all the $(N-1)$ worst vectors simultaneously and then finding the transmit code, the orthogonal projection is done individually i.e, one worst vector after the other. It picks the first worst eigen vector, and then searches for the next worst eigen vector in the orthogonal subspace of the first one. It again searches for the third worst eigen vector in the subspace orthogonal to the second one. It continues this for $(N-1)$ times (iterations), where N being the total number of dimensions of the transmit signal. After $(N-1)$ iterations, only one dimension is left, which gives us the best transmit signal. After each iteration, as we are projecting orthogonal to the worst eigen vector, the resulting eigen spectrum of the \mathbf{C} matrices will have a tighter χ bound than the

bound before that particular iteration. If there are a total of “ T ” targets, then after the $(N-1)$ iterations, we will have $(T-1)$ number of eigen values corresponding to $(T-1)$ pairs of targets. Now the \mathbf{C} matrix of each pair of targets has only one eigen value associated with it. These eigen values are precisely the same values we would get if the transmit code given by the Algorithm is used as a solution to the equation (4.1). There is no eigen bound as there was in Alg-1, but an exact correlation value can be derived between the targets by using the transmit code given by the Algorithm. As this Algorithm makes sure that it projects orthogonal to all the $(N-1)$ dimensions unlike Algorithm-1, we expect it to perform better than Algorithm-1.

The flow chart of Algorithm-2 is shown in Fig 4.5.

Algorithm-2

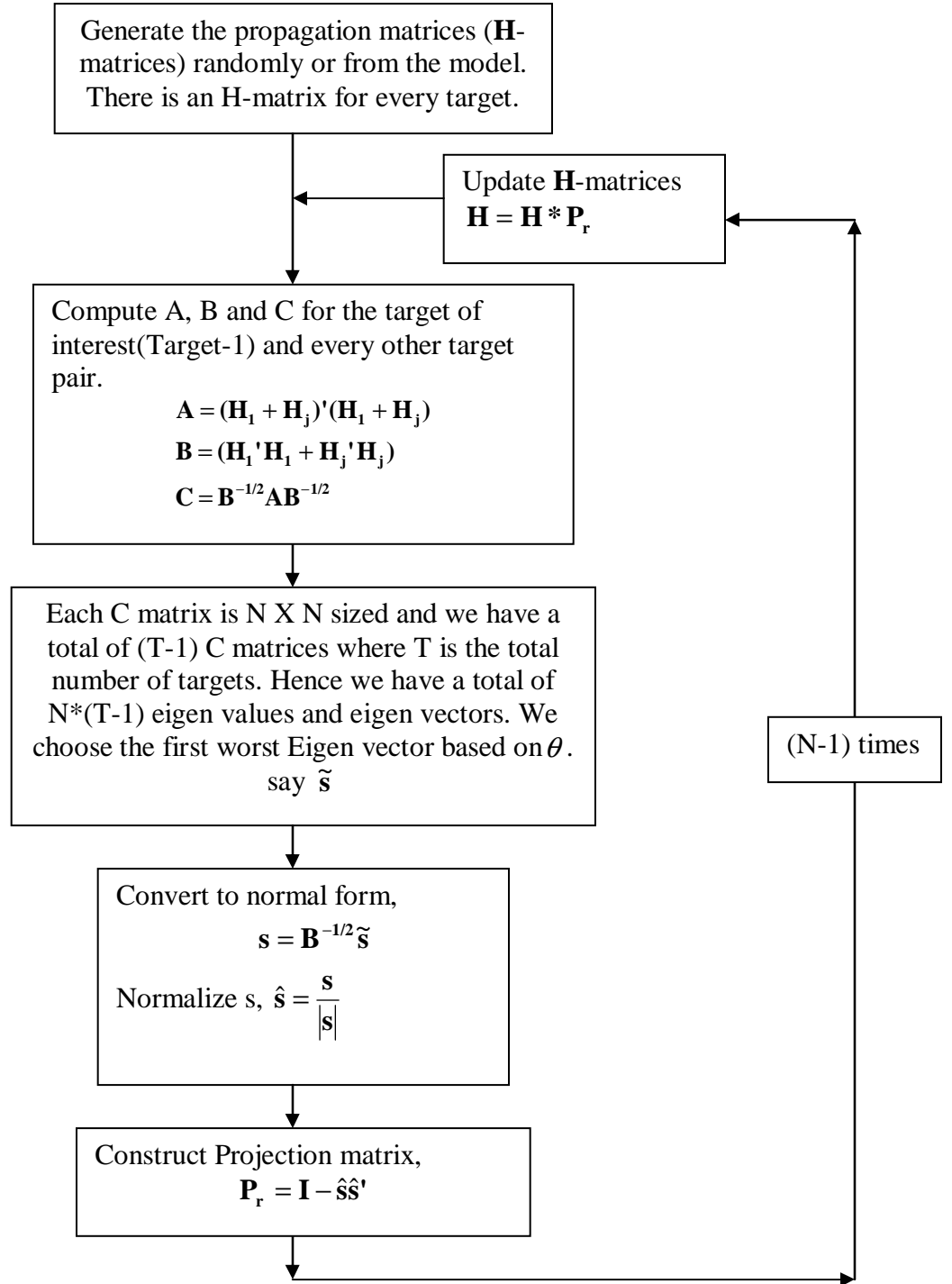


Fig 4.5: Flow chart of Algorithm-2

4.4 Performance of Algorithm-2

The performance of Alg-2 has been evaluated by first generating the \mathbf{H} -matrices randomly. Both the real as well as the imaginary parts of the complex elements have been generated from a Gaussian distribution with 0 mean and variance 1. The \mathbf{H} -matrices that are used for analysis of this Algorithm are exactly the same \mathbf{H} -matrices that were used for the analysis of Algorithm-1.

$M = 100$; $N = 40$ and $T = 10$.

The results are as shown in the following figures.

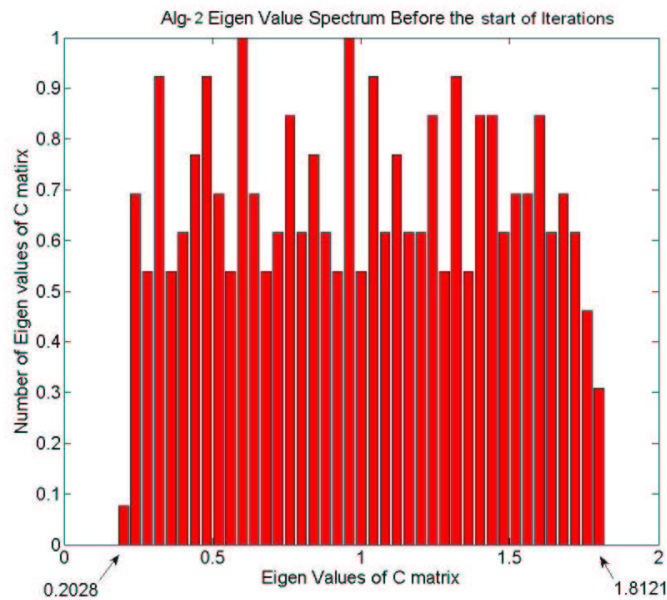


Fig 4.6: Eigen spectrum before the start of iterations.

The Fig 4.6 shows the spectrum of eigen values of the \mathbf{C} matrices before any iterations. As can be seen from the figure, the bound is quite loose with minimum value = 0.2028 ($\theta = 52.86$ degrees) and maximum value = 1.8121 ($\theta = 54.3$ degrees). From the θ value it is decided that 1.8121 is the worst eigen value and the

corresponding eigen vector is picked to search for a better code in its orthogonal space. A projection matrix is then constructed using this eigen vector and the \mathbf{H} -matrices are updated. Now a new set of \mathbf{C} matrices are formed between the main target and all the other targets, and again a worst eigen vector is picked to form a projection matrix to project orthogonal to that vector and the \mathbf{H} -matrices are updated once again. This process is repeated $(N-1)$ times.

Fig 4.7 histogram shows the eigen value spectrum after the first iteration.

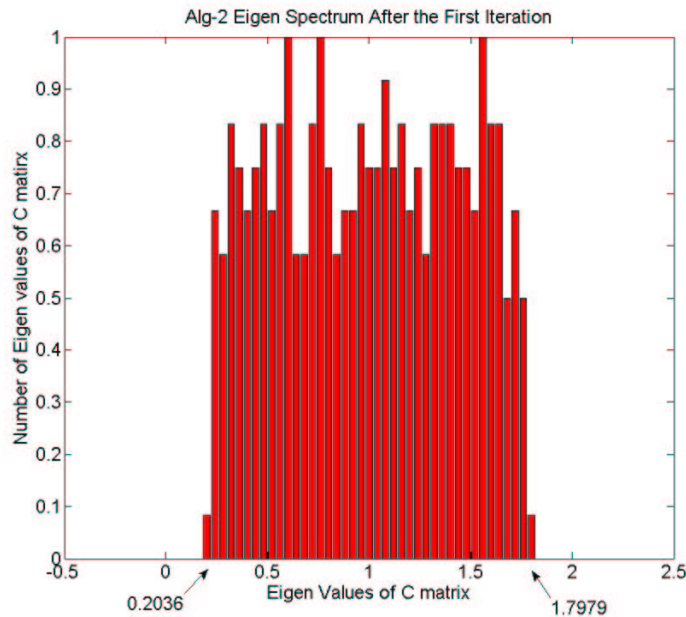


Fig 4.7: Eigen Spectrum after the first iteration.

As can be seen from Fig 4.7, the worst eigen value has been brought closer to 1 compared to the values before the first iteration. In this new spectrum, again the worst eigen vector is chosen based on the worst eigen value, which in this case is 1.7979 ($\theta = 52.93$ degrees) and a better code is searched for in the orthogonal space of its corresponding eigen vector.

The eigen value spectrum after Iteration = 27 is shown in Fig 4.8.

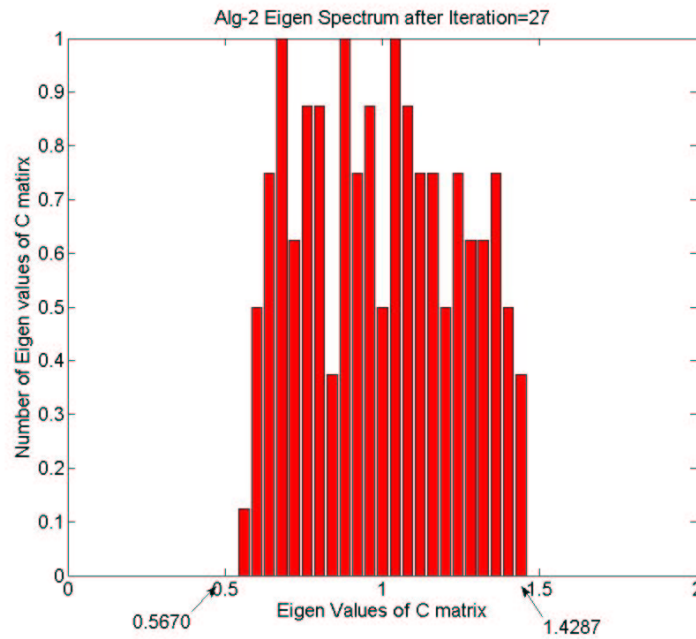


Fig 4.8: Eigen spectrum after Iteration=27

The eigen value spectrum after Iteration = 40 is shown in Fig 4.9.

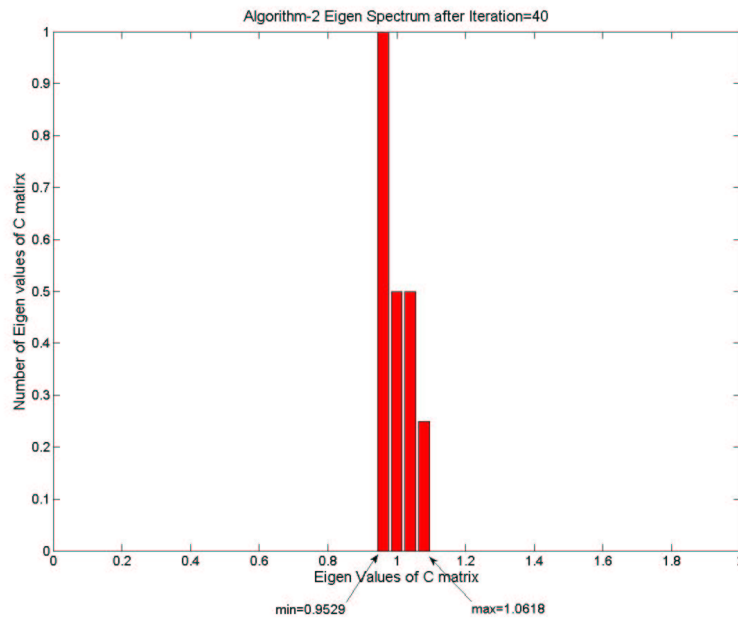


Fig 4.9: Eigen spectrum after Iteration=40

Hence, the worst eigen value has been tightened from a value of 1.8121 ($\theta = 54.3$ degrees) in the beginning, to a value of 1.0168 ($\theta = 3.54$ degrees) after $(N-1)$ iterations. The corresponding correlation coefficient value is 0.1386 corresponding to $\phi = 82.03$ degrees. This means that the response from the most correlated target is at an angle of 82.03 degrees to the response from the main target of interest. Hence we have minimized the maximum correlation to 0.1386 (-17dB).

A plot that shows the convergence of bounds of the eigen values of the \mathbf{C} matrices with respect to the iteration number is shown in Fig 4.10. In order to distinctly identify the curves, smaller values of M , N and T have been chosen.

$M=20; N=6; T=8$

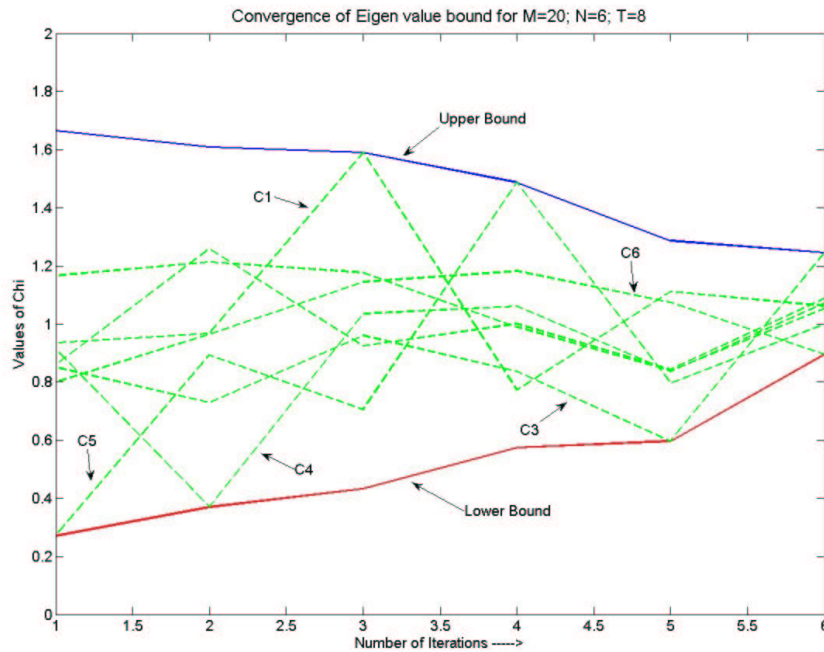


Fig 4.10: Plot showing convergence of the χ bound with respect to iteration number.

The above figure shows the convergence of the eigen value bound with respect to the iteration number. From the figure it can be noted that, the bound has converged from Iteration-1 to Iteration-6. The solid lines on top and bottom represent the maximum and minimum eigen values after its corresponding iteration. The dashed lines in the middle are the lines joining the worst eigen values of its respective **C**-matrix. That is, each dashed line corresponds to one particular **C** matrix, and is a plot of worst eigen values of that particular **C** matrix, over all the iterations. Hence, we observe that the worst eigen value after the first iteration is from **C5** matrix (i.e., the **C** matrix formed between Target-1 which our target of interest and Target-6) and worst eigen value after the second iteration is from **C4** and so on. A list of all the iterations is given below,

Iteration-1 → Worst eigen value picked from **C5** (Target-1 and Target-6)

Iteration-2 → Worst eigen value picked from **C4** (Target-1 and Target-5)

Iteration-3 → Worst eigen value picked from **C1** (Target-1 and Target-2)

Iteration-4 → Worst eigen value picked from **C5** (Target-1 and Target-6)

Iteration-5 → Worst eigen value picked from **C3** (Target-1 and Target-4)

Iteration-6 → Worst eigen value picked from **C3** (Target-1 and Target-4)

Therefore, the Eigen value bound has been converged from min = 0.2706 and max = 1.6647 to min = 0.8966 and max = 1.2452 in Fig 4.10.

4.5 Analysis of the optimization criterion χ using numerically generated input values.

As the optimization criterion χ directly relates to the real part of the complex correlation and not to the magnitude of the correlation, a very important question that needs to be answered is, how acceptable is it to use χ as a criterion to derive a transmit signal that tries to minimize the correlation between dissimilar targets? A plot between the correlation coefficient (ξ) and $|1-\chi|$ clearly answers the question. The H-matrices are generated randomly and are used as inputs to Algorithm-2. The correlation coefficient and $|1-\chi|$ values are calculated using the transmit signal given by the Algorithm. The plot is as shown in Fig 4.11.

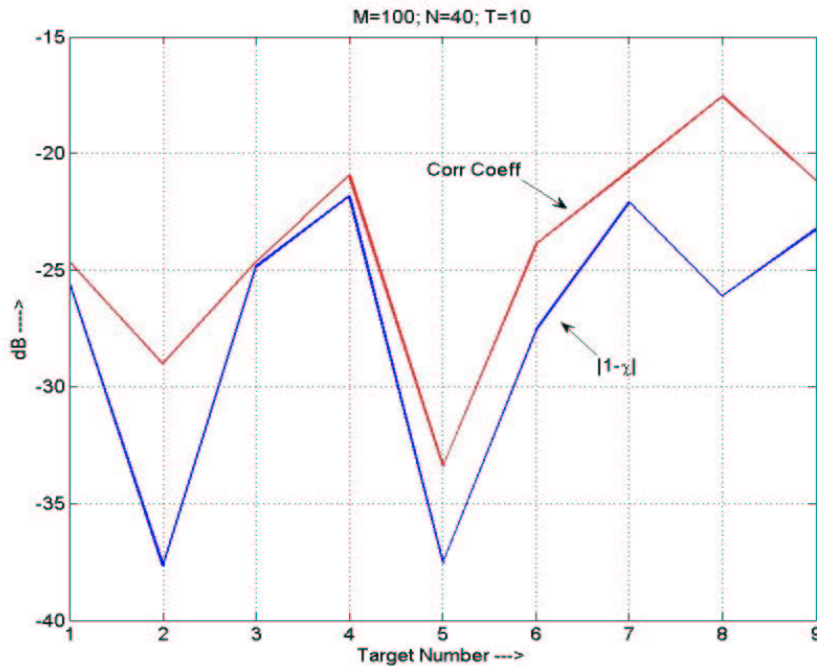


Fig 4.11: Plot showing the correlation coefficient curve and $|1-\chi|$ curve.

From Fig 4.11, it can be clearly seen that the correlation coefficient plot closely follows the $|1-\chi|$ plot. The value $|1-\chi|$ gives us the absolute value of the real part of the complex correlation and the correlation coefficient represents the magnitude of the complex correlation. Hence, it can be seen from the plot that by reducing the real part, in most cases we are reducing the magnitude of the complex correlation. Thus, the optimization criterion χ is an acceptable criterion that can be used to minimize the correlation between dissimilar targets.

4.6 Comparison of Algorithm-1 to Algorithm-2

The performances of Algorithm-1 and Algorithm-2 have been compared for different values of M , N and T . Both the Algorithms have been compiled for 20 Monte Carlo iterations. After each Monte-Carlo iteration, Algorithm-1 and Algorithm-2 give their respective solutions using which the χ -values and the correlation values have been calculated using equations (3.10) and (3.29) as,

$$\chi = \frac{\mathbf{s}'\mathbf{A}\mathbf{s}}{\mathbf{s}'\mathbf{B}\mathbf{s}} \quad \xi = \frac{|\boldsymbol{\rho}_i' \boldsymbol{\rho}_t|}{\|\boldsymbol{\rho}_i\| \|\boldsymbol{\rho}_t\|}$$

A χ -value histogram and a maximum correlation coefficient value histogram are plotted for all the 20 Monte-Carlo iterations collectively. Having plotted these histograms for both the Algorithms, the performances have been compared in terms of standard deviation of the χ -values and mean of the maximum correlation coefficient values. As the bound of χ -values is of main interest, we considered the standard deviation of the χ -value distribution as a measure of performance of the

Algorithms. The mean of χ s in all the cases is approximately 1, hence, only the standard deviation of the values will be discussed in this report. Thus, lower the standard deviation tighter is the χ - bound and better is the performance of the Algorithm. Also, we intend the maximum correlation coefficient histogram to have a mean as low as possible. Lower the mean, better is the performance of the Algorithm.

Fig 4.12 shows the different cases for which the comparisons are made.

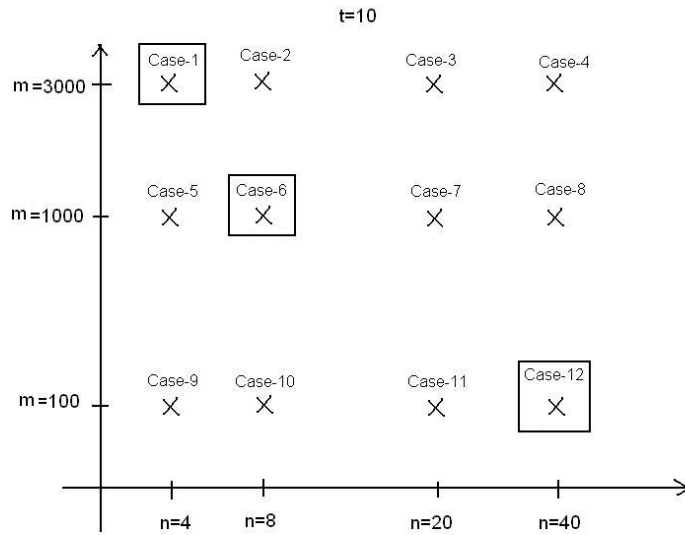


Fig 4.12: Different cases that Algorithm-1 and Algorithm -2 have been compared in.

The Algorithms have been compared for 12 different cases corresponding to different values of M , N and T as shown in Fig 4.11. Showing the results of all the 12 cases would be redundant to come to a conclusion, hence, the three most important cases will be discussed, which are indicated by a square box, in Fig 4.12. The value of M has been varied from 100 to 3000 and the value of N has been varied from 4 to 40, whereas the value of T has been kept constant at 10.

4.6.1 Case – 1: ($M=3000$; $N=4$; $T=10$)

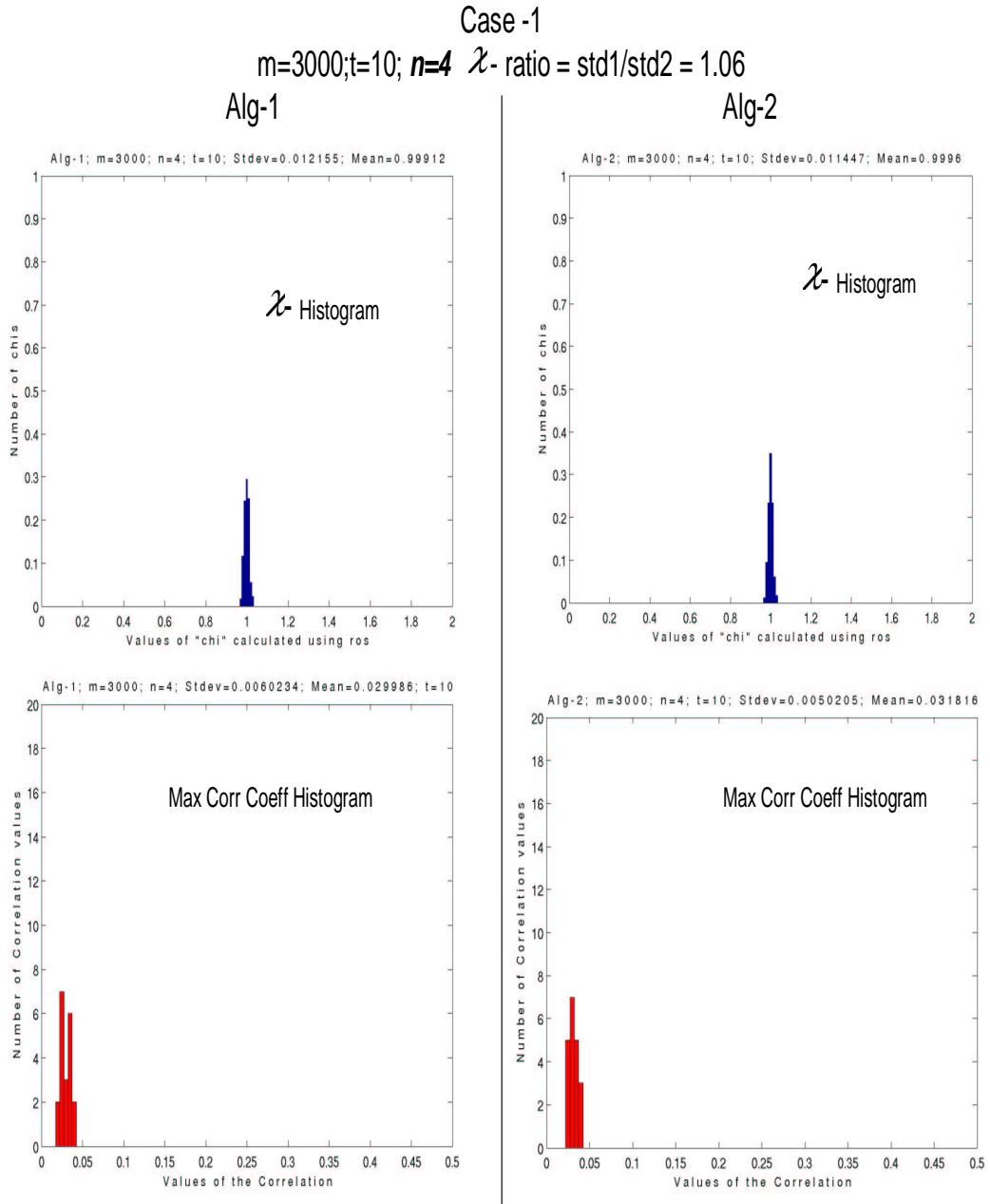


Fig 4.13: Comparison of Histograms of χ and maximum Correlation coefficient values, for Alg-1 and Alg-2 for case1

The Fig 4.13 shows a comparison between the histograms of χ -values as well as maximum correlation coefficients for Alg-1 and Alg-2. The plots on the left side show the histograms corresponding to Alg-1 and the plots on the right correspond to Alg-2. As can be seen from Fig 4.13, there is not much improvement in the chi standard deviation of Alg-2 from Alg-1. The ratio of the standard deviation of the distribution of χ of Alg-1 to Alg-2 is about 1. The mean of the maximum correlation coefficient values for Alg-1 is 1.061 times that of Alg-2.

4.6.2 Case – 6: ($M=1000$; $N=8$; $T=10$)

In this case, the value of M has been decreased from 3000 to 1000 and the value of N has been increased from 4 to 8. The histograms of Alg-1 and Alg-2 are shown in Fig 4.14.

Again, in this case the ratio of the standard deviation of χ values for Alg-1 to Alg-2 is not too high and is only 1.11. And the mean of the maximum correlation of Alg-1 is almost same as that of Alg-2.

Case -6

$m=1000; t=10; n=8$ χ ratio = std1/std2 = 1.11

Alg-1

Alg-2

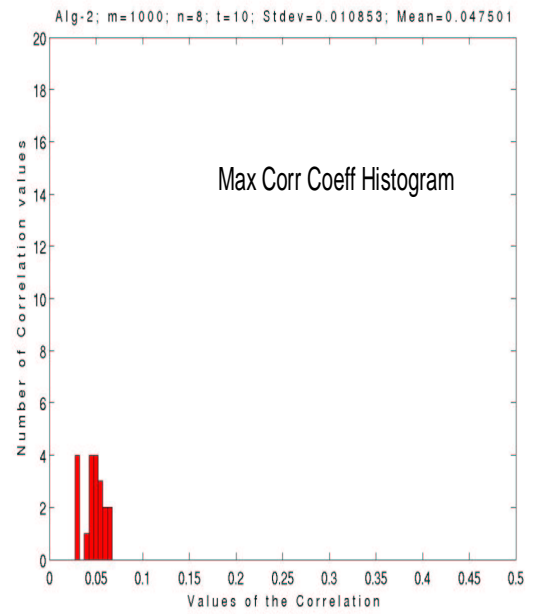
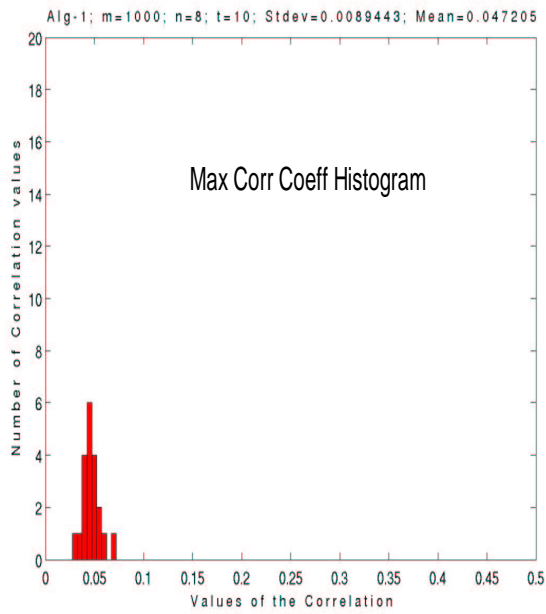
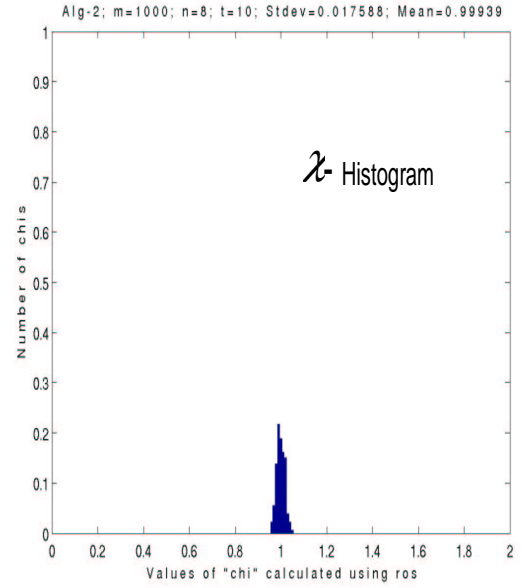
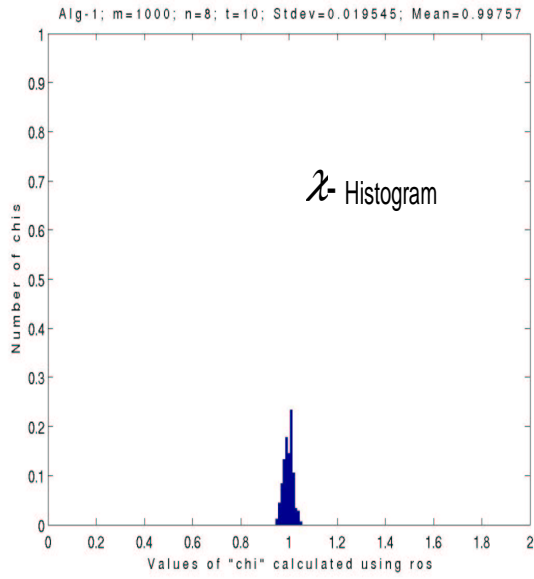


Fig 4.14: Comparison of Histograms of χ and Correlation for Alg-1 and Alg-2 for case-6

4.6.3 Case – 12: ($M=100$; $N=40$; $T=10$)

In this case, the value of M has been decreased from 1000 to 100 and the value of N has been increased from 8 to 40. The histograms of Alg-1 and Alg-2 are as shown in Fig 4.15,

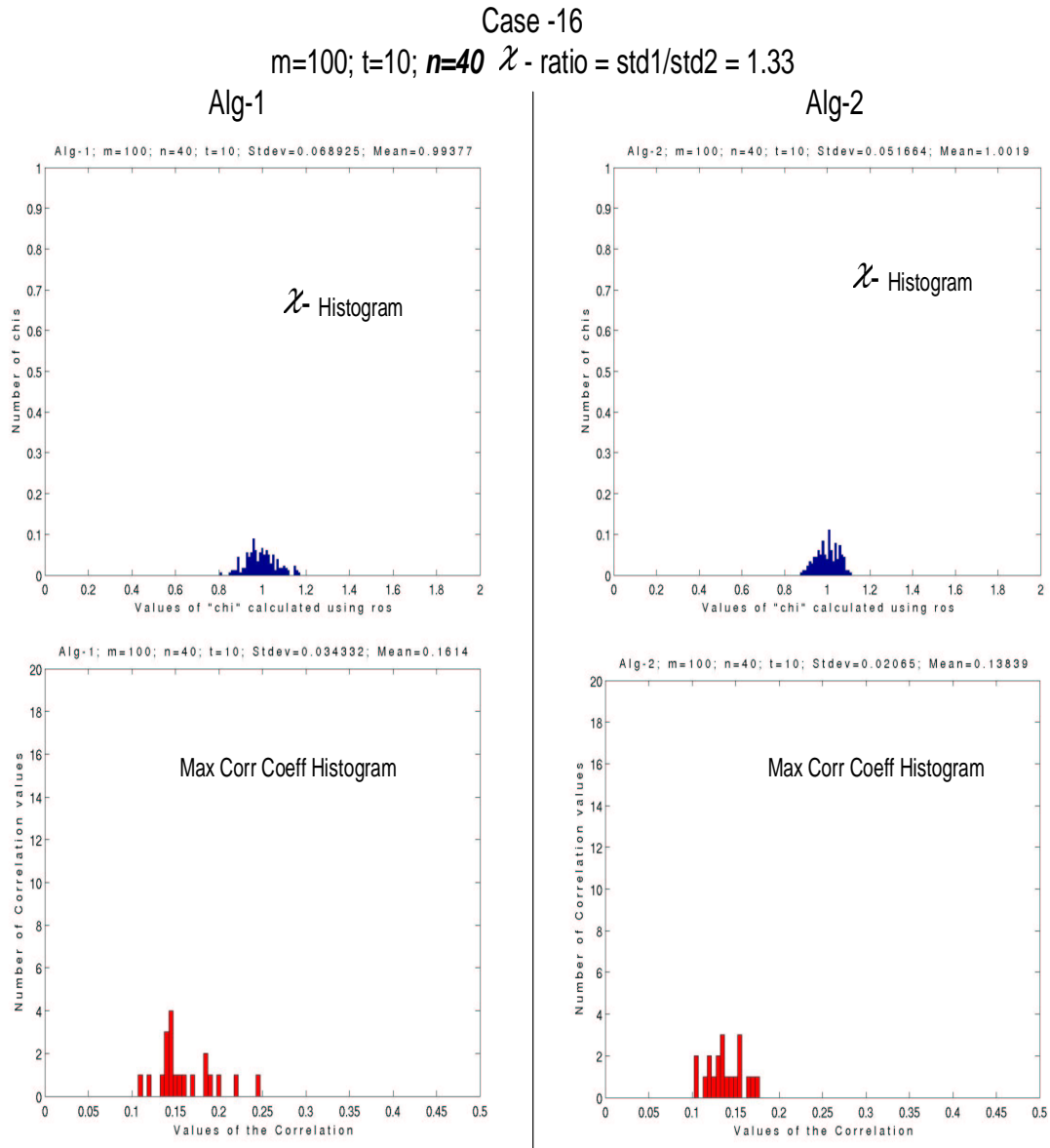


Fig 4.15: Comparison of Histograms of χ and Correlation for Alg-1 and Alg-2 for Case-12

The ratio of standard deviations of χ values from Alg-1 to Alg-2 in this case is 1.33 and the ratio of mean of maximum correlation coefficient for Alg-1 to Alg-2 is 1.165.

Summarizing all the above cases, a plot of the standard deviation values with respect to the transmit signal dimension can be plotted for both Alg-1 and Alg-2. The plot is as shown in Fig 4.16.

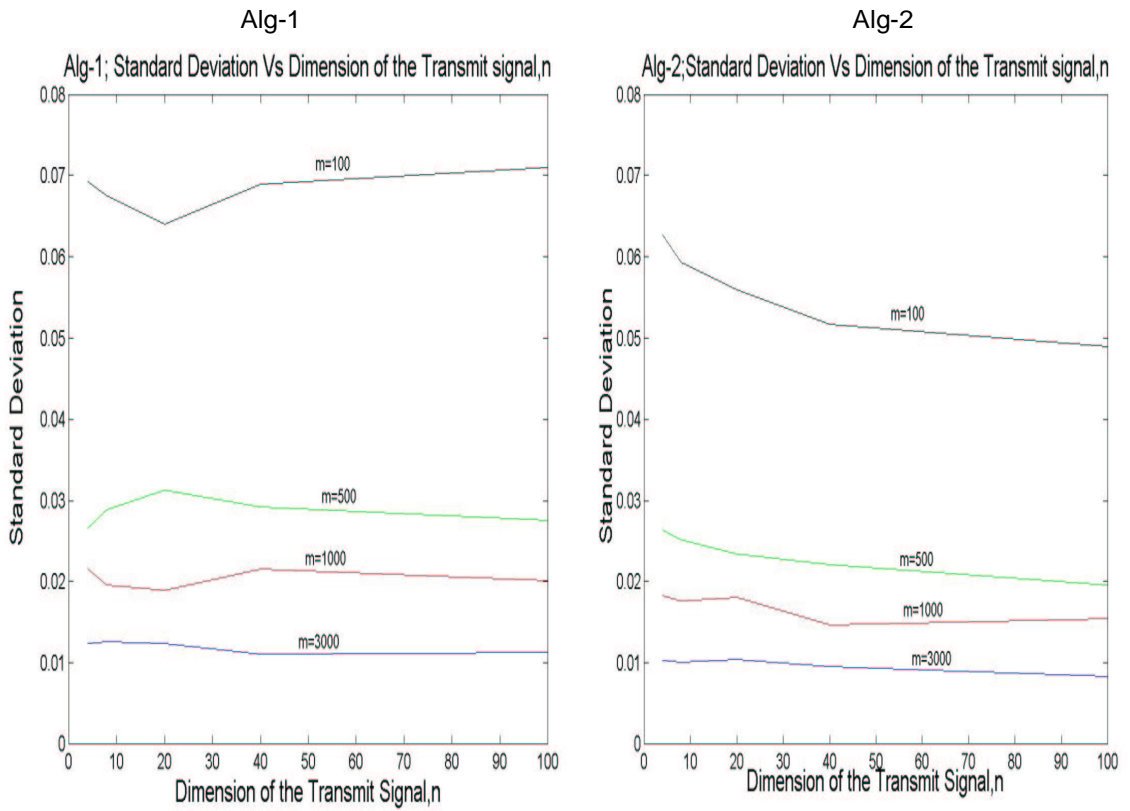


Fig 4.16: Plots of standard deviation of χ with respect to the transmit signal dimension for Alg-1 and Alg-2. (m is the total number of measurements taken.)

The standard deviation values for Alg-1 are very close to that of Alg-2 for $M=3000$; 1000; 500. However, Alg-2 performs better than Alg-1 for $M=100$.

Similarly a plot showing the mean of the maximum correlation coefficient values with respect to the dimension of the transmit signal is as shown in Fig 4.17.

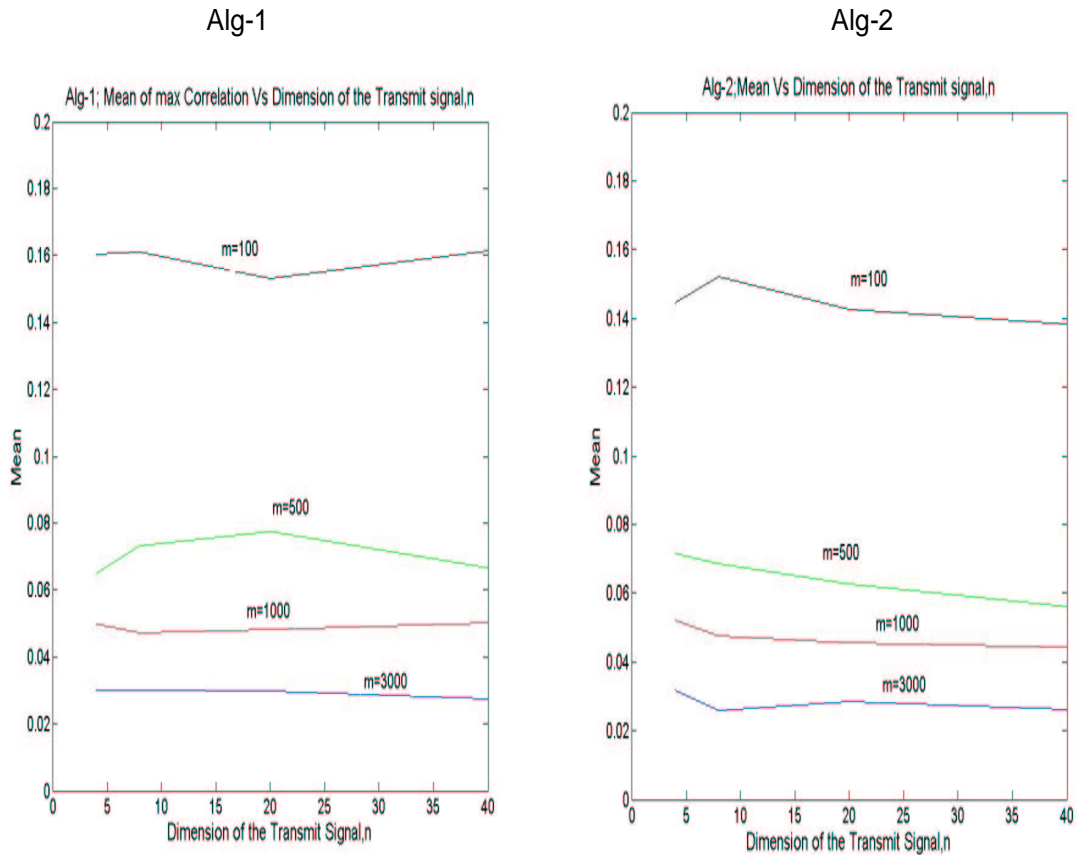


Fig 4.17: Plot showing the mean of max correlation with respect to the transmit signal dimension for Alg-1 and Alg-2.

Therefore, from the above cases it is very difficult to come to a precise conclusion about the performance of the Algorithms. For \mathbf{H} -matrices generated from single Gaussian distribution, though there is an improvement in the standard deviation of Alg-2 compared to Alg-1 for all cases, the improvement is not a very significant one. Also, the means of the maximum correlation for Alg-2 are approximately equal to

that of Alg-1. Therefore, we can say that for constant **H**-matrices (Matrices generated from single Gaussian distribution) the performance of both the Algorithms in terms of standard deviation of χ values and mean of the maximum correlation values is very similar.

The **H**-matrices whose elements have been generated from Gaussian distributions of different means and different variances have been generated and the performances of Algorithms have been analyzed in those cases as well.

4.7 **H** matrices generated from Gaussian distributions with different Means and different Standard Deviations

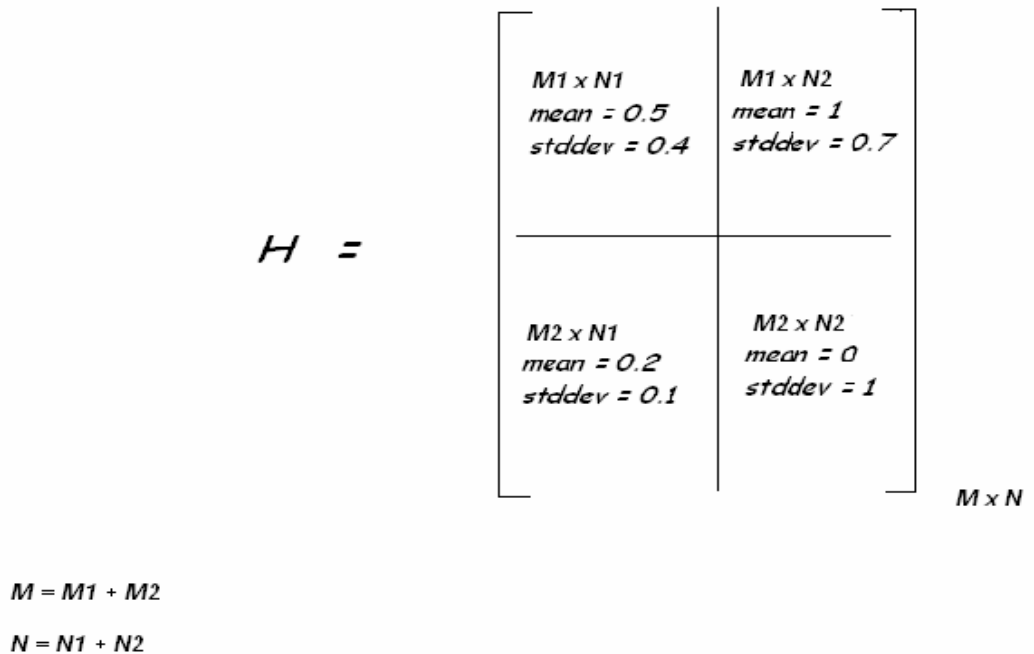


Fig 4.18: Four blocks of the “Varying H-matrices” with different mean and different standard deviations.

Each element in this kind of \mathbf{H} -matrices has been selected randomly from four different Gaussian distributions having different means and different variances. A single \mathbf{H} matrix of $M \times N$ dimension has been divided into 4 blocks, so that the elements in these blocks can be chosen from Gaussian distributions having different means and different standard deviations. Both the real and imaginary parts have been generated independent of each other and have been joined to form a complex element. All the 4 blocks together make up a single \mathbf{H} matrix. The division of the \mathbf{H} -matrix into different blocks is as shown in the Fig 4.18.

The elements in the first block have been picked randomly from a Gaussian distribution of 0.5 mean and 0.4 standard deviation. The second, third and fourth blocks have elements from Gaussian distributions with means 1, 0.2 and 0 and standard deviations 0.7, 0.1, 1 respectively. All these four blocks have been joined to form one single \mathbf{H} -matrix of dimension $M \times N$. Every target has a corresponding \mathbf{H} -matrix. These \mathbf{H} -matrices for each target has been generated independently.

Therefore, using these new \mathbf{H} -matrices as inputs to Algorithm-1 and Algorithm-2, their performances have been analyzed in the same manner as in the previous section.

4.7.1 Case – 1: ($M=3000$; $N=4$; $T=10$)

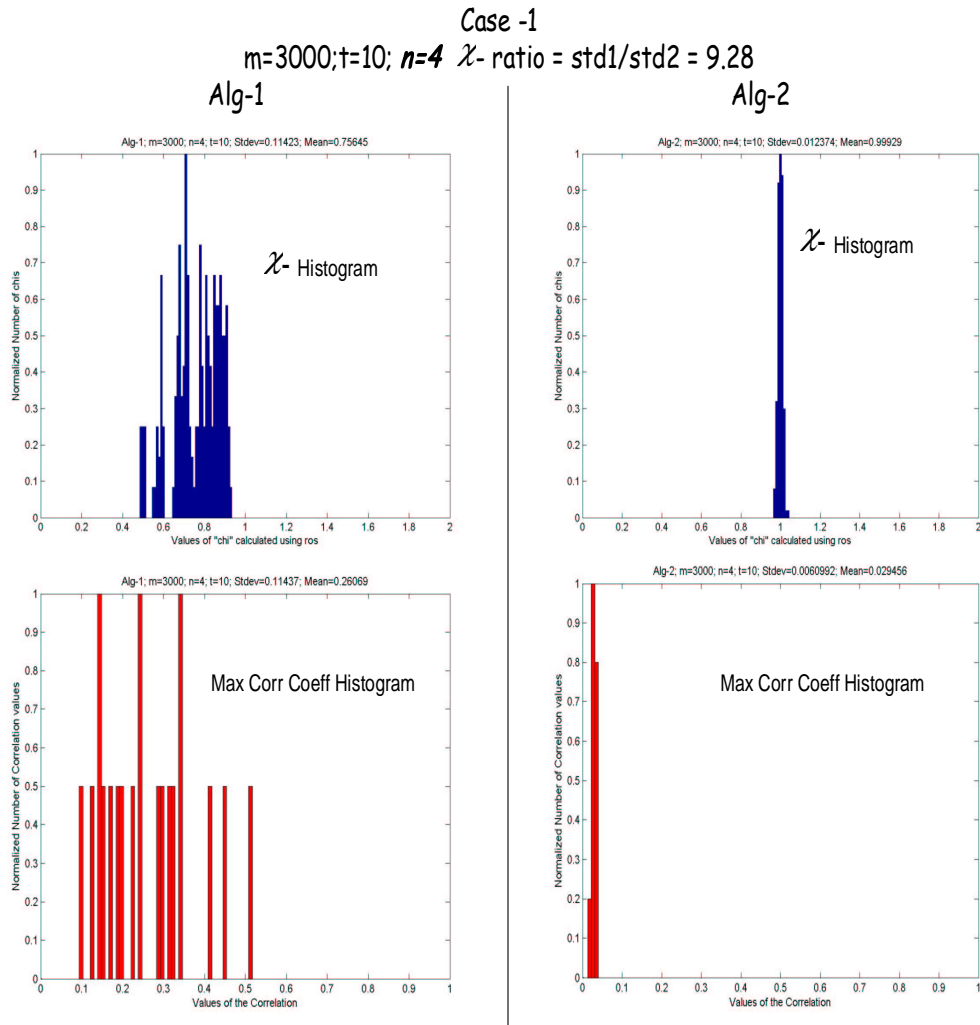


Fig 4.19: Comparison of Histograms of χ and Correlation for Alg-1 and Alg-2 for case-1

In this case, $M=3000$; $N=4$ and $T=10$, the standard deviation of the χ values for Alg-2 is 9.28 times that of Alg-1. The histograms are as shown in Fig 4.19. The ratio of the means of the maximum correlation coefficients for Alg-1 to Alg-2 is 8.85. A significant improvement compared to a similar case of constant- \mathbf{H} matrices. (Matrices with generated from Gaussian distribution of constant mean constant variation).

4.6.2 Case – 2: ($M=1000$; $N=8$; $T=10$)

In this case, the value of M has been decreased from 3000 to 1000 and the value of N increased from 4 to 8. The histograms of Alg-1 and Alg-2 are as shown in Fig 4.20,

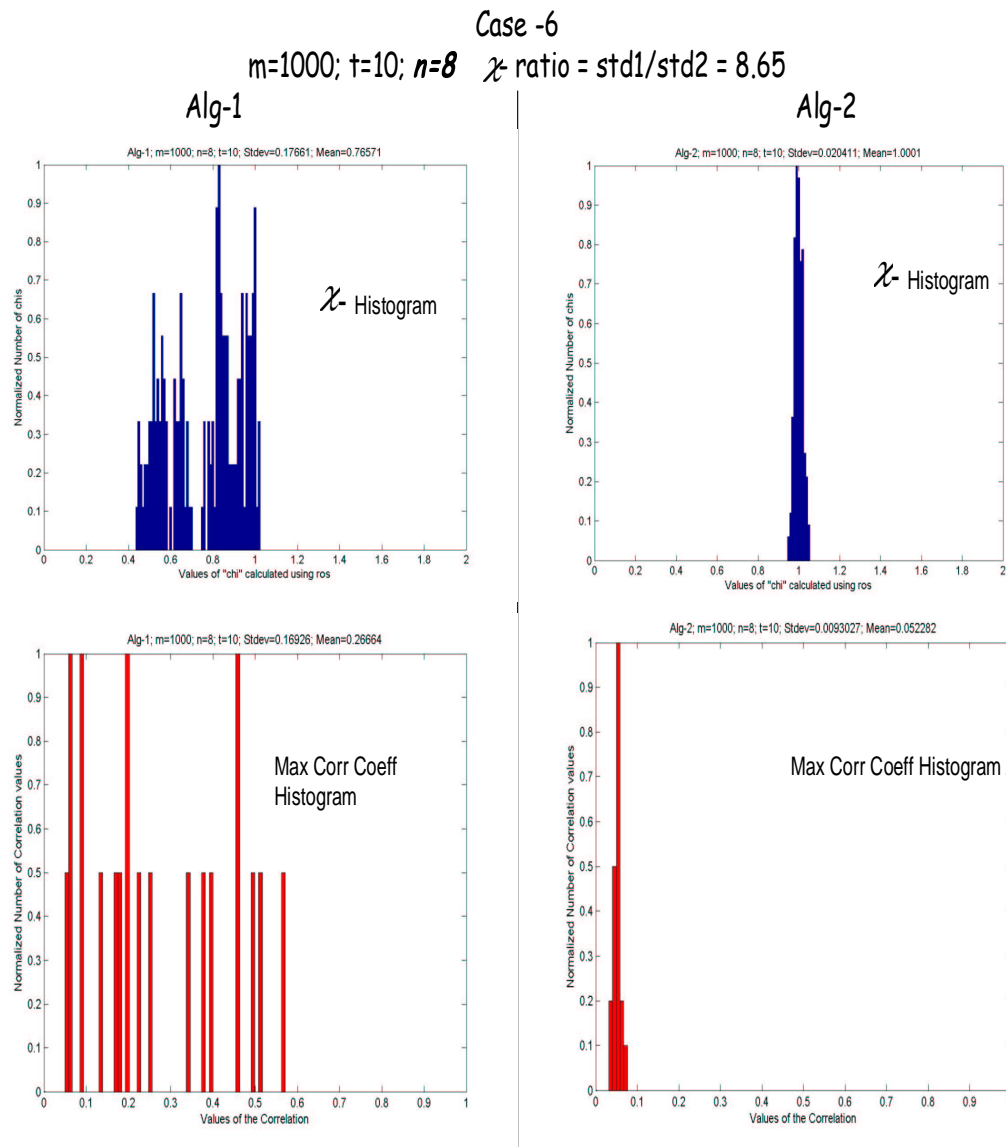


Fig 4.20: Comparison of Histograms of χ and Correlation for Alg-1 and Alg-2 for Case-6

The χ standard deviation ratio of Alg-1 to Alg-2 is 8.65. And the maximum correlation coefficient mean ratio is 5.1

4.6.3 Case – 12: ($M=100$; $N=40$; $T=10$)

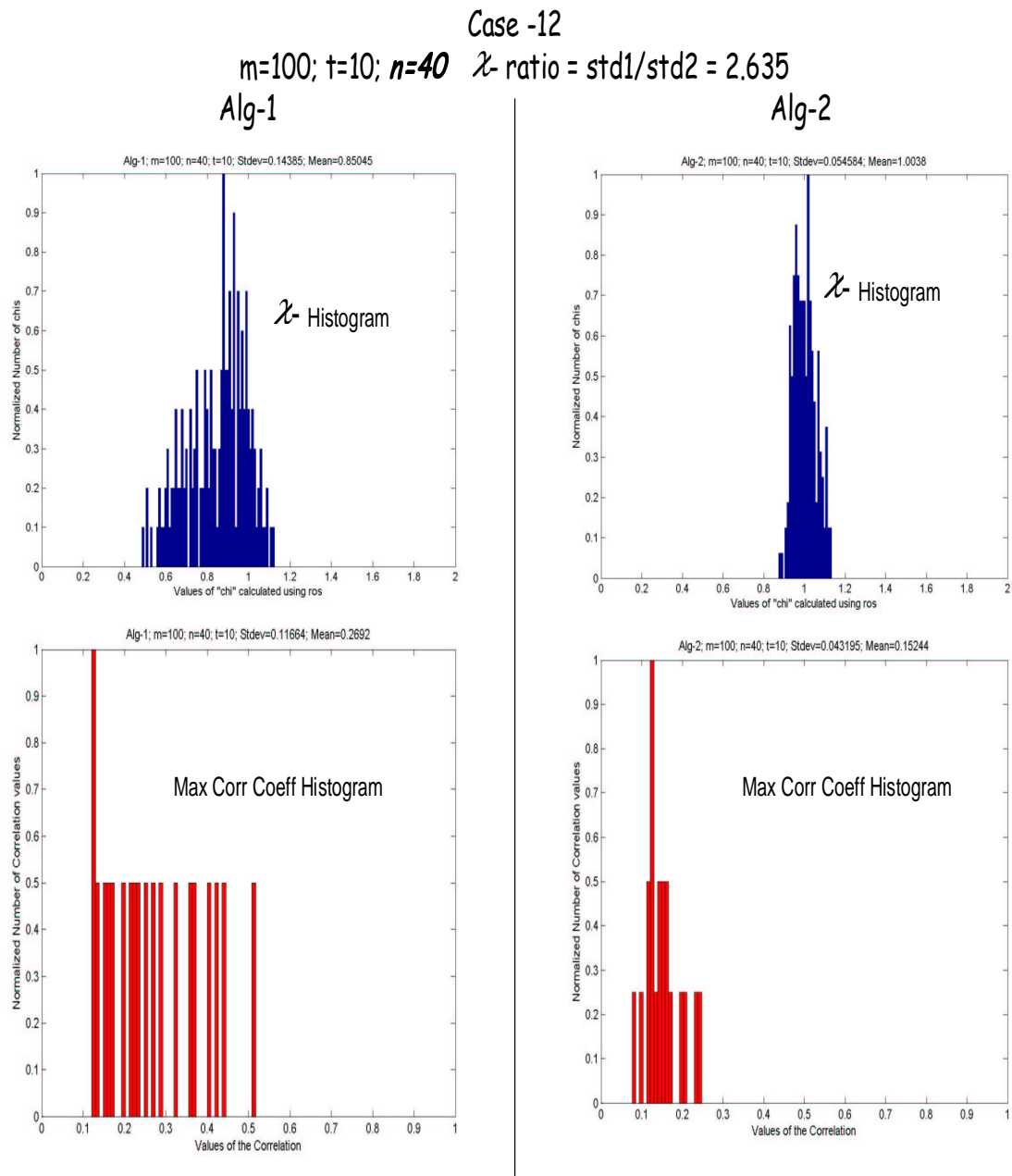


Fig 4.21: Comparison of Histograms of χ and Correlation for Alg-1 and Alg-2 for case-12

In this case, the value of M has been decreased from 1000 to 100 and the value of N has been increased from 8 to 40. The histograms of Alg-1 and Alg-2 are as shown in

Fig 4.21. The χ standard deviation ratio of Alg-1 to Alg-2 is 2.635, and the maximum correlation mean ratio of Alg-1 to Alg-2 is 1.276.

Plots summarizing all the above cases are as shown below,

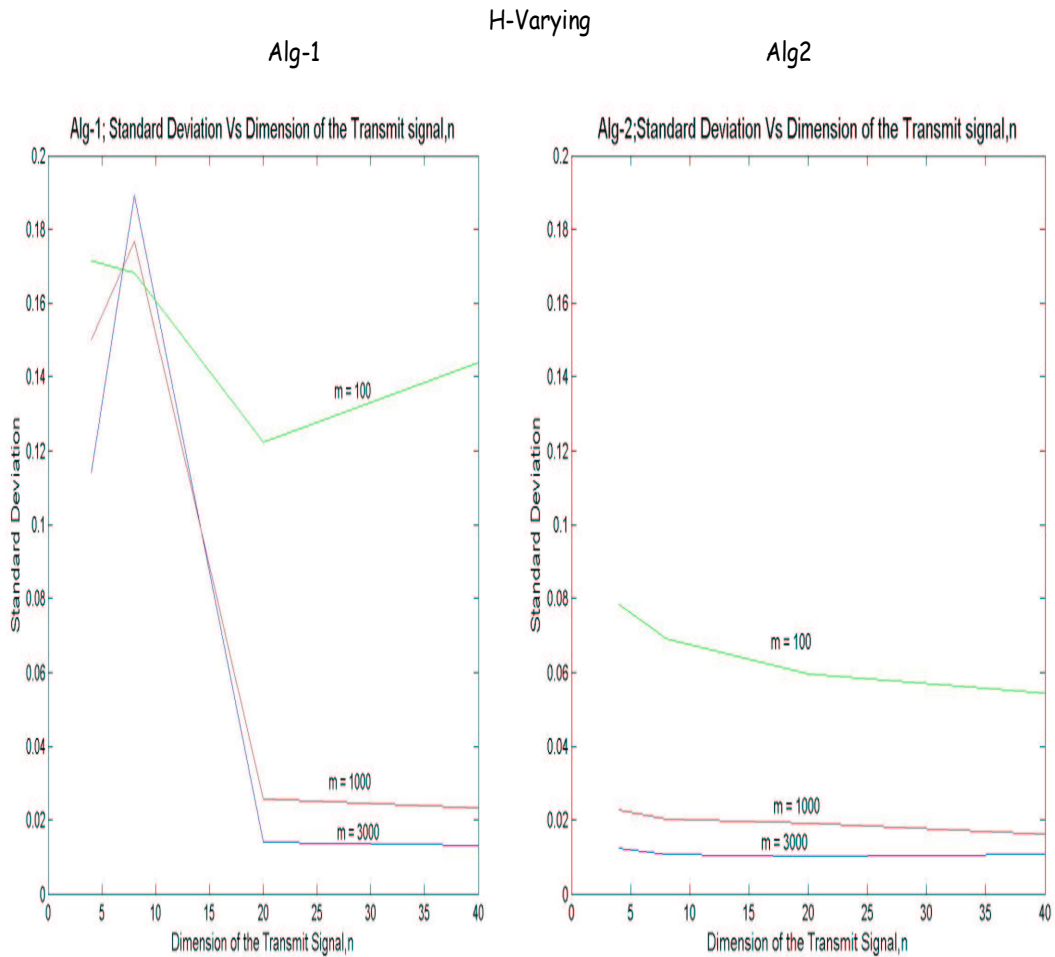


Fig 4:22: Plots of standard deviation of χ with respect to the transmit signal dimension for Alg-1 and Alg-2.

From the Fig 4.22, it has been observed that Alg-2 has much lower χ standard deviations than those of Alg-1, for lower transmit signal dimensions, however, both

the Algorithms give approximately the same standard deviations for large number of measurements (M) and higher number of transmit signal dimensions (N).

Plots showing the variation in mean with respect to the transmit signal dimension is as shown below.

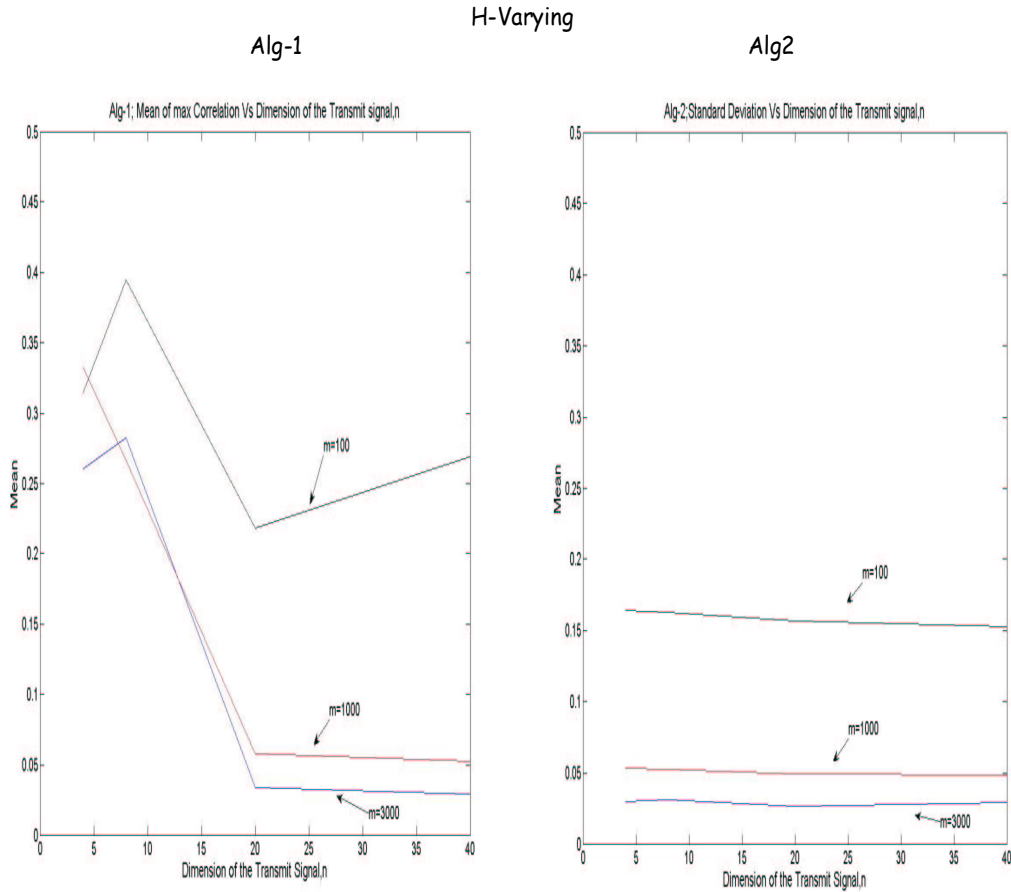


Fig 4:23: Plot showing the mean of max correlation with respect to the transmit signal dimension for Alg-1 and Alg-2.

From Fig 4.23, it is very clear that Alg-2 provides much lower maximum correlations than Alg-1 for low transmit signal dimensions, where as they give almost the same results for higher number of measurements and higher transmit signal dimensions.

Therefore, from all the above cases in this section, we conclude that, when varying- \mathbf{H} matrices (\mathbf{H} -matrices generated from different Gaussian distribution) are used, there is a significant improvement in the performance of Algorithm-2 compared to Algorithm-1 in terms of standard deviation of χ -values and means of the maximum correlations coefficients for low transmit signal dimensions. However, both the Algorithms give approximately same results when there are a high number of measurements (M) and high number of transmit signal dimensions (N).

From all the cases in both the sections, that is, for constant \mathbf{H} -matrices and varying- \mathbf{H} matrices, the conclusions made are as follows.

- 1) Higher the total number of measurements (M) and higher the total number of dimensions of the transmit signal (N), better is the performance of both the Algorithms.
- 2) For \mathbf{H} matrices generated from a single Gaussian distribution, it is very difficult to say which Algorithm performs better, as, both the Algorithms give approximately same results (Standard Deviations of χ - values and Means of the maximum correlation coefficients) for the same values of M , N and T .
- 3) For \mathbf{H} matrices generated from different Gaussian distributions having different means and different variances, there is a significant improvement in the performance of Algorithm-2 compared to Algorithm-1 in terms of standard deviation of χ -values and means of the maximum correlation coefficients for low transmit signal dimensions. However, both the Algorithms give approximately same results when high number of

measurements (M) and high number of transmit signal dimensions (N) are used.

Hence, as the performance of Algorithm-2 is either same or better than that of Algorithm-1 for all the cases that have been discussed, Algorithm-2 is considered as a better and effective algorithm and will be used in all the future experiments in this study. Therefore, it is very clear from the above discussion that the performance of Algorithm-2 not only depends on the total number of measurements (M), the number of dimensions of the transmit signal (N) and the total number of targets (T) but also depends on the structure of the H-matrices. Now the only question that remains is, in general, how useful is the solution given by Algorithm-2?

In order to answer this question, we compared the performance of the transmit signal given by Algorithm-2 to the performance of solution given by Genetic Algorithm and randomly generated codes. This comparison will be discussed in the next section.

4.8 Comparison of Algorithm-2 solution with Genetic Algorithm Solution and Randomly Generated Solutions

4.8.1 Genetic Algorithm:

Genetic Algorithm is a process in which, the best solution is derived by first considering a group of possible solutions. Then out of this group, a group of fit solutions is selected and are combined or mutated to come up with a new generation of better solutions. The fitness of a solution is decided by how well the solution satisfies the given criteria of the problem. After the mutation, a new group of fit

solutions is selected out of the second generation of solutions using the criteria to come up with a third generation of more fit solutions. This process is continued till there is no more improvement in the criteria and the fittest of the last generation solutions is considered to be the best solution [11].

In our case, the criteria that was used by the genetic Algorithm was,

$$\beta_t = \frac{|\rho_1' \rho_t|^2}{|\rho_1|^2 |\rho_t|^2} \quad \text{where } t \in \{2,3,4,\dots,T\}$$

where,

$$\rho_i = \mathbf{H}_i \mathbf{s}$$

And we seek a solution \mathbf{s} that minimizes the largest value in the set of values of β_t (Mini-Max solution). The varying-H matrices were generated with $M=100$; $N=8$ and $T=10$ in order to be used by the Genetic Algorithm. The set of β_t value that the Genetic Algorithm came up with using its best solution are as shown in Table-1

T	β_t	Target-6	0.0002
Target-2	0.0001	Target-7	0.0002
Target-3	0.0000	Target-8	0.0002
Target-4	0.0002	Target-9	0.0000
Target-5	0.0011	Target-10	0.0008

Table-1: Table showing the set of β_t values obtained using the code given by Genetic Algorithm.

The maximum β_t value in the above table is 0.0011 corresponding to target-5.

Therefore the genetic Algorithm can minimize the maximum correlation energy between ρ_1 and ρ_t to 0.0011. That is -30 dB.

4.8.3 Randomly Generated Codes

A randomly generated code is used to compute the set of β_t -values. The β_t -values obtained using a randomly generated code is shown in Table-2,

Random Code -1		Random Code -2		Random Code -3	
T	β_t	T	β_t	T	β_t
Target-2	0.1249	Target-2	0.1041	Target-2	0.1662
Target-3	0.0791	Target-3	0.0275	Target-3	0.1387
Target-4	0.0691	Target-4	0.0162	Target-4	0.1202
Target-5	0.0317	Target-5	0.0610	Target-5	0.1119
Target-6	0.0472	Target-6	0.0481	Target-6	0.1716
Target-7	0.1318	Target-7	0.0259	Target-7	0.1957
Target-8	0.0612	Target-8	0.0479	Target-8	0.1459
Target-9	0.0788	Target-9	0.0317	Target-9	0.2026
Target-10	0.0573	Target-10	0.0080	Target-10	0.1178

Table-2: Table showing the set of β_t values obtained using three randomly generated codes.

The maximum β_i value given by Random code-1, Random code-2 and Random code-3 are 0.1318 (-8.6dB), 0.1041 (-9.8dB) and 0.2026(-7dB) respectively.

4.8.3 Algorithm -2:

In order to compare the results of the Genetic Algorithm and Algorithm-2, same set of H-matrices were used as inputs to Algorithm-2 as were used for the Genetic Algorithm. The set of β_i values that the Algorithm solution came up with are as shown in Table-3.

T	β_i	Target-6	0.0003
Target-2	0.0162	Target-7	0.0175
Target-3	0.0021	Target-8	0.0019
Target-4	0.0092	Target-9	0.0057
Target-5	0.0041	Target-10	0.0124

Table-3: Table showing the set of β_i values obtained using the code given by Algorithm-2.

The maximum β_i value in this case is 0.0175, that is, -17.56dB, corresponding to target-7.

Max β_t			
Random Codes	-9dB	-10dB	-7dB
Algorithm-2 Code	-18dB		
Genetic Algorithm Code	-30dB		

Table-3: Table showing Max β_t values obtained using 3 randomly generated codes, Algorithm-2 Code, and Genetic Algorithm Code.

Therefore, Algorithm-2 code is better than a Random Code-1, Random code-2 and Random code-3 by 8.96dB, 7.76dB and 11.56dB respectively and the Genetic Algorithm performs better than Algorithm-2 code by 12dB in terms of the maximum β_t value. Though the genetic Algorithm is better than Algorithm-2, there is no mathematical basis for the functioning of it. Also, the genetic Algorithm takes a huge amount of time to come up with the best solution. For this particular case, it took about 12 hours to come up with the best code, whereas Algorithm-2 gave us the best solution in less than 30 seconds. Therefore, though the genetic Algorithm is better by 12 dB compared to Algorithm-2, it cannot be used in situations where processing time is an important factor.

4.8.3 Comparison with Random Codes:

The performance of the solution given by Algorithm-2 has been compared with codes generated randomly, for different cases of M , N and T . This comparison tells us

whether our Algorithm is actually working as we intended or is giving some random solution. Every element in the random code is generated from a Gaussian distribution of 0 mean and variance 1.

The comparison will be done on the same cases as was done in the previous sections.

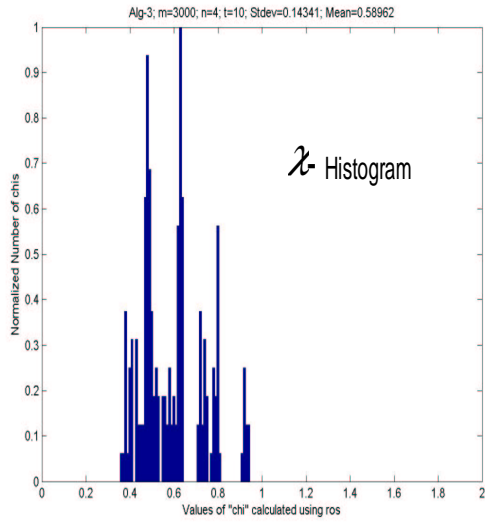
4.8.1.1 Case – 1: ($M=3000$; $N=4$; $T=10$)

The histograms given by the random code and Algorithm-2 code are as shown in Fig 4.23. The χ histogram obtained by using the random code has a very loose bound. Not a single χ -value is equal to 1. Also, the maximum correlation coefficient histogram has very high values. On the other hand, the histogram given by Alg-2 code is very tightly bound and has its mean at 1. The correlation histogram has very low maximum correlation coefficient values. Hence it is very clear from the Fig 4.24 that Alg-2 performs much better than a Random code for this case.

Case -1

$m=3000; t=10; n=4$ λ - ratio = $\text{std3}/\text{std2} = 11.59$

Alg-0



Alg-2

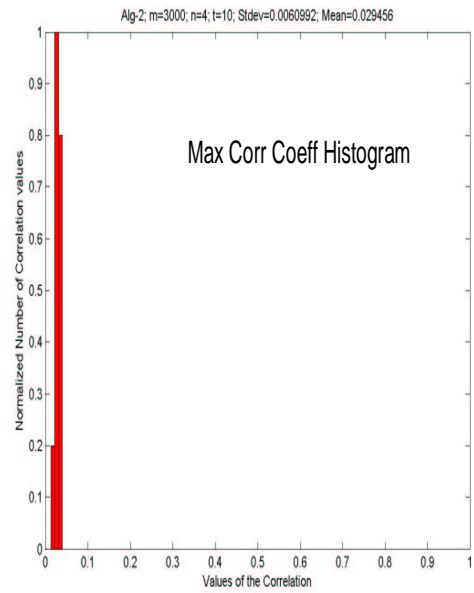
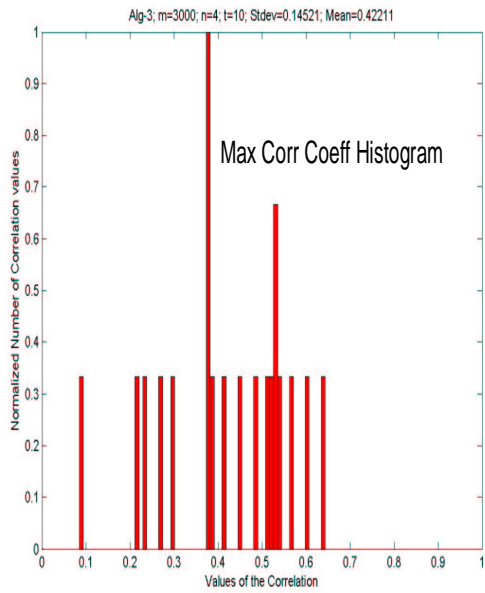
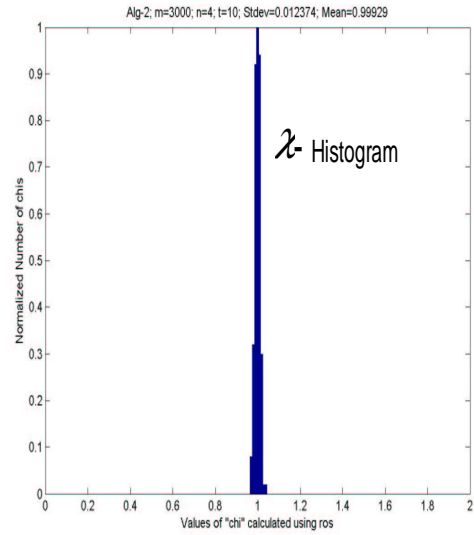


Fig 4.24: Comparison of Histograms of χ and Correlation for Alg-1 and Alg-2 for case-1

4.8.1.2 Case – 6: ($M=1000$; $N=8$; $T=10$)

In this case, the value of M has been decreased from 3000 to 1000 and the value of N has been increased from 4 to 8. The histograms of Alg-2 and Random Code are as shown in Fig 4.25.

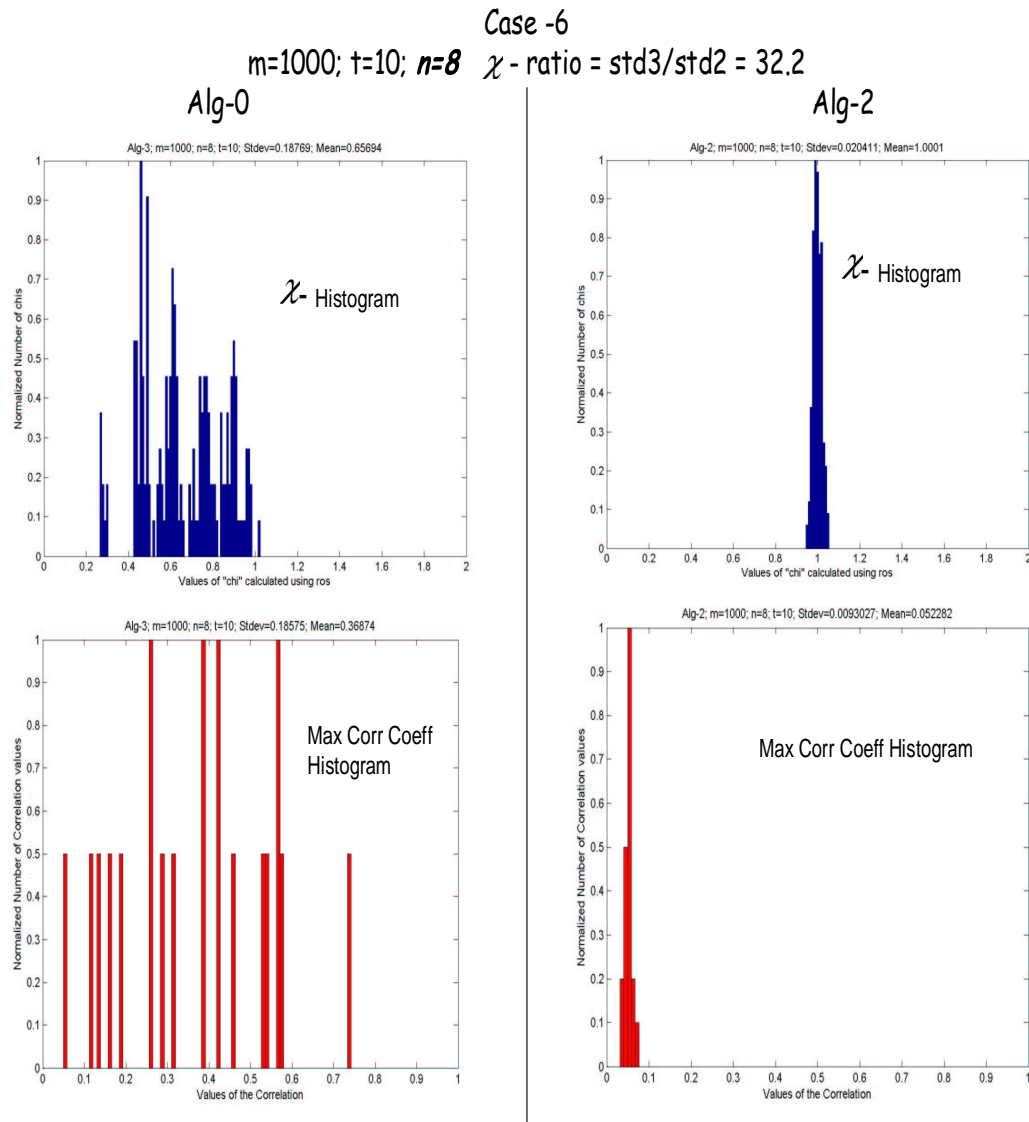


Fig 4.25: Comparison of Histograms of χ and Correlation for Alg-1 and Alg-2 for case 6

Again in terms of the tightness of the χ bound and the maximum correlation coefficient values, solution given by Alg-2 is much better than a randomly picked code.

4.8.1.3 Case – 3: ($M=100$; $N=40$; $T=10$)

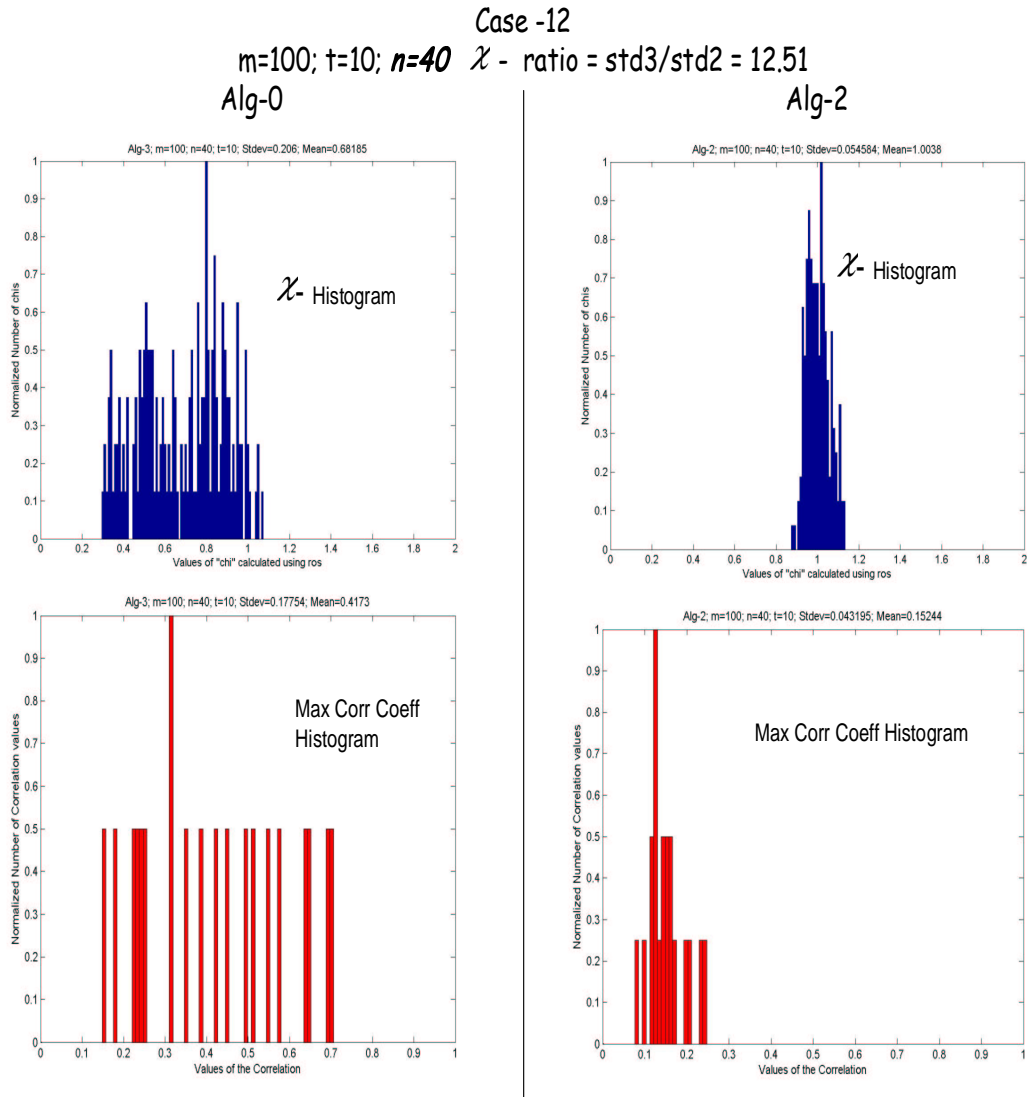


Fig 4.26: Comparison of Histograms of χ and Correlation for Random Code and Alg-2 for case1

In this case, the value of M has been decreased from 1000 to 100 and the value of N has been increased from 8 to 40. The histograms of Alg-2 and Random Code are as shown in Fig 4.26. In this case also, Alg-2 solution is better than a random code.

Therefore from the above cases it can be concluded that Algorithm-2 gives us a much better solution than a randomly generated code, irrespective of M , N and T values.

CHAPTER - 5

5. Simulation of a Radar Model

The results shown previously for the performance of the Algorithms were obtained using the propagation matrices (**H**-matrices) generated randomly from Gaussian distributions. In order to evaluate the performance of Algorithm-2 with results obtained using the propagation matrices that closely resemble the actual physical conditions that the transmit signal would undergo; a physical radar model has been designed that completely represents a side looking Synthetic Aperture Radar model.

The different parts of the radar model are, the space-time transmit signal, the target set and the space-time receive measurements. Each one of them will be discussed in the next few sections.

5.1 Transmit Signal Model

The transmit signal in our model is represented as a set of complex valued samples lying in a multi-dimensional space. This multi-dimensional space consists of temporal subspace as well as spatial subspace. Consequently, the complex valued samples of the transmit signal will have a temporal component as well as a spatial component.

The temporal component of the samples is denoted in time and frequency, thus the total number of dimensions in temporal subspace given by Z_t is 2.

Let K be the total number of transmit temporal samples. These are the transmit samples transmitted at different times and at different frequencies but, by the same

transmit element. Therefore, the temporal position vector of the k -th transmit sample is given in time and frequency as,

$$\bar{z}_k^t = [t_k, \omega_k]^T \quad (5.1)$$

Similarly, the spatial component of the samples are represented in 3 dimensions, i.e, X, Y, and Z directions, hence the total number of dimensions in transmit spatial subspace given by Z_s is 3.

Let J be the total number of samples in the spatial subspace. In other words, the number of samples in the spatial subspace is equal to the number of transmit elements used in the radar model. Each transmit element transmits a sample at a particular time and at a particular frequency, hence, we can have multiple samples transmitted at the same time and at the same frequency but by different transmit elements (differing spatially). Thus, the total number of transmit spatial samples at a given time is equal to the total number transmit elements used in the model.

The spatial position vector of the j -th transmit sample given in 3 coordinate axes is defined as,

$$\bar{z}_j^s = [x_j, y_j, z_j]^T \quad (5.2)$$

Combining both temporal and spatial subspaces, there are a total of $Z = Z_t + Z_s$ dimensions, i.e., 5 in the total subspace.

Hence, the total number of spatial and temporal samples is given by $N = JK$, that is, all the samples transmitted at different times and at different frequencies by different transmit elements.

The overall position vector of the jk -th sample defined in the combined space of temporal and spatial is given by,

$$\bar{z}_{jk} = [x_j, y_j, z_j, t_k, \omega_k]^T \quad (5.3)$$

Where, \bar{z}_{jk} defines the complete position of a transmit sample in both spatial subspace as well as the temporal subspace.

The value of the jk -th complex valued sample can be denoted with respect to its position vector as,

$$s(\bar{z}_{jk}) = s_{jk}$$

All the complex values are arranged into a single complex vector of size $N (J*K) \times 1$ as,

$$\mathbf{s} = [(s_1^s)^T, (s_2^s)^T, (s_3^s)^T, \dots, (s_K^s)^T]^T \quad (5.4)$$

Similarly, the position vectors can be written with 'n' as its index as, $\bar{z}_{jk} = \bar{z}_n$.

Where, the mapping of n, j and k is given by,

$$n = (kJ + j) - J$$

Where, $1 \leq j \leq J$ and $1 \leq k \leq K$

Hence, $1 \leq n \leq N = JK$

The description of the transmit signal discussed before, as a set of complex samples is given in a general form. In our radar model, the transmit signal has been defined as a weighted superposition of a set of wide time width and wide bandwidth orthonormal basis functions. It is then described in terms of a set of complex valued samples obtained by sampling the windowed fourier transformation of every single

pulse. This design of transmit signal as a superposition of different basis functions is as follows.

In general, a real valued transmit signal can be described as,

$$v_s(t) = \text{Re}\{S(t)e^{-j\omega_c t}\} \quad (5.5)$$

where, $S(t) \rightarrow$ Complex function constructed as a weighted superposition of complex basis functions $\psi_{pq}(t)$.

$P \rightarrow$ An odd integer number indicating the total number of slow time functions and p is its index.

$Q \rightarrow$ An odd integer number indicating the total number of fast time functions and q is its index.

$\omega_c \rightarrow$ Real valued carrier frequency in radians given by, ($\omega_c = 2\pi f_c$)

$f_c \rightarrow$ Carrier frequency in (Hz).

The complex basis functions $\psi_{pq}(t)$ are given by,

$$\psi_{pq}(t) = s_p(t) \sum_u f_q(t - uT_o) e^{j\omega_c u T_o} \quad (5.6)$$

where, $T_o \rightarrow$ Signal repetition interval (sec). ($T_o = 1/f_o$)

$f_o \rightarrow$ Signal Repetition Frequency (Hz).

$U \rightarrow$ An odd integer indicating total number of pulses transmitted.

$s_p(t) \rightarrow$ One of the P slow-time functions, each with a narrow bandwidth and

time width T . Each $s_p(t)$ function is denoted by integer p , which

$$\text{ranges from, } -\left(\frac{P-1}{2}\right) \leq p \leq \left(\frac{P-1}{2}\right)$$

$f_q(t) \rightarrow$ One of the Q fast-time functions, each with a narrow time width and

a wide bandwidth B . Each $f_q(t)$ function is denoted by q , which

$$\text{ranges from, } -\left(\frac{Q-1}{2}\right) \leq q \leq \left(\frac{Q-1}{2}\right)$$

A train of U pulses can be denoted by $\sum_u f_q(t - uT_o)e^{j\omega_c uT_o}$. Each pulse in the pulse

train is described by the fast-time function $f_q(t)$. Hence, there is an entire pulse train

for every fast-time function $f_q(t)$.

The pulses are represented by u , where u is an odd integer, ranging from

$$-\left(\frac{U-1}{2}\right) \leq u \leq \left(\frac{U-1}{2}\right)$$

The complex function $S(t)$ is given by,

$$S(t) = \sum_p \sum_q S_{pq} \psi_{pq}(t) \quad (5.7)$$

$$S(t) = \sum_p \sum_q S_{pq} s_p(t) \sum_u f_q(t - uT_o)e^{j\omega_c uT_o} \quad (5.8)$$

where, S_{pq} are the complex weights of the basis functions.

All the fast-time basis functions are derived from a main function called the mother function $g_f(t)$. Each fast-time function $f_q(t)$ is a slightly time delayed version of the mother function.

i.e.
$$f_q(t) = g_f(t - \tau_q) e^{j\omega_c \tau_q} \quad \text{Where, } \tau_q \ll T_o \quad (5.9)$$

Where, τ_q is defined as the time delay used to generate the fast-time basis functions.

Similarly, the slow-time functions are also derived from the mother-function $g_s(t)$.

Each slow-time function is a frequency shifted version of the main mother-function.

As it is a frequency shifted function, the mother function and the slow-time basis function are represented in frequency domain as, $G_s(\omega)$ and $S_p(\omega)$ respectively [13].

The slow-time basis function is given as,

$$S_p(\omega) = G_s(\omega - \omega_p) \quad \text{where, } \omega_p \ll \omega_o \quad (5.10)$$

Where, ω_p is the frequency shift used to generate the slow-time basis functions.

Substituting the above equations of fast-time and slow-time basis functions and taking a windowed fourier transformation, the equation of our transmit signal (5.8) is transformed as,

$$s(uT_o, \omega) = \sum_p g_s(uT_o) e^{ju\omega_p T_o} \sum_q S_{pq} G_f(\omega) e^{-j\omega u T_o} e^{-j(\omega - \omega_c)\tau_q} \quad (5.11)$$

The windowed fourier transform of S(t) is now sampled. After windowing, if the frequency spectrum is sampled at Nyquist rate, then there will be an overall of $2BT$ samples which is much higher than the time-bandwidth product of the windowed signal, BT_o . Hence, the signal needs to be shifted back to uT_o so that the spectrum

can be sampled with higher spacing. This shifting is performed by multiplying the frequency spectrum by $e^{j\omega u T_o}$. Therefore, the Nyquist spacing for the shifted version of the windowed transmit signal is ω_o , however, it was chosen to oversample the spectrum with a spacing of $\omega_o / 2$ between the samples, so that more of the signal can be seen in the time-domain. Hence, there is a total of $\omega = v(\omega_o / 2)$ number of frequency samples where, 'v' is an integer value that varies from

$$-\left(\frac{V-1}{2}\right) \leq v \leq \left(\frac{V-1}{2}\right)$$

Therefore, there are an overall of UV number of complex transmit samples.

Thus, $s(uT_o, \omega)$ can be denoted as s_{uv} and is given by,

$$s_{uv} = \sum_p g_s(uT_o) e^{ju\omega_p T_o} \sum_q S_{pq} G_f\left(\frac{v\omega_o}{2}\right) e^{-j\left(\frac{v\omega_o}{2} - \omega_c\right)\tau_q} \quad (5.12)$$

A new term, ψ_{uv}^{pq} has been defined as,

$$\psi_{uv}^{pq} = g_s(uT_o) e^{ju\omega_p T_o} G_f\left(\frac{v\omega_o}{2}\right) e^{-j\left(\frac{v\omega_o}{2} - \omega_c\right)\tau_q} \quad (5.13)$$

Substituting the above term in (5.12) we have,

$$s_{uv} = \sum_p \sum_q \psi_{uv}^{pq} S_{pq} \quad (5.14)$$

Where, s_{uv} are the total number of temporal-samples of the transmit signal and S_{pq} are the complex weights of PQ number of basis functions. Hence, the complex temporal samples have been successfully written in terms of complex weights of the basis functions defined earlier in this chapter. Now, the Algorithm that has been

developed in this study needs to find the best possible “weights” for the basis functions which will give us the lowest possible correlation between the target of interest and some other target in a target grid.

Reindexing, the samples can be denoted with a single index using the mappings as,

$$p, q \rightarrow r : p, q, \text{ indices are mapped to } r \text{ by, } r = (pQ + q) + \left(\frac{PQ + 1}{2} \right)$$

Range of p , q , and r are given as,

$$\begin{aligned} -\left(\frac{P-1}{2} \right) &\leq p \leq \left(\frac{P-1}{2} \right), \\ -\left(\frac{Q-1}{2} \right) &\leq q \leq \left(\frac{Q-1}{2} \right) \\ 1 &\leq r \leq R = PQ \end{aligned}$$

Similarly, $u, v \rightarrow k : p, q$, indices are mapped to r by, $k = (uV + v) + \left(\frac{UV + 1}{2} \right)$

Range of p , q , and r are given as,

$$\begin{aligned} -\left(\frac{U-1}{2} \right) &\leq u \leq \left(\frac{U-1}{2} \right), \\ -\left(\frac{V-1}{2} \right) &\leq v \leq \left(\frac{V-1}{2} \right) \\ 1 &\leq k \leq K = UV \end{aligned}$$

Therefore, the equation (5.14) can be written in a reindexed form as,

$$s_k = \sum_r \psi_{kr} S_r \quad (5.15)$$

where, s_k is a set of K samples and can be written in a vector form as,

$$\mathbf{s}^t = [s_1, s_2, s_3, \dots, s_k]^T \quad (5.16)$$

S_r is a set of R complex values and can be written in a vector form as,

$$\mathbf{S}^t = [S_1, S_2, S_3, \dots, S_R]^T \quad (5.17)$$

and ψ_{kr} is a matrix of $K \times R$ size give as,

$$\boldsymbol{\Psi} = \begin{bmatrix} \psi_{11} & \psi_{12} & \psi_{13} & \dots & \dots & \dots & \psi_{1R} \\ \psi_{21} & \psi_{22} & \psi_{23} & \dots & \dots & \dots & \psi_{2R} \\ \psi_{31} & \psi_{32} & \psi_{33} & \dots & \dots & \dots & \psi_{3R} \\ \vdots & & \ddots & & & & \\ \vdots & & & \ddots & & & \\ \vdots & & & & \ddots & & \\ \psi_{K1} & \psi_{K2} & \psi_{K3} & & & & \psi_{KK} \end{bmatrix} \quad (5.18)$$

The superscript ‘ t ’ indicates the temporal subspace.

Using the above representation of the samples, the model equation (5.15) can be written as,

$$\mathbf{s}^t = \boldsymbol{\Psi} \mathbf{S}^t \quad (5.19)$$

Equation (5.19) gives us one vector of \mathbf{s}^t , corresponding to one transmit element. As a space-time transmit signal is being defined, more than one transmit element are to be considered. Let us say there is a total of ‘ J ’ number of transmit elements. Therefore the model equation (5.15) will change to,

$$s_{jk} = \sum_r \psi_{kr} S_{jr} \quad (5.20)$$

$$\mathbf{s}_j^t = \boldsymbol{\Psi} \mathbf{S}_j^t \quad (5.21)$$

Which defines the transmit sample vector for a specific transmit element j .

Including the spatial dimension in our model equation (5.15) we have,

$$\begin{aligned} \mathbf{s}_k^s &= \sum_r \psi_{kr} \mathbf{S}_r^s \\ \mathbf{s}_k^s &= \sum_r \psi_{kr} \mathbf{I}_J \mathbf{S}_r^s \end{aligned} \quad (5.22)$$

Where,

$$\begin{aligned} \mathbf{s}_k^s &= [s_{1k}, s_{2k}, s_{3k}, \dots, s_{Jk}]^T \\ \mathbf{S}_r^s &= [S_{1r}, S_{2r}, S_{3r}, \dots, S_{Jr}]^T \end{aligned}$$

A matrix, \mathbf{D}_{kr}^{ψ} is defined such that $\mathbf{D}_{kr}^{\psi} = \psi_{kr} \mathbf{I}_J$

Therefore, equation (5.22) is transformed into,

$$\mathbf{s}_k^s = \sum_r \mathbf{D}_{kr}^{\psi} \mathbf{S}_r^s \quad (5.23)$$

Another matrix, \mathbf{F}_k is defined such that,

$$\mathbf{F}_k = [\mathbf{D}_{k1}^{\psi}, \mathbf{D}_{k2}^{\psi}, \dots, \mathbf{D}_{kR}^{\psi}]$$

Therefore substituting \mathbf{F}_k in equation (5.23) we have,

$$\mathbf{s}_k^s = \mathbf{F}_k \mathbf{S} \quad (5.24)$$

Finally the model equation (5.24) can be written as,

$$\mathbf{s} = \mathbf{F} \mathbf{S} \quad (5.25)$$

Where,

$$\begin{aligned} \mathbf{F} &= [\mathbf{F}_1, \mathbf{F}_2, \dots, \mathbf{F}_k]^T \\ \mathbf{s} &= [(\mathbf{s}_1^t)^T, (\mathbf{s}_2^t)^T, (\mathbf{s}_3^t)^T, \dots, (\mathbf{s}_J^t)^T]^T \\ \mathbf{S} &= [(\mathbf{S}_1^t)^T, (\mathbf{S}_2^t)^T, (\mathbf{S}_3^t)^T, \dots, (\mathbf{S}_J^t)^T]^T \end{aligned}$$

5.2 Target Model

A total of N_t number of targets lying on the ground was considered to define the target model. These targets lie in a Y dimensional space. Each target has a position vector associated with it and is given by \bar{y}_t . The complex scattering coefficient of each target is given by γ_t , hence there are N_t number of scattering values given by the γ vector as,

$$\gamma = [\gamma_1, \gamma_2, \gamma_3, \dots, \gamma_{N_t}]^T \quad (5.29)$$

Therefore, the entire target model can be described by the position vectors of the targets as well as the complex scattering values.

The arrangement of the target system used in the model will be discussed in the future sections. The above description only gives a general overview of a target system.

5.3 Receiver Measurements

The receiver measurements are described in the same way as the transmit signal. The receive measurements in this model are represented as a set of complex valued samples lying in a multi-dimensional space. This multi-dimensional subspace consists of temporal subspace and spatial subspace. Consequently, the received complex valued samples will have a temporal component as well as a spatial component.

The temporal component of the samples is denoted in time and frequency, therefore, the total number of dimensions in temporal subspace given by X_t is 2.

Let K' be the total number of receive temporal samples. These are the receive samples received at different times and at different frequencies but by the same receive element.

Therefore, the temporal position vector of the k' -th receive sample is given in time and frequency as,

$$\bar{x}_{k'}^t = [t_{k'}, \omega_{k'}]^T \quad (5.30)$$

Similarly, the spatial component of the samples are represented in 3 dimensions, i.e., X, Y, and Z directions, hence the total number of dimensions in receive spatial subspace given by X_s is 3.

Let ' T ' be the total number of receive samples in the spatial subspace. In other words the number of samples in the spatial subspace is equal to the number of receive elements used in the radar model. Each receive element receives a sample at a particular time and at a particular frequency, hence we can have multiple samples received at the same time and at the same frequency but by different receive elements (differ spatially). Therefore, the overall spatial samples is equal to the total number of receive elements used in the model.

Thus, the spatial position vector of the i -th transmit sample given in 3 coordinate axes is defined as,

$$\bar{x}_i^s = [x_i, y_i, z_i]^T \quad (5.31)$$

Combining both temporal and spatial subspaces, there are a total of $X = X_t + X_s$ dimensions, i.e., 5 in the combined subspace.

Hence, the total number of spatial and temporal samples is given by $M = IK'$, that is, all the samples received at different times, at different frequencies by different receive elements.

The overall position vector of the ik' -th sample defined in the combined space of temporal and spatial subspaces is given by,

$$\bar{x}_{ik'} = [x_i, y_i, z_i, t_{k'}, \omega_{k'}]^T \quad (5.31)$$

Where, $\bar{x}_{ik'}$ defines the complete position of a receive sample in both spatial subspace as well as the temporal subspace.

The value of the ik' -th complex valued sample can be denoted with respect to its position vector as,

$$r(\bar{x}_{ik'}) = r_{ik'}$$

The complex values are arranged into a single complex vector of size $M(I*K') \times 1$ as,

$$r = [(r_1^s)^T, (r_2^s)^T, (r_3^s)^T, \dots, (r_K^s)^T]^T \quad (5.32)$$

Similarly, the position vectors can also be written with 'm' as their index as,

$$\bar{x}_{ik'} = \bar{x}_m$$

Where, the mapping of m , i and k' is given by,

$$m = (k'I + i) - I$$

where, $1 \leq i \leq I$ and $1 \leq k' \leq K'$

hence, $1 \leq m \leq M = IK'$

5.4 Model Equations

From Chapter-2, Equation (2.4) gives the relation between the received signal vector \mathbf{r} to the transmit signal vector \mathbf{s} and the scattering value vector $\boldsymbol{\gamma}$ as,

$$\mathbf{r} = \sum_t \gamma_t \mathbf{H}_t \mathbf{s} + \mathbf{n} \quad (5.33)$$

Where, \mathbf{n} is an M dimensional complex vector representing random noise.

The most important part of the above relation is the propagation matrix, \mathbf{H}_t which of the dimension M x N. In order to derive the propagation matrix, the following parameters are to be discussed first.

$\overline{\overline{K_\theta}}$ \rightarrow This is a frequency matrix which accounts for the change of phase with respect to the transmitter position, temporal frequency and time. Basically it accounts for the change in phase of the transmit signal as it travels from transmitter to the target. It has a dimension of $Y \times Z$.

$\overline{\overline{K_\phi}}$ \rightarrow This is also a frequency matrix which accounts for the change in phase of the signal from the target to the receiver. It's a $Y \times X$ dimension vector.

$g_h^t(k', k : t)$ \rightarrow It's a complex weighting function that relates the temporal samples of the transmit signal to the temporal receive samples for a given target 't'. We will be discussing more about the kind of weighting function used in the model in the future section.

$g_{hJ}^s(j, t) \rightarrow$ It's again a complex weighting function that weights the spatial transmit samples. It can be viewed as a transmit antenna pattern that corresponds to beam shaping or antenna tapering characteristic.

$g_{hI}^s(i, t) \rightarrow$ A complex weighting function that weights the spatial receive samples. It can be viewed as a receive antenna pattern that corresponds to beam shaping or antenna tapering characteristic.

The \mathbf{H}_t matrix is described as an $M \times N$ dimensional matrix given by,

$$\mathbf{H}_t^{mn} = g_h(m, n : t) e^{-j\bar{x}_m^s T \bar{K}_\phi^s T \bar{y}_t} e^{-j\bar{y}_t T \bar{K}_\theta^s z_n^s} e^{-j\bar{y}_t T (\bar{K}_\phi^t + \bar{K}_\theta^t) z_n^t} \quad (5.34)$$

Separating the above expression into temporal and spatial parts using various mappings described above as,

$$H_t^{mn} = g_h^s(i, j : t) e^{-j\bar{x}_m^s T \bar{K}_\phi^s T \bar{y}_t} e^{-j\bar{y}_t T \bar{K}_\theta^s z_n^s} g_h^t(k', k : t) e^{-j\bar{y}_t T (\bar{K}_\phi^t + \bar{K}_\theta^t) z_n^t} \quad (5.35)$$

Where,

$$g_h(m, n : t) = g_h^s(k', i; k, j : t) = g_h^s(i, j : t) g_h^t(k', k : t) \quad (5.36)$$

Therefore the temporal part is given by a $K' \times K$ matrix as,

$$\mathbf{H}_t^t = \mathbf{H}_{k'k}^t = g_h^t(k', k : t) e^{-j\bar{y}_t T (\bar{K}_\phi^t + \bar{K}_\theta^t) z_n^t} \quad (5.37)$$

and the spatial part is given as a matrix of $I \times J$ dimension as,

$$\mathbf{H}_t^s = \mathbf{H}_{ij}^s = g_h^s(i, j : t) e^{-j\bar{x}_m^s T \bar{K}_\phi^s T \bar{y}_t} e^{-j\bar{y}_t T \bar{K}_\theta^s z_n^s} \quad (5.38)$$

The combined \mathbf{H}_t matrix can be written as,

$$\mathbf{H}_t = \mathbf{H}_t^t \otimes \mathbf{H}_t^s \quad (5.39)$$

(where, \otimes denotes a Kronecker product)

Hence from the equation (2.7) we know that the response vector of target 't' is given by,

$$\boldsymbol{\rho}_t = \mathbf{H}_t \mathbf{s} \quad (5.40)$$

Also, using the transmit signal model equation, in which the transmit signal has been described to be a weighted superposition of orthonormal basis functions. Hence from equation (5.25) we have,

$$\mathbf{s} = \mathbf{F} \mathbf{S} \quad (5.41)$$

Where, \mathbf{s} is an N dimensional vector containing the transmit signal space-time samples and \mathbf{S} is a W - dimensional transmit weight vector that gives the weights for the transmit signal basis functions.

Substituting \mathbf{s} in the above equation we have,

$$\begin{aligned} \boldsymbol{\rho}_t &= \mathbf{H}_t \mathbf{F} \mathbf{S} \\ \boldsymbol{\rho}_t &= \mathbf{H}_t' \mathbf{S} \end{aligned} \quad (5.42)$$

Where,
$$\mathbf{H}_t' = \mathbf{H}_t \mathbf{F} = \mathbf{H}_t (\boldsymbol{\psi} \otimes \mathbf{I}_j) \quad (5.43)$$

Hence, the propagation matrices i.e., \mathbf{H}_t matrices, that give the relation between the response vectors and the transmit signal samples, have been converted to \mathbf{H}_t' matrices that relate the response vectors to the weight vector of the basis functions of the transmit signal.

5.5 Default values used in the Radar Model

Let us consider a radar system which is flying at an altitude ' h ' with a velocity ' v ' in the x -direction. Let the radar be looking at a target grid of $N_x \times N_y$, and the center of the target is located at $x = 0$; $y = Y_0$. The radar setup is as shown in Fig 5.1.

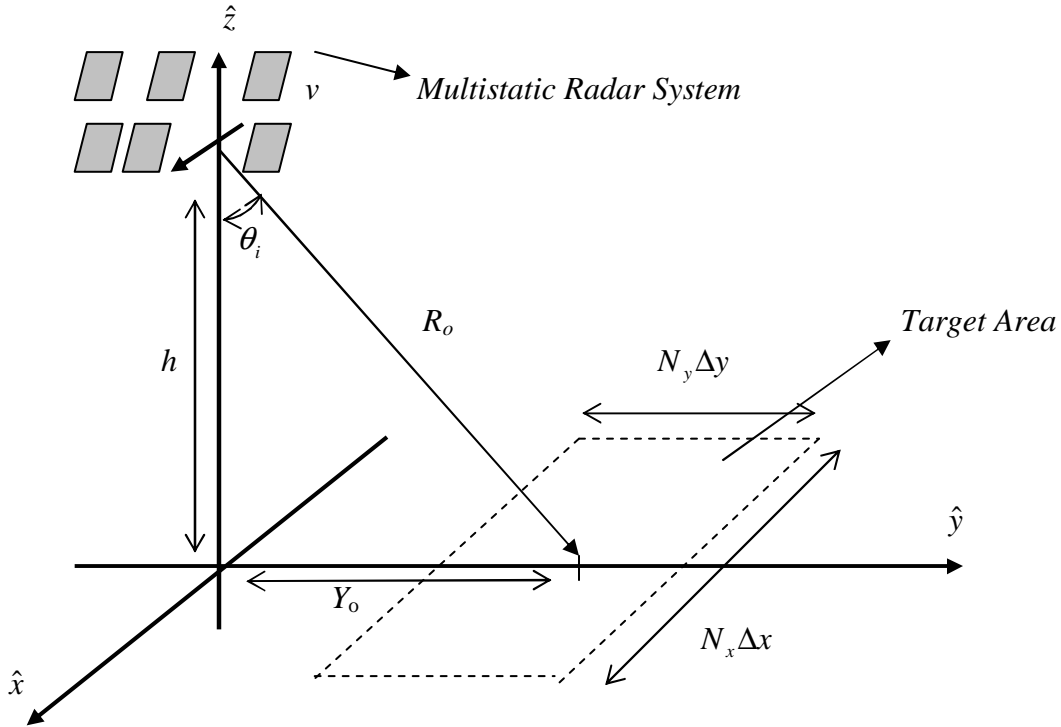


Fig 5.1: Multistatic Synthetic Aperture Radar System

- **Transmit temporal position vectors** – The transmit temporal position vector has been defined to be in a two dimensional space of time and frequency as,

$$\bar{z}_k^t = [t_k, \omega_k]^T \quad (5.44)$$

As discussed before, the frequency domain of a single pulse of the transmit signal is sampled at a rate of $(\omega_0/2)$, hence there are a total of V frequency samples

spaced $\omega_o / 2$ apart and a total of U samples in the time domain spaced T_o distance apart. Therefore, the transmit element position vector can be written as,

$$\bar{z}_k^t = [uT_o, v(\omega_o / 2)]^T \quad (5.45)$$

Where, the mapping of k , u , and v are given as,

$$k = (uV + v) + \left(\frac{UV + 1}{2} \right)$$

- **Receive Temporal Position vectors** – Similar to the transmit temporal position vectors, the received position vectors also lie in a two dimensional space of time and frequency and is given by,

$$\bar{x}_k^t = [t_{k'}, \omega_{k'}]^T \quad (5.46)$$

A receive window of duration $-T_o \leq t \leq T_o$ has been used for the complex weighting function defined by $g_h^t(k', k : t)$ that weights the receive samples accordingly. The frequency spectrum of this window has been sampled using the Nyquiste criteria, resulting in frequency samples placed ω_o distance apart. Therefore, there are a total of V' receive frequency samples and a total of U' time samples corresponding to U' received pulses. Hence, the receive position vector can be defined as,

$$\bar{x}_k^t = [u'T_o, v'\omega_o]^T \quad (5.47)$$

Where, $-\left(\frac{U'-1}{2}\right) \leq u' \leq \left(\frac{U'-1}{2}\right)$, $-\left(\frac{V'-1}{2}\right) \leq v' \leq \left(\frac{V'-1}{2}\right)$

$$k' = (u'V' + v') + \left(\frac{U'V' + 1}{2} \right), 1 \leq k' \leq K' = U'V'$$

Now, we define relations between, the total number of transmit pulses U , the total number of receive pulses U' , the total number of transmit frequency samples V and the total number of receive frequency samples V' as,

$U' = U + 2$ -- The model has been designed in such a way that the receiver receives two pulses more than the number of pulses actually transmitted.

$V' = \frac{V-1}{2}$ or $V' = \frac{V+1}{2}$ -- Based on the sampling rates of windowed transmit signal spectrum and response signal spectrum, it is very clear that the total number of receive frequency samples are approximately half of the total number of transmitted frequency samples.

- **Target Position vectors** – The target position vector have been defined to be in a four dimensional subspace. In those four dimensions, three dimensions correspond to X, Y, and Z directions, where, the targets lie in the X-Y plane and Z corresponds to the height of the targets. The other dimension corresponds to the velocity of the target. The target position vectors have been defined as,

$$\bar{y}_t = [n_x \Delta x, n_y \Delta y, z_t, v_t]^T \quad (5.48)$$

Where, $-\left(\frac{N_x-1}{2}\right) \leq n_x \leq \left(\frac{N_x-1}{2}\right)$ and $-\left(\frac{N_y-1}{2}\right) \leq n_y \leq \left(\frac{N_y-1}{2}\right)$

Where, N_x and N_y are the total number of targets in X and Y axis respectively.

The mapping of n_x, n_y and t is shown as,

$$t = (n_x N_y + n_y) + \left(\frac{N_x N_y + 1}{2} \right) \quad \text{Where, } 1 \leq t \leq N_x N_y$$

- **Temporal Complex Weighting function** – The temporal complex function has been defined as a function that weights and relates transmit temporal samples to receive temporal samples.

It can also be seen as a receive window that has a time width of $-T_o \leq t \leq T_o$, and windows the receive pulse. This weighting function is such that for targets below the center target in a target grid, it includes energy not only from a particular receive pulse corresponding to a particular transmit pulse; it also includes the energy from the pulse transmitted before that particular pulse. Similarly for targets above the center target, it includes energy from a particular pulse as well as energy from the pulse transmitted after the particular pulse. This weighting is function as,

$$g_h^t(k', k : t) = g_h^t(u', v'; u, v : n_x, n_y)$$

$$\begin{aligned}
g_h^t(u', v'; u, v : n_x, n_y) = & \\
& \frac{1. \sin\left(\frac{\pi(2v'-v)}{2}\right)}{V. \sin\left(\frac{\pi(2v'-v)}{V}\right)} [\delta(u'-u) + e^{+jv\pi} \delta(u'-u-1)] \Rightarrow \text{for } -n_y > 0 \\
& \frac{1. \sin\left(\frac{\pi(2v'-v)}{2}\right)}{V. \sin\left(\frac{\pi(2v'-v)}{V}\right)} \delta(u'-u) \Rightarrow \text{for } -n_y = 0
\end{aligned} \tag{5.49}$$

$$\frac{1 \cdot \sin\left(\frac{\pi(2v'-v)}{2}\right)}{V \cdot \sin\left(\frac{\pi(2v'-v)}{V}\right)} [\delta(u'-u) + e^{+jv\pi} \delta(u'-u+1)] \Rightarrow \text{for } -n_y < 0$$

where, $\delta(t) = 1$ for $u = 0$ and $\delta(t) = 0$ for $u \neq 0$

$$\frac{1 \cdot \sin\left(\frac{\pi(2v'-v)}{2}\right)}{V \cdot \sin\left(\frac{\pi(2v'-v)}{V}\right)} = 1/2 \text{ for } 2v' = v \quad (5.50)$$

$$\frac{1 \cdot \sin\left(\frac{\pi(2v'-v)}{2}\right)}{V \cdot \sin\left(\frac{\pi(2v'-v)}{V}\right)} = \frac{1 \cdot \sin\left(\frac{\pi(2v'-v)}{2}\right)}{V \cdot \sin\left(\frac{\pi(2v'-v)}{V}\right)} \text{ for } 2v' \neq v \quad (5.51)$$

- **Spatial complex weighting function** – As stated before, the spatial complex functions weight the spatial receive samples. This function has been set as 1 in the model, which means there are no weights attached to the spatial samples.

$$g_{hl}^s(i, t) = g_{hj}^s(j, t) = 1$$

- $\overline{\overline{K}}_\theta$ and $\overline{\overline{K}}_\phi$ - The frequency matrices $\overline{\overline{K}}_\theta$ and $\overline{\overline{K}}_\phi$ are defined as,

$$\overline{\overline{K}}_\theta = \frac{\omega_c}{c} \begin{bmatrix} \frac{-1}{R_o} & 0 & 0 & \frac{-v}{R_o} & 0 \\ 0 & \frac{-h^2}{R_o^3} & \frac{-hY_o}{R_o^3} & 0 & \frac{Y_o}{\omega_c R_o} \\ 0 & \frac{-hY_o}{R_o^3} & \frac{-Y_o^2}{R_o^3} & 0 & \frac{-h}{\omega_c R_o} \\ 0 & 0 & 0 & 0 & -1 \end{bmatrix} \quad (5.52)$$

Separating the spatial part and the temporal part we have,

$$\overline{\overline{K}}_{\theta}^s = \frac{\omega_c}{c} \begin{bmatrix} \frac{-1}{R_o} & 0 & 0 \\ 0 & \frac{-h^2}{R_o^3} & \frac{-hY_o}{R_o^3} \\ 0 & \frac{-hY_o}{R_o^3} & \frac{-Y_o^2}{R_o^3} \\ 0 & 0 & 0 \end{bmatrix} \quad \overline{\overline{K}}_{\theta}^t = \frac{\omega_c}{c} \begin{bmatrix} \frac{-v}{R_o} & 0 \\ 0 & \frac{Y_o}{\omega_c R_o} \\ 0 & \frac{-h}{\omega_c R_o} \\ 0 & -1 \end{bmatrix}$$

Similarly, $\overline{\overline{K}}_{\phi}$ is defined as,

$$\overline{\overline{K}}_{\phi} = \frac{\omega_c}{c} \begin{bmatrix} \frac{-1}{R_o} & 0 & 0 & \frac{-v}{R_o} & 0 \\ 0 & \frac{-h^2}{R_o^3} & \frac{-hY_o}{R_o^3} & 0 & \frac{Y_o}{\omega_c R_o} \\ 0 & \frac{-hY_o}{R_o^3} & \frac{-Y_o^2}{R_o^3} & 0 & \frac{-h}{\omega_c R_o} \\ 0 & 0 & 0 & 0 & -1 \end{bmatrix} \quad (5.53)$$

$$\overline{\overline{K}}_{\phi}^s = \frac{\omega_c}{c} \begin{bmatrix} \frac{-1}{R_o} & 0 & 0 \\ 0 & \frac{-h^2}{R_o^3} & \frac{-hY_o}{R_o^3} \\ 0 & \frac{-hY_o}{R_o^3} & \frac{-Y_o^2}{R_o^3} \\ 0 & 0 & 0 \end{bmatrix} \quad \overline{\overline{K}}_{\phi}^t = \frac{\omega_c}{c} \begin{bmatrix} \frac{-v}{R_o} & 0 \\ 0 & \frac{Y_o}{\omega_c R_o} \\ 0 & \frac{-h}{\omega_c R_o} \\ 0 & -1 \end{bmatrix}$$

(For more information on the derivation of these frequency matrices, please refer the reference [3])

- **Target Spacing** – Targets are spaced one resolution cell apart in the model.

The resolution in the Doppler direction is given by [14],

$$\Delta x = \frac{cR_o}{2UT_o v f_c} \quad (5.54)$$

And the resolution in the range directions is given by,

$$\Delta y = \frac{cR_o}{2BY_o}. \quad (5.55)$$

(The description of the Radar Model has been taken from references [14])

5.6 Numerical Values for the Model

The numerical values of the various parameters used in the model have been derived by applying several constraints on to the model. One such constraint is that the resolutions along the along-track axis and the cross-track axis have been made equal. From this constraint we can derive expressions for bandwidth B and total time width T as,

$$B = \sqrt{\frac{N_x N_y v f_c}{\beta Y_o}} \quad (5.56)$$

and

$$T = \sqrt{\frac{N_x N_y Y_o}{\beta v f_c}} \quad (5.57)$$

Where, β is the ratio of total number of targets to the product of time and bandwidth and is given as,

$$\beta = \frac{N_x N_y}{BT} \quad (5.58)$$

The expressions for U and V have can also be derived from the above constraint as,

$$U = \frac{N_x}{\sqrt{\beta}} \quad (5.579)$$

and
$$V = \frac{2N_y}{\sqrt{\beta}} \quad (5.60)$$

From the discussion in previous sections, we know that,

$$T_o = \frac{T}{U} \quad (5.61)$$

Also, the fast time function delay has been set as, $\tau_q = \frac{q}{B}$ (5.62)

And the slow-time function frequency shift is defined as, $\omega_p = 2\pi\left(\frac{p}{T}\right)$ (5.63)

Since the total number of samples received, must be greater than the total number of targets, to have an unambiguous image, we can say that the total number of receive elements must be greater than β . i.e.,

$$I > \beta = \frac{N_x N_y}{BT} \quad (5.64)$$

A term η has been defined, which gives the ratio of the beam width of the radar to the spatial resolution. This term helps in defining the spatial extent of the receive elements, given by L_x .

$$\eta = \frac{\Delta x_s}{\Delta x} \quad (5.65)$$

where, Δx_s is the main beam width given by,

$$\Delta x_s = \frac{cR_o}{f_c L_x} \quad (5.66)$$

Therefore, the spatial extent of the receive elements is given by,

$$L_x = \frac{cR_o}{f_c \eta \Delta x} \quad (5.67)$$

Numerical Values:

Following are the numerical values that have been given as inputs to the Algorithm.

These values resemble closely the parameters of a low-orbit radar would have.

The values of β and η are assumed as,

$$\beta = 4.2$$

$$\eta = 5$$

$$N_x = N_y = 31$$

Therefore, the derived values are,

$$B = 3.123 \times 10^5 \text{ Hz}$$

$$T = 7.327 \times 10^{-4} \text{ s}$$

$$T_o = 4.844 \times 10^{-5} \text{ s}$$

$$U = 15$$

$$V = 31$$

$$f_o = 2.065 \times 10^4 \text{ Hz}$$

$$\text{del}_x = \text{del}_y = 679.3 \text{ m}$$

$$L_x = 2.286 \text{ m}$$

Using all the numerical values mentioned in this section as inputs to the Algorithm, the complex propagation matrices (\mathbf{H}' -matrices) are obtained for every single target in the target grid.

Hence, these \mathbf{H}' - matrices are used as inputs to our Algorithm to derive an optimal space-time signal. The performance of Algorithm-2 with the new model will be analyzed in the subsequent chapters.

CHAPTER - 6

6. Analysis of Algorithm-2 using the Radar Model

A radar model has been designed as discussed in the previous chapter. This chapter evaluates the performance of Algorithm-2 using inputs to the algorithm from the radar model. It answers various questions on the performance of the Algorithm based on the variation of the total number of basis functions. It has been found that as the total number of basis functions are increased, the chances of the Algorithm coming up with a best code also increases. This poses a question as to how far can the total number of basis functions can be increased? An upper limit on the total number of basis functions is also derived in this chapter. It has also been shown that as the total number of transmit elements are increased from 1 to 2, the performance of the algorithm improves, but the ambiguity plot ceases to remain invariant. Also, a comparison of the final code given by the Algorithm with a randomly generated code has been done, which gives us an idea about the efficacy of the final result given by the Algorithm.

6.1 Performance Analysis of Algorithm-2 with the Radar Model

Having designed the model, the numerical values discussed in the previous chapter have been used as inputs to the model. A 31×31 grid i.e., $N_x=31$ and $N_y=31$, has been chosen for the analysis of the algorithm performance as it closely resembles a practical physical model. Also, having a bigger grid would require huge amount of processing time and system memory. Thus, substituting the numerical values, the \mathbf{H} '

matrices are generated for every single target on the grid. These \mathbf{H}' matrices are then used as inputs to the Algorithm. Ideally, all the \mathbf{H}' - matrices corresponding to all the targets should be used as inputs to the algorithm. But based on observations made on the performance of the model, only the \mathbf{H}' matrices corresponding to the targets on the Cross-Track Axis are used.

The observations made were,

- 1) The Ambiguity function for a standard transmit signal is symmetric about along track and cross track axis. Hence, the targets lying only in one quadrant can be considered rather than all the four quadrants of the grid. This would speed up the process of finding the best code.
- 2) The Ambiguity function of a space-time signal transmitted using one transmit element is invariant of the target of interest. That is no matter which target we consider as the target of interest in the grid, we would get the same ambiguity pattern with respect to that particular target.
- 3) The model has an error in generating the \mathbf{H}' matrices for the targets along the Along Track Axis.

Hence, in view of the above observations, only the targets along the cross-track axis in the grid have been considered. For these targets, the performance of the algorithm for different values of P and Q has been analyzed.

For all the following cases shown in the next few sections, the total number of transmit elements used is 1 i.e., $J=1$ and the total number of receive elements used are 15 i.e., $I=15$. The total number of P s and Q s are varied over the several cases shown.

6.1.1 Case-1($P=1$; $Q=1$; $J=1$):

The total number of slow-time functions ' P ' is set to 1 and the total number of fast-time functions ' Q ' is also set to 1.

The Ambiguity (Correlation) plots obtained using the transmit code generated by the Algorithm are as shown in Fig 6.1

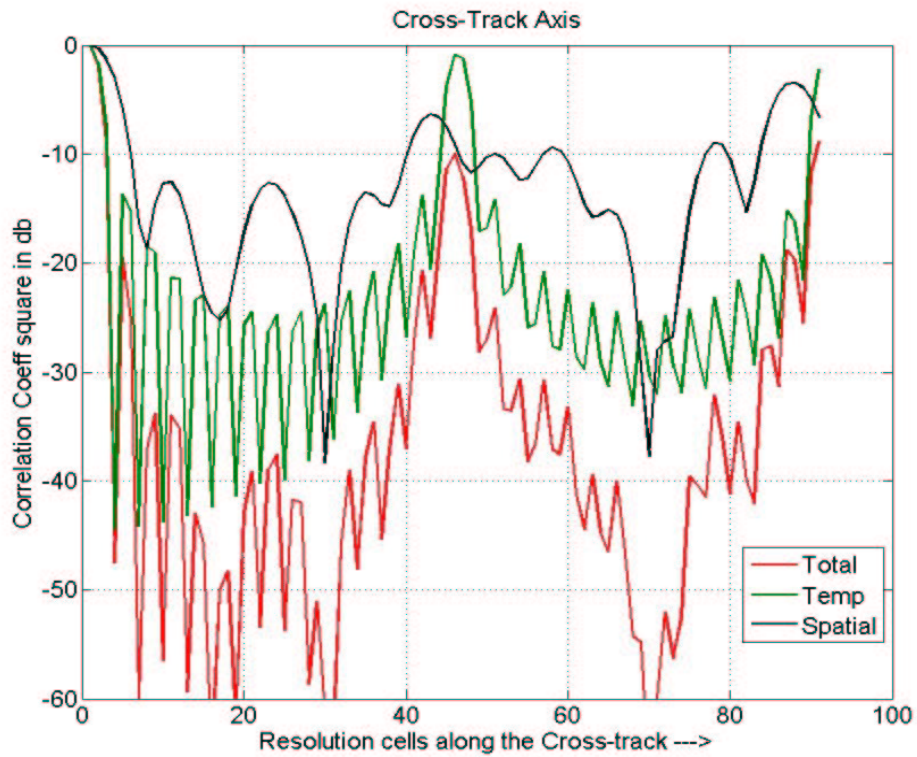


Fig 6.1: Spatial, Total and Temporal Ambiguity plot along the Cross Track axis for $P=1$; $Q=1$.

The green plot in Fig 6.1 indicates the Temporal ambiguity plot which conveys by how much the maximum correlation is reduced when only the temporal aspect of the transmit signal is considered. Since P and Q are equal to 1, the algorithm does not

have much freedom to find the best code. Hence, the maximum temporal ambiguity is down only by 1dB. The black plot shows the spatial ambiguity plot along the cross-track axis. Furthermore, when the temporal and spatial plots are added in dB, the total ambiguity pattern is obtained in dB which is indicated by the red curve in the figure. From Fig 6.1 we can see that the total maximum correlation has been lowered by 9dB.

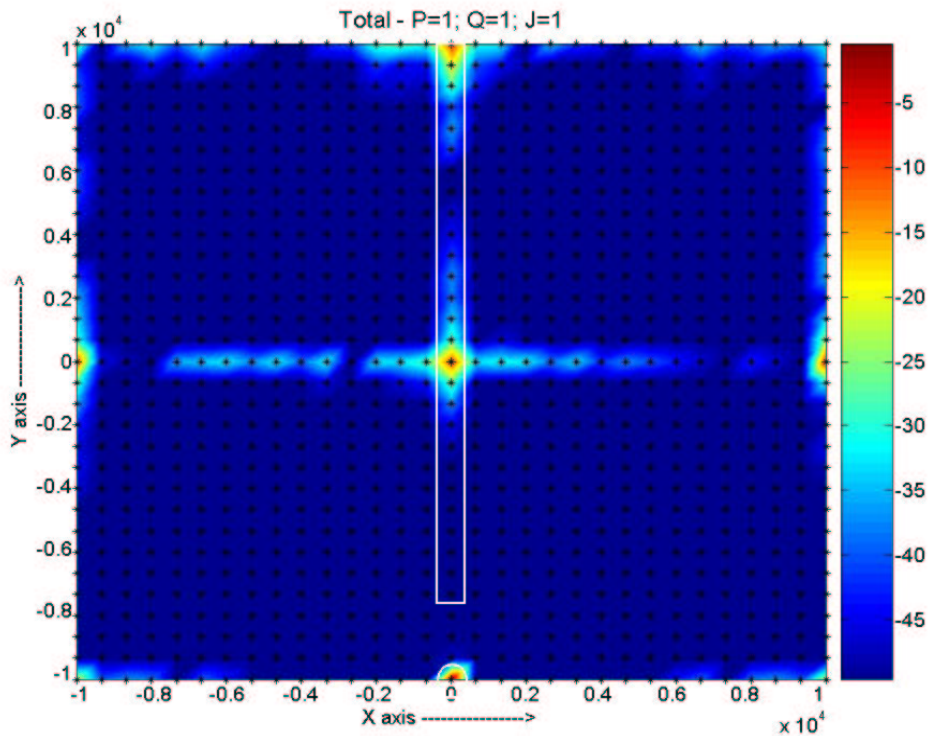


Fig 6.2: A 2-D plot of the correlation of the target of interest and all the targets in the grid (2-D ambiguity plot) for $P=1$; $Q=1$.

Fig 6.2 shows the correlation of the main target of interest with all other targets in the grid, obtained using the transmit signal given by the Algorithm. The targets in the rectangular box are the targets on which the algorithm has worked and the target in the circle is the target of interest. Red color in the above plot, indicates a very high

correlation, where as the dark blue color indicates very low correlation. The bright spots along the corners and the center of the grid indicate Doppler and Range ambiguities. An ideal two dimensional plot should have a red spot on the target of interest, which indicates a high correlation of the target with itself and dark blue color everywhere else.

6.1.2 Case 2 ($P=3; Q=3; J=1$):

In this case, the total number of slow-time functions, P is set to 3 and the total number of fast-time functions, Q is also set to 3.

The Ambiguity (Correlation) plot obtained by using the transmit code generated by the Algorithm is as shown in Fig 6.3.

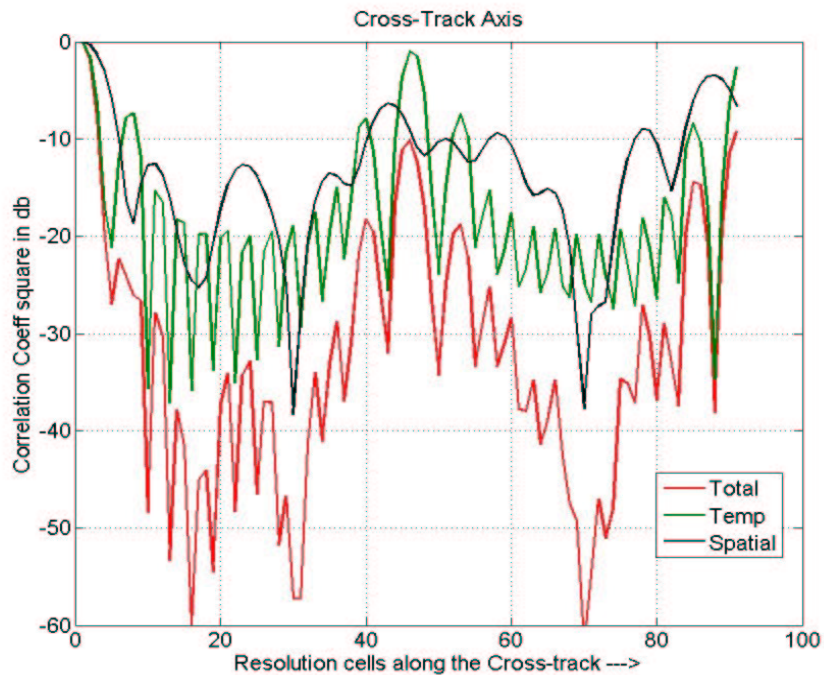


Fig 6.3: Spatial, Total and Temporal Ambiguity plot along the Cross Track axis for $P=3; Q=3$.

As can be seen from the fig. 6.3, the total ambiguity plot has a maximum total correlation of -10dB which indicates that there has not been much of an improvement when compared to a case of $P=1$ and $Q=1$. Improvement will be noticed as P and Q further increased. The 2-D plot of this case is as shown in Fig 6.4.

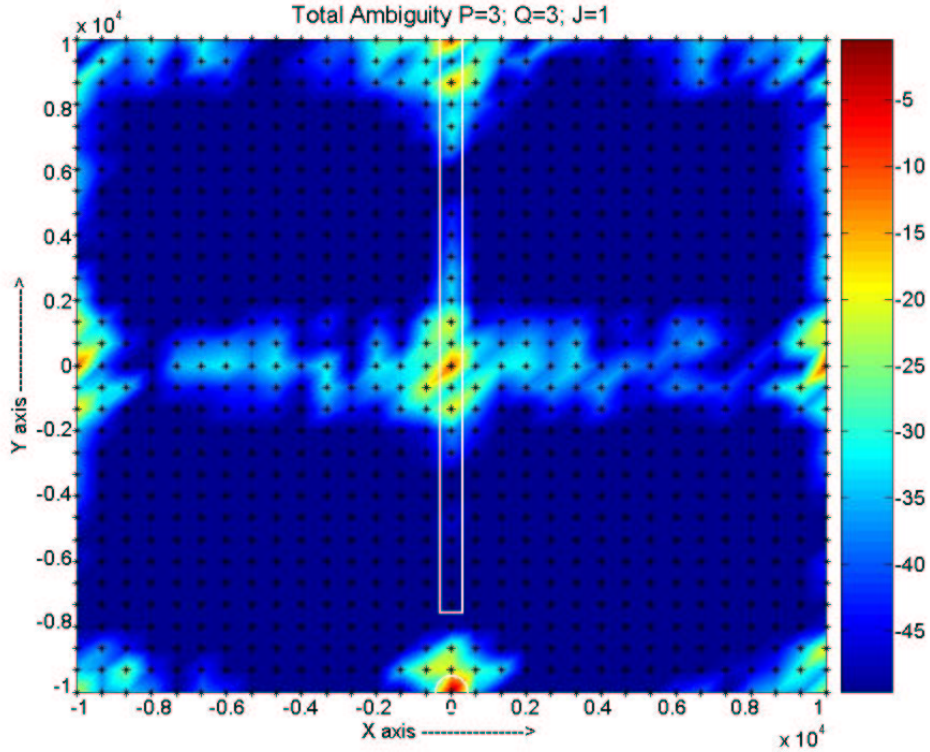


Fig 6.4: A 2-D plot of the correlation of the target of interest and all the targets in the grid (2-D ambiguity plot) for $P=3$; $Q=3$.

6.1.3 Case 3 ($P=5$; $Q=5$; $J=1$):

The total number of slow-time functions, P is set to 5 and the total number of fast-time functions, Q is also set to 5.

The Ambiguity (Correlation) plots obtained by using the transmit code generated by the Algorithm are as shown in Fig 6.5 and Fig 6.6.

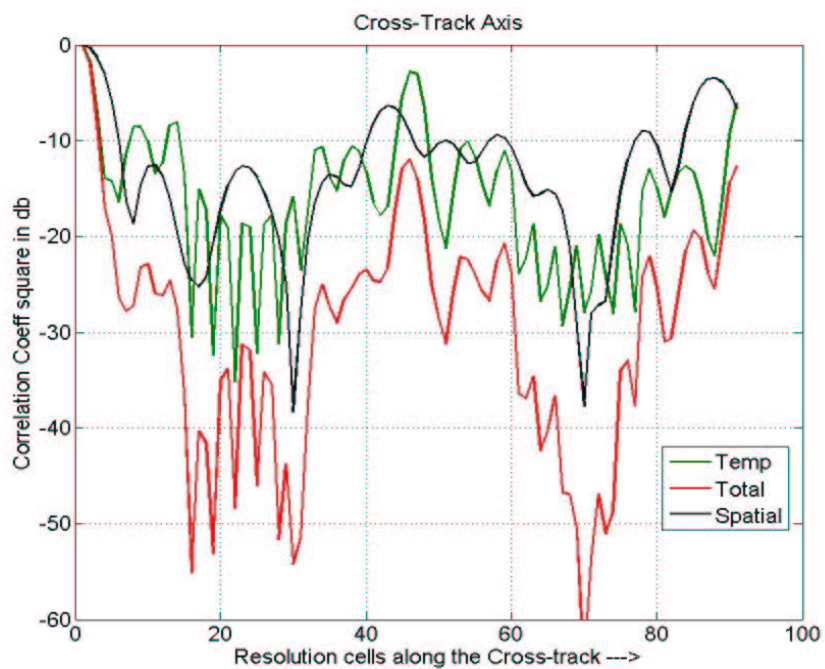


Fig 6.5: Spatial, Total and Temporal Ambiguity plot along the Cross Track axis for $P=5; Q=5$.

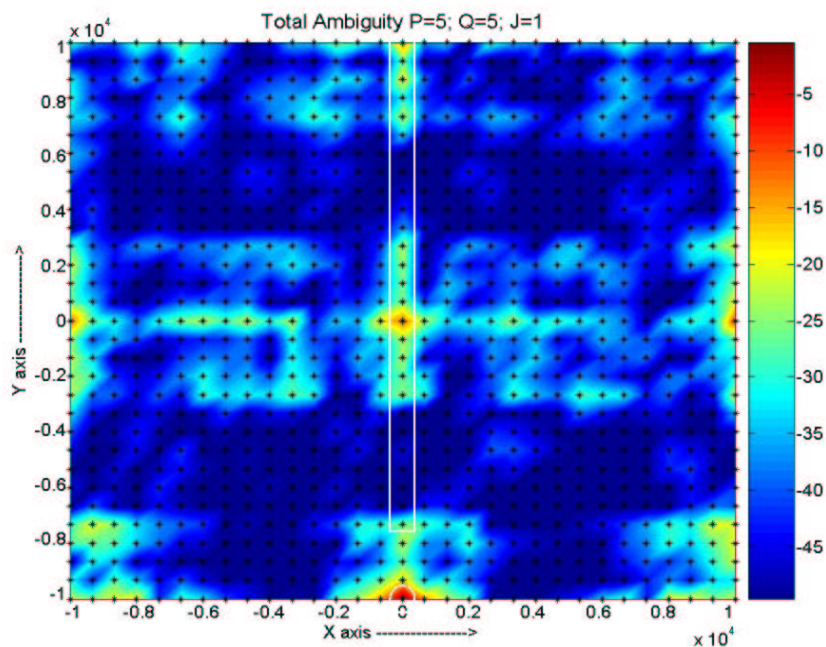


Fig 6.6: A 2-D plot of the correlation of the target of interest and all the targets in the grid (2-D ambiguity plot) for $P=5; Q=5$.

In this case, the maximum total ambiguity is about -12dB which shows an improvement of 3dB when compared to the case where $P=1; Q=1$ and an improvement of 2dB when compared to the case of $P=3; Q=3$.

6.1.4 Case 4 ($P=7; Q=7; J=1$):

The total number of slow-time functions, P is set to 7 and the total number of fast-time functions, Q is also set to 7.

The Ambiguity (Correlation) plots obtained by using the transmit code generated by the Algorithm are as shown in Fig 6.7 and Fig 6.8..

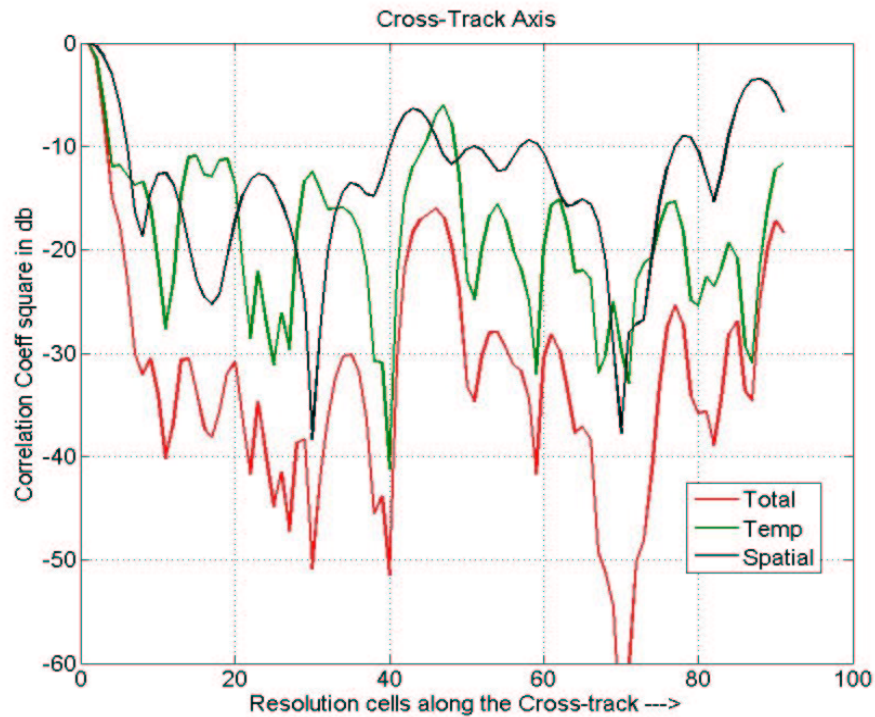


Fig 6.7: Spatial, Total and Temporal Ambiguity plot along the Cross Track axis for $P=7; Q=7$.

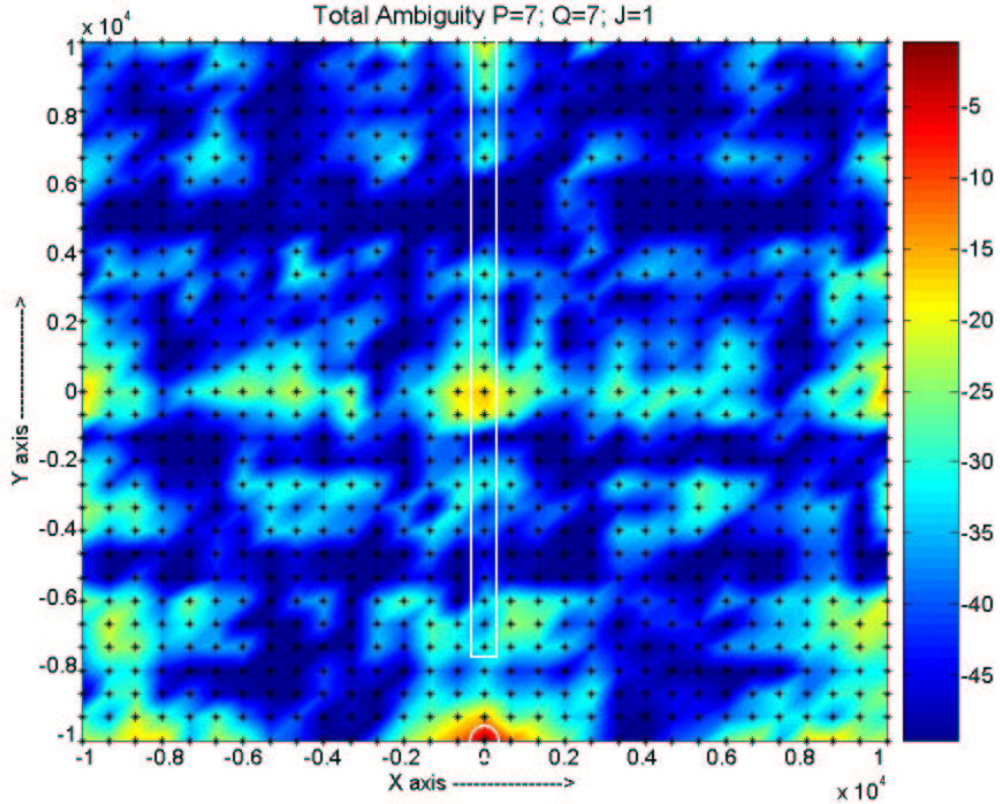


Fig 6.8: A 2-D plot of the correlation of the target of interest and all the targets in the grid (2-D ambiguity plot) for $P=7$; $Q=7$.

In this case the total maximum ambiguity is about -16dB. There is a considerable improvement when compared to the previous cases. This is attributed to the increased dimension of the transmit signal which is given by, $J*P*Q$. In this case, the transmit signal has a dimension of 49, hence the algorithm has a subspace having 49 dimensions to search for the best code, compared to the previous cases, case-1, case-2, and case-3 where the dimensions were 1, 9 and 25 respectively.

6.1.5 Case 5 ($P=9$; $Q=9$; $J=1$):

The total number of slow-time functions, P is set to 9 and the total number of fast-time functions, Q is also set to 9.

The Ambiguity (Correlation) plots obtained by using the transmit code generated by the Algorithm are as shown in Fig 6.9.

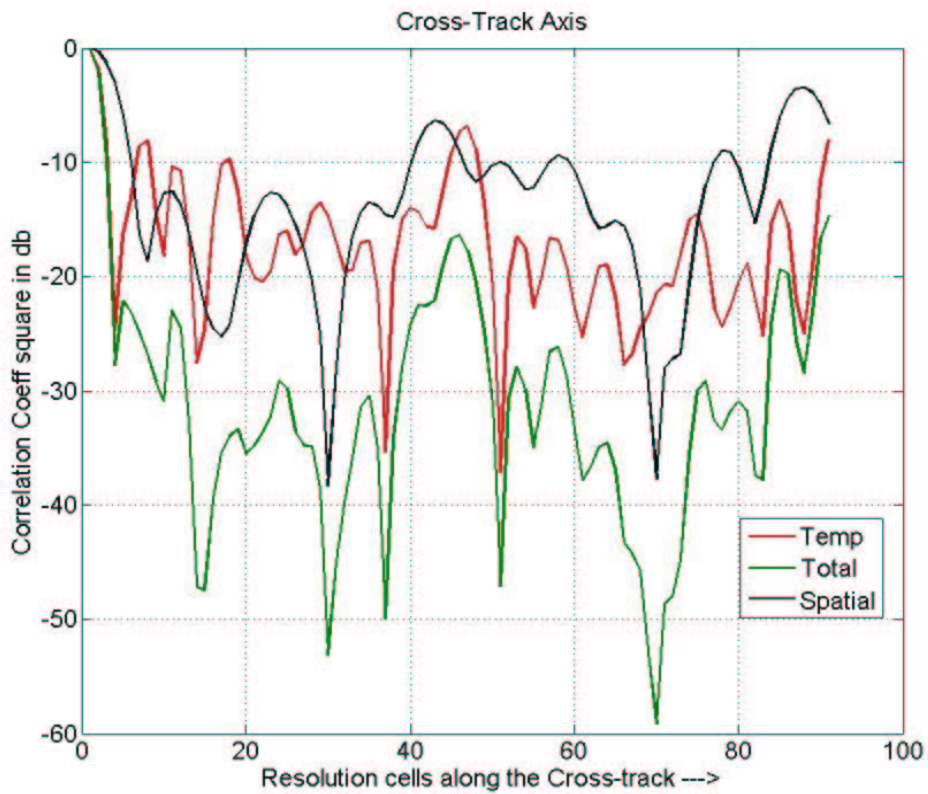


Fig 6.9: Spatial, Total and Temporal Ambiguity plot along the Cross Track axis for $P=9$; $Q=9$

In this case there is not much of an improvement in the total maximum ambiguity as compared to a case where $P=7$ and $Q=7$. It is equal to -15dB.

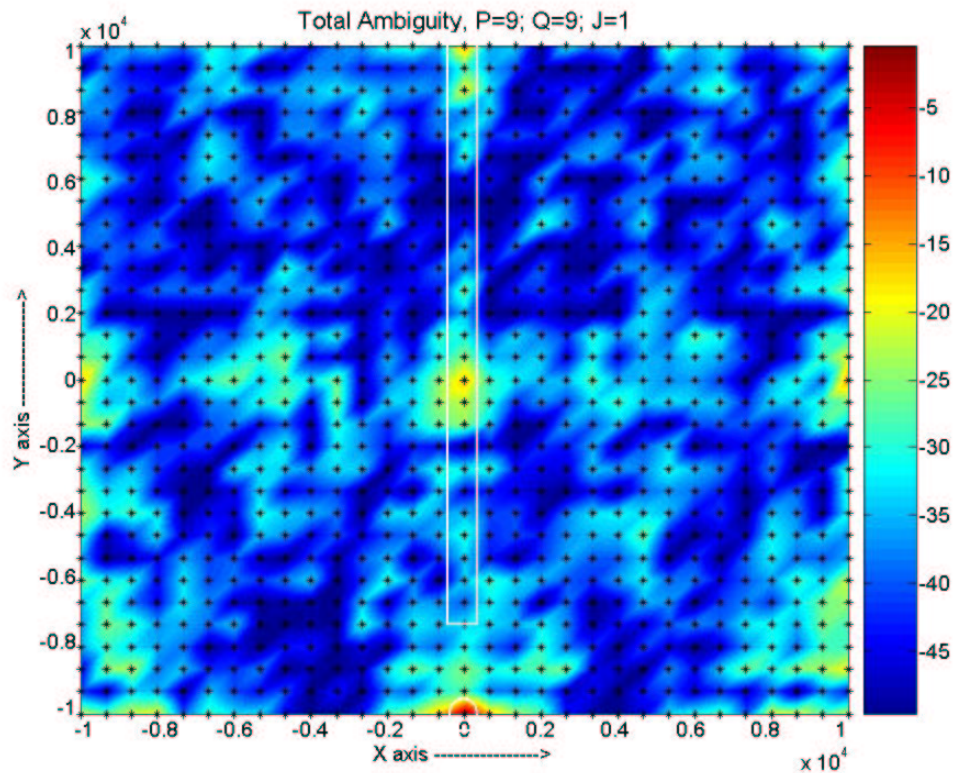


Fig 6.10: A 2-D plot of the correlation of the target of interest and all the targets in the grid (2-D ambiguity plot) for $P=9$; $Q=9$.

6.1.6 Case 6 ($P=11$; $Q=11$; $J=1$):

The total number of slow-time functions, P is set to 11 and the total number of fast-time functions Q , is also set to 11.

The Ambiguity (Correlation) plots obtained by using the transmit code generated by the Algorithm are as shown in Fig 6.11 and Fig 6.12.

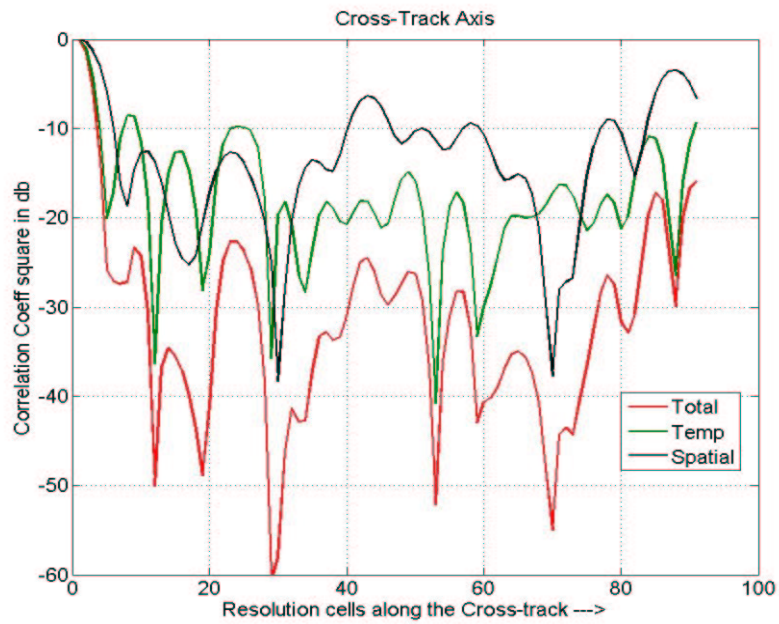


Fig 6.11: Spatial, Total and Temporal Ambiguity plot along the Cross Track axis for $P=11; Q=11$.

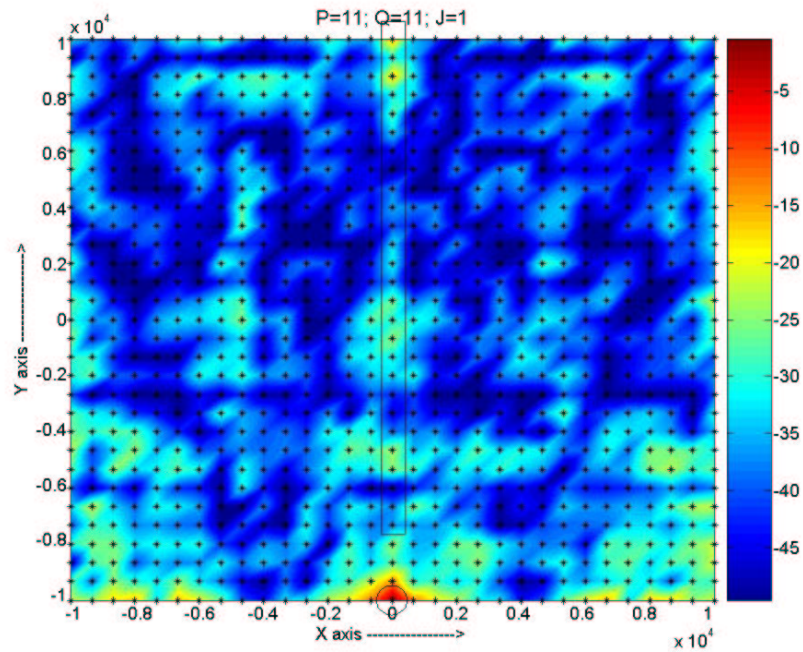


Fig 6.12: A 2-D plot of the correlation of the target of interest and all the targets in the grid (2-D ambiguity plot) for $P=11; Q=11$.

This is the final case that will be discussed for one transmit element. There is a limit on how much the values of P and Q can be increased. This limit will be discussed later in this section. The maximum values that could be assigned to P and Q were $P=11$ and $Q=11$. The maximum total ambiguity for this case is -16dB. An improvement of 7dB as compared to the standard transmit signal ($P=1$; $Q=1$ and $J=1$) is observed.

Hence from the all the cases discussed, it is clear that as the total number of basis functions is increased, the maximum correlation drops by a great extent. This is because, as the total number of basis functions is increased, that is, as the total number of slow-time and fast-time functions are increased, the Algorithm achieves more flexibility to come up with a better code. In other words, more the number of basis functions, bigger is the subspace in which the Algorithm can search for the best code, hence the possibility of coming up with the best possible code improves.

The limit on the number of P s and Q s is discussed as follows.

As discussed before, the fast time functions are a time shifted form of the mother function $g_f(t)$. The shift in time is given as, τ_q where,

$$\tau_q \ll T_o$$

Where, T_o is the pulse repetition time.

When more than one fast time functions are considered, in order to differentiate between two consecutive pulses, the duration of total number of fast time functions should not exceed the pulse repetition time.

i.e.,

$$Q\tau_q \ll T_o \quad (6.1)$$

Hence, the total number of fast time functions (Q) should be selected in such a way that the combined duration should not exceed the pulse repetition time.

$$Q \leq \frac{T_o}{\tau_q}$$

Similarly, a limit can be defined for slow-time functions as well. As it is known, the slow-time functions are a frequency shifted version of the mother function $G_f(\omega)$.

The frequency shift is defined as ω_p where,

$$\omega_p \ll \omega_o$$

where, ω_o is the pulse repetition frequency.

Hence the frequency extent of the total number of slow-time functions should not exceed the pulse repetition frequency. Therefore a limit on the number of P's used can be set,

$$P \ll \frac{\omega_o}{\omega_p} \quad (6.2)$$

6.2 Analysis of the Algorithm with 2 Transmit Elements ($J = 2$)

Having analyzed the Algorithm for all the cases with 1 transmit element ($J=1$), the Algorithm has been analyzed for 2 transmit elements that is $J=2$. By doing this, a spatial dimension has been included to the transmit signal. Hence, there are two transmit elements at different spatial position vectors.

Same cases of P and Q will be considered as were considered for 1 transmit element.

6.2.1 Case 1 ($P=1; Q=1; J=2$):

The total number of slow-time functions ' P ' is set to 1 and the total number of fast-time functions ' Q ' is also set to 1.

The Ambiguity (Correlation) plot obtained using the transmit code generated by the Algorithm is as shown in Fig 6.13. Only the total ambiguity plot along the cross-track axis will be shown, as the temporal ambiguity plot cannot be plotted for $J=2$ unlike $J=1$ cases.

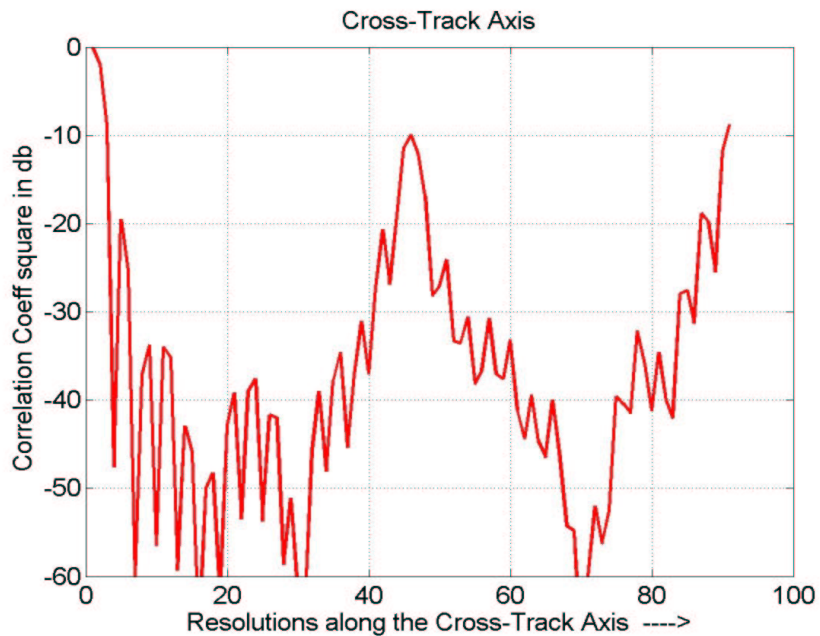


Fig 6.13: Total Ambiguity plot along the Cross Track axis for $P=1; Q=1$.

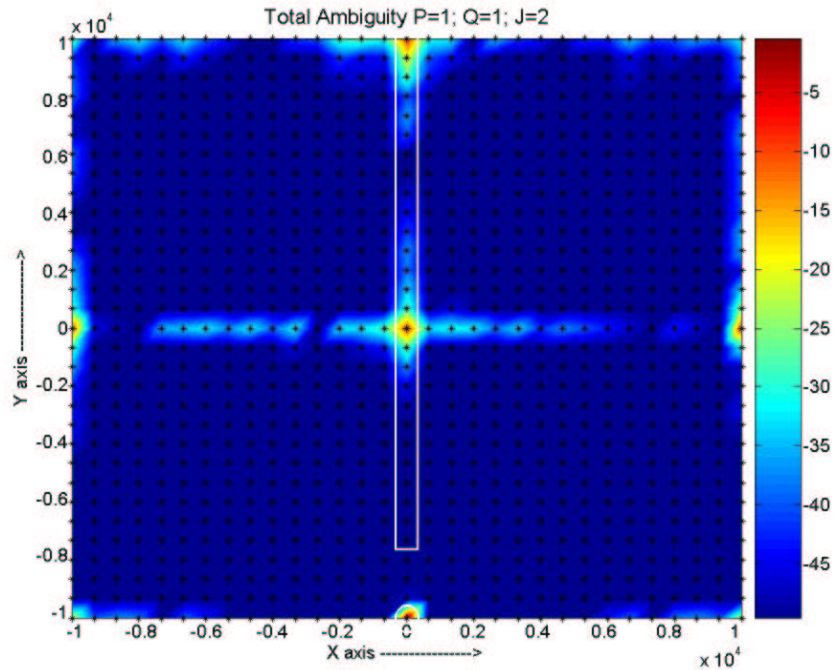


Fig 6.14: A 2-D plot of the correlation of the target of interest and all the targets in the grid (2-D ambiguity plot) for $P=1$; $Q=1$.

From the ambiguity plot it is noticed that the maximum total correlation is about -9dB. More improvement can be seen as the number of P 's and number of Q 's is increased. The 2-D plot for this particular case is as shown Fig 6.14.

Here again, similar to $J=1$ 2-D plots, red color indicates high correlation and dark blue color indicates a very low correlation between the target of interest and the other target.

6.2.2 Case 2 ($P=3$; $Q=3$; $J=2$):

The total number of slow-time functions, P is set to 3 and the total number of fast-time functions, Q is also set to 3.

The Ambiguity (Correlation) plots obtained by using the transmit code generated by the Algorithm are as shown in Fig 6.15 and Fig 6.16.

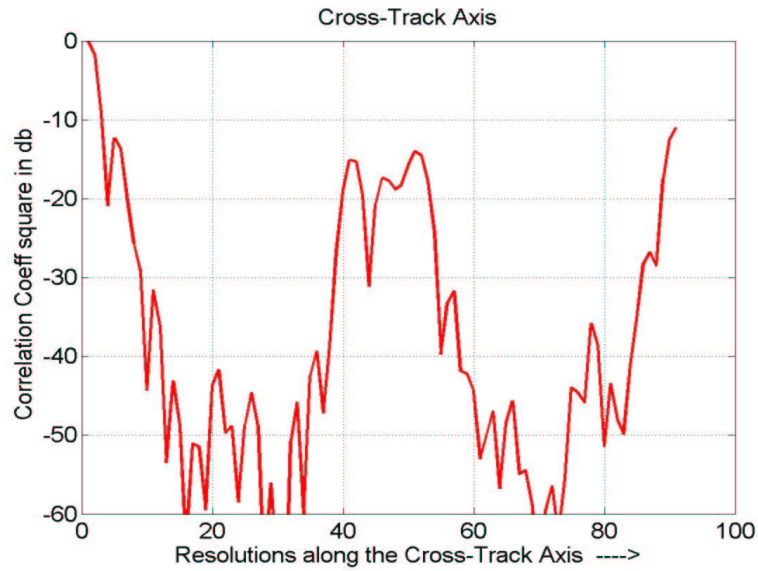


Fig 6.15: Total Ambiguity plot along the Cross Track axis for $P=3$; $Q=3$.

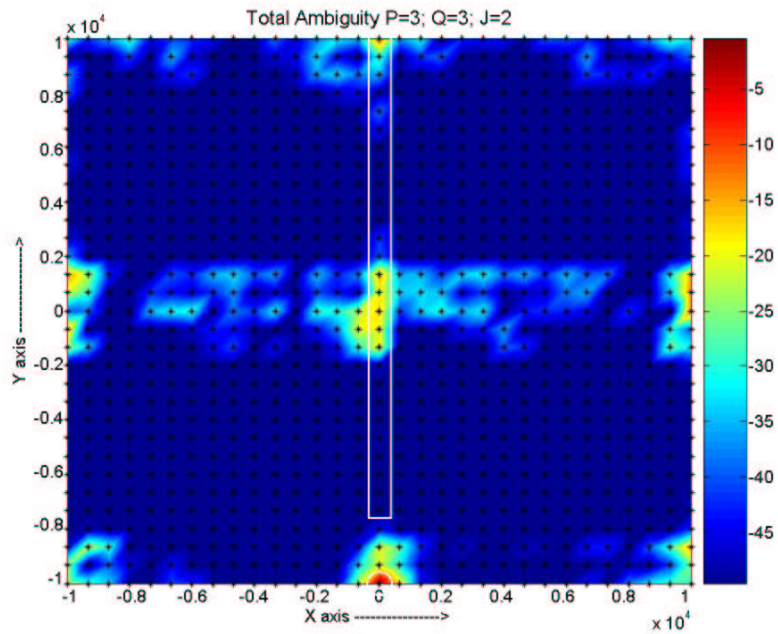


Fig 6.16: A 2-D plot of the correlation of the target of interest and all the targets in the grid (2-D ambiguity plot) for $P=3$; $Q=3$.

The total ambiguity plot has a maximum total correlation of -11dB. This is an improvement of 2-dB when compared to the previous case.

6.2.3 Case 3 ($P=5; Q=5; J=2$):

The total number of slow-time functions P is set to 5 and the total number of fast-time functions Q is also set to 5.

The Ambiguity (Correlation) plots obtained by using the transmit code generated by the Algorithm are as shown in Fig 6.17 and Fig 6.18..

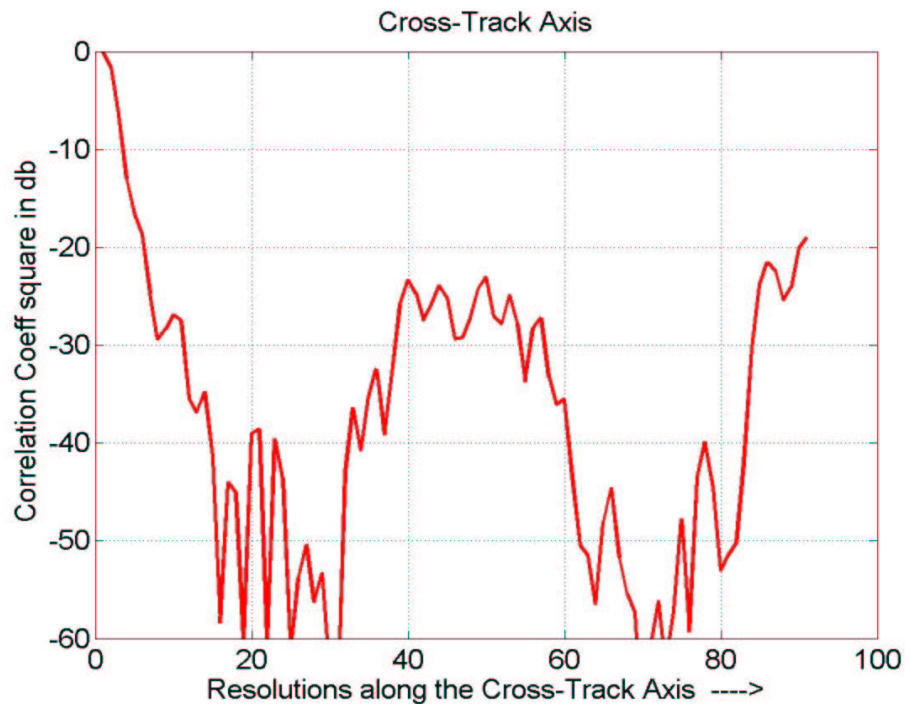


Fig 6.17: Total Ambiguity plot along the Cross Track axis for $P=5; Q=5$.

In this case, the maximum total ambiguity is about -19dB which is an improvement of 8dB as compared to the case where $P=5$; $Q=5$ and an improvement of 10dB as compared $P=3$; $Q=3$ case.

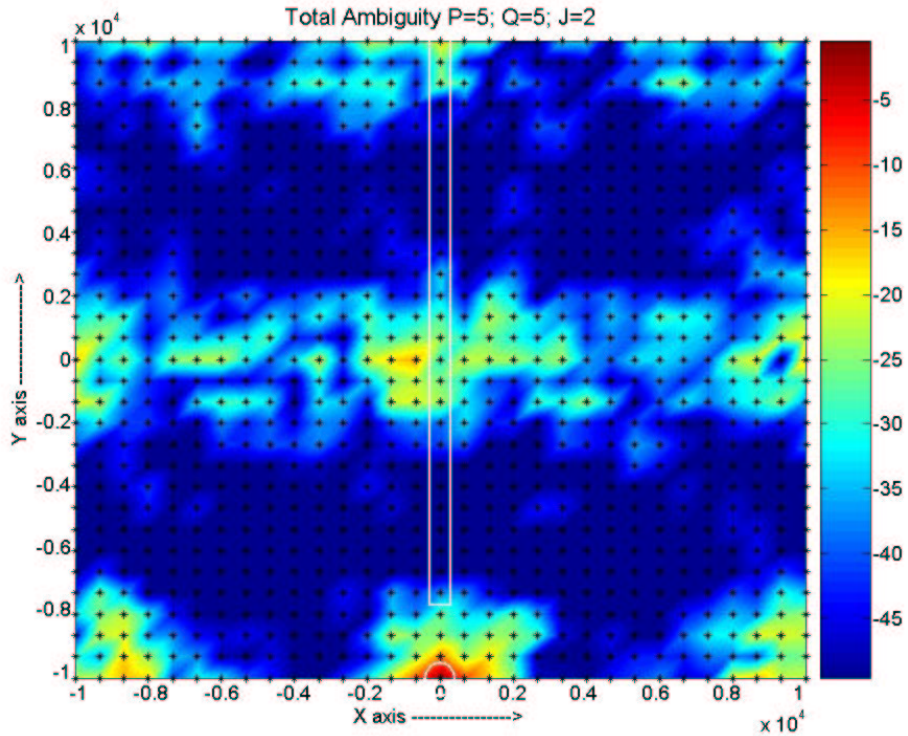


Fig 6.18: A 2-D plot of the correlation of the target of interest and all the targets in the grid (2-D ambiguity plot) for $P=5$; $Q=5$.

6.2.4 Case 4 ($P=7$; $Q=7$; $J=2$):

The total number of slow-time functions P is set to 7 and the total number of fast-time functions Q is also set to 7.

The Ambiguity (Correlation) plots obtained by using the transmit code generated by the Algorithm are as shown in Fig 6.19 and Fig 6.20.

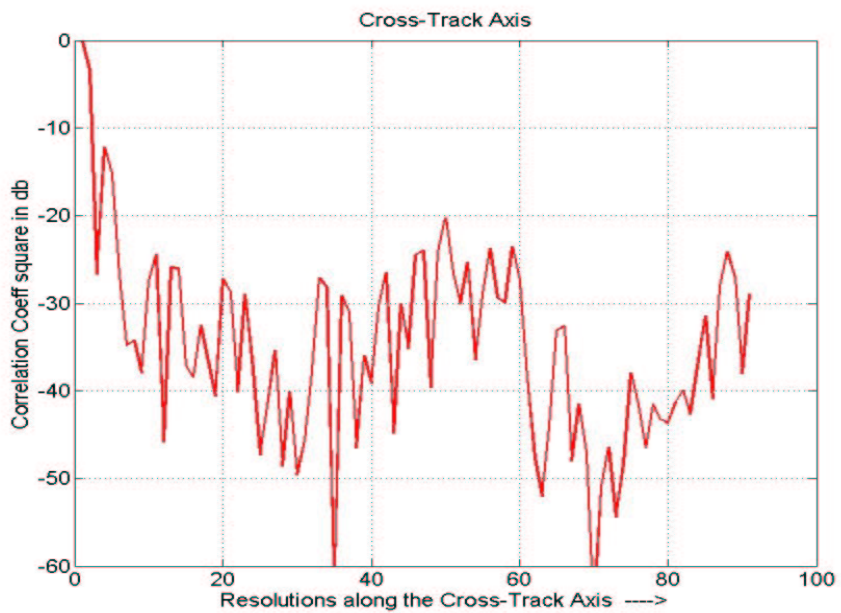


Fig 6.19: Total Ambiguity plot along the Cross Track axis for $P=7$; $Q=7$.

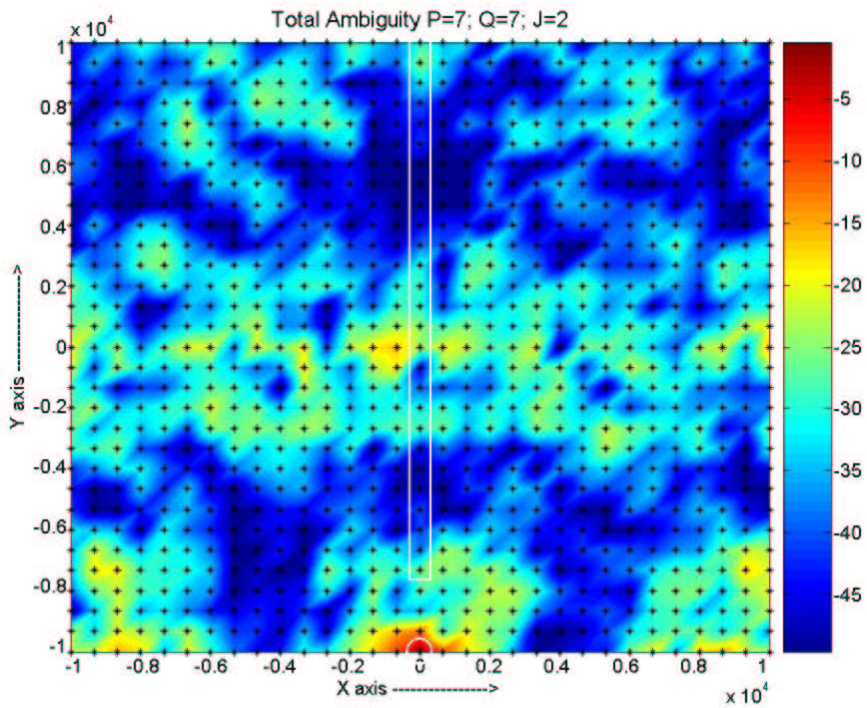


Fig 6.20: A 2-D plot of the correlation of the target of interest and all the targets in the grid (2-D ambiguity plot) for $P=7$; $Q=7$.

In this case the total maximum ambiguity is about -24dB. A considerable improvement is observed when compared to the previous cases.

6.2.5 Case 5 ($P=9; Q=9; J=2$):

The total number of slow-time functions P is set to 9 and the total number of fast-time functions Q is also set to 9.

The Ambiguity (Correlation) plots obtained by using the transmit code generated by the Algorithm are as shown in Fig 6.21 and Fig 6.22.

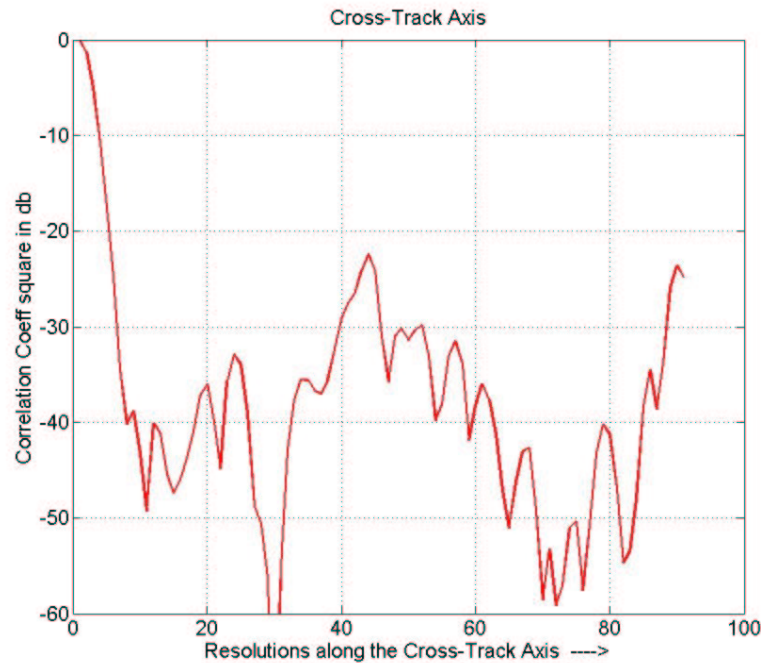


Fig 6.21: Total Ambiguity plot along the Cross Track axis for $P=9; Q=9$

In this case there is a not much improvement in the total maximum ambiguity compared to a case where $P=7$ and $Q=7$. It is again equal to -24dB.

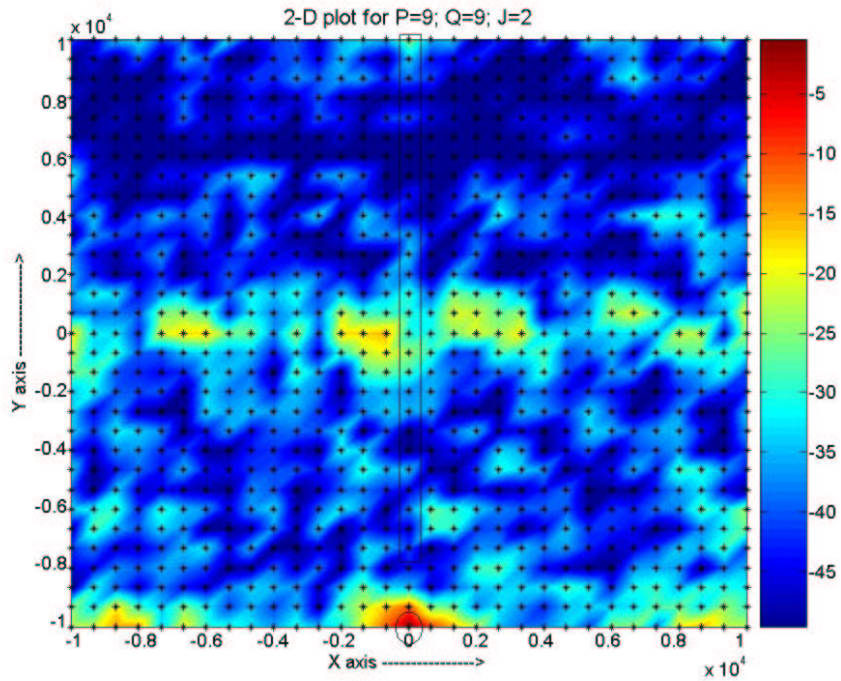


Fig 6.22: A 2-D plot of the correlation of the target of interest and all the targets in the grid (2-D ambiguity plot) for $P=9$; $Q=9$.

6.2.6 Case 6 ($P=11$; $Q=11$; $J=2$):

The total number of slow-time functions P is set to 11 and the total number of fast-time functions Q is also set to 11.

The Ambiguity (Correlation) plots obtained by using the transmit code generated by the Algorithm are as shown in Fig 6.23 and Fig 6.24.

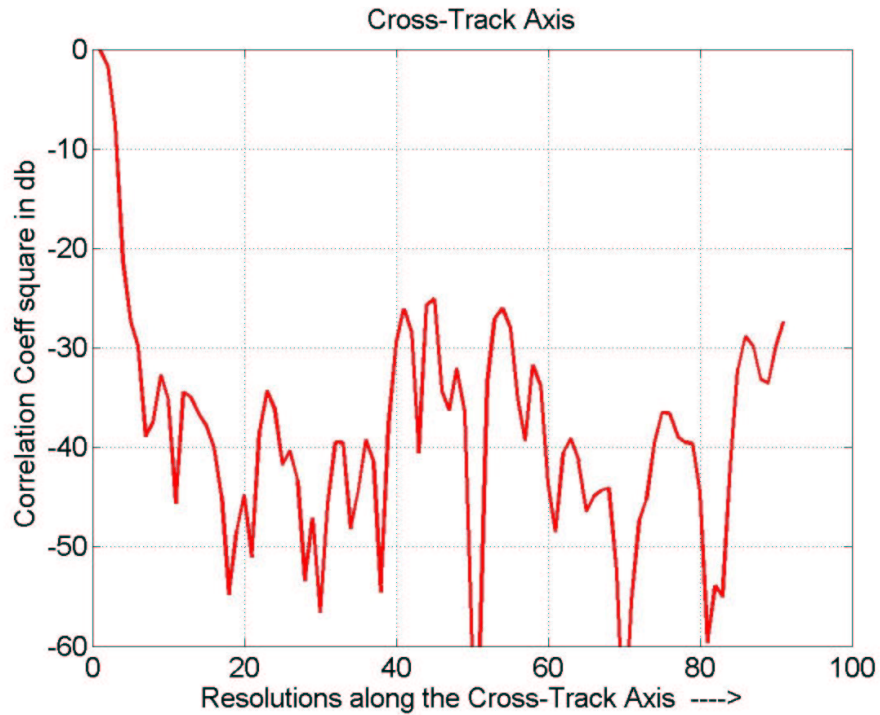


Fig 6.23: Total Ambiguity plot along the Cross Track axis for $P=11$; $Q=11$.

This is the final case that will be analyzed for two transmit elements. As explained before, the maximum values that could be assigned are $P=11$ and $Q=11$. The maximum total ambiguity obtained for this case is -28dB.

This was the best result which was achieved in terms of reducing the maximum correlation using two transmit elements. It is the maximum correlation of the main target of interest with all the other targets that our algorithm worked on.

The two dimensional image of the entire grid is as shown below.

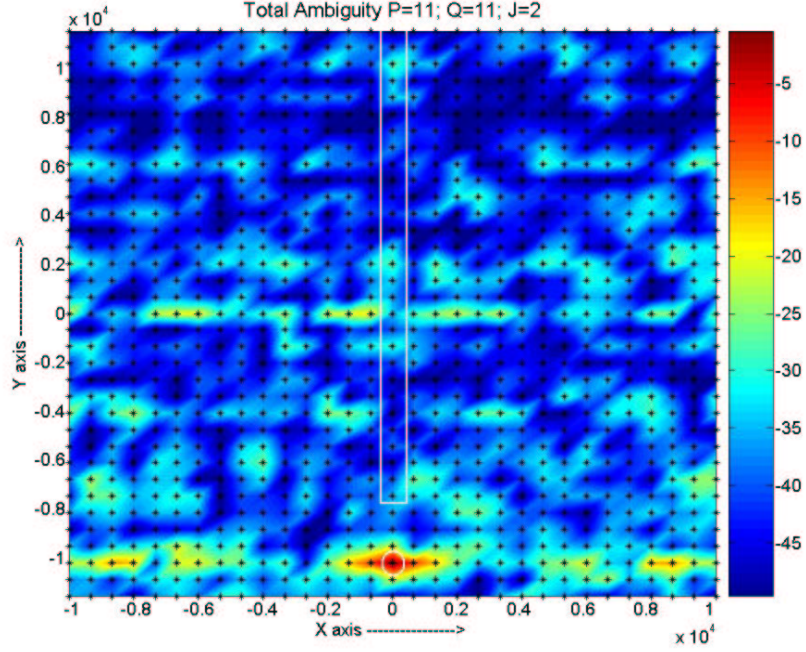


Fig 6.24: A 2-D plot of the correlation of the target of interest and all the targets in the grid (2-D ambiguity plot) for $P=11$; $Q=11$.

The observations made from the two dimensional plot are,

- 1) The correlation of the target of interest with any other target is not invariant when the target of interest is changed. That is, the correlation value of the target of interest and some other target at certain resolution cells away will not be exactly same as the correlation between a different target of interest and another target which is same resolution cells away.
- 2) The 2-D total ambiguity plot is rotationally symmetric, which is according to one of the properties of the ambiguity function that states that [2],

$$\chi(T_R, f_d) = \chi^*(-T_R, -f_d) \quad (6.3)$$

Therefore,

$$|\chi(T_R, f_d)|^2 = |\chi(-T_R, -f_d)|^2 \quad (6.4)$$

Where, T_R is the time delay and f_d is the Doppler frequency.

6.3 Comparison of $P=11$; $Q=11$ and $J=2$ case with Standard Code ($P=1$; $Q=1$) and Three random codes.

The lowest maximum correlation that has been achieved for $J=2$ is -28dB. In order to see the efficacy of the Algorithm, the result is compared with the maximum correlations obtained using a standard code i.e., a code with $P=1$; $Q=1$ and $J=1$, and also with 3 different random codes which are complex vectors in which each element is generated randomly from a Gaussian distribution of mean 0 and variance 1.

6.3.1 Standard Code ($P=1$; $Q=1$)

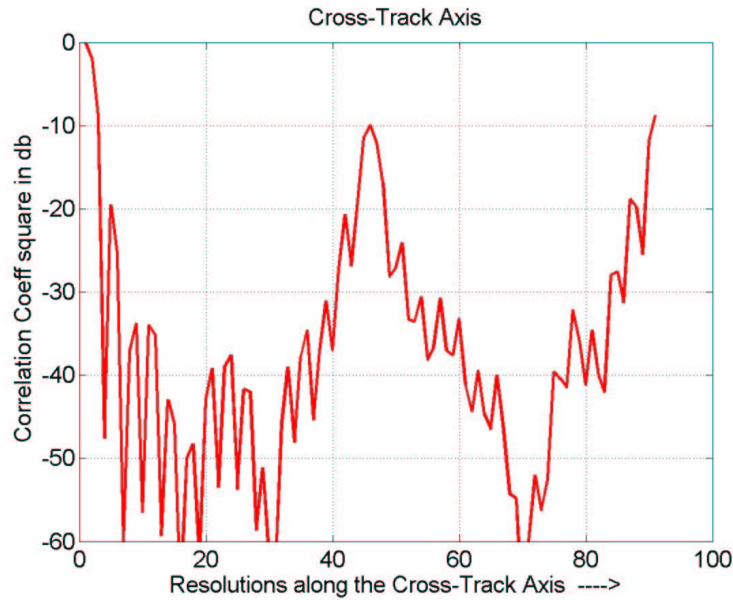


Fig 6.25: Total Ambiguity plot along the Cross Track axis for $P=1$; $Q=1$.

Fig 6.25 shows the total ambiguity plot for a standard case. And the maximum Correlation = -9dB.

6.3.2 Random Code-1

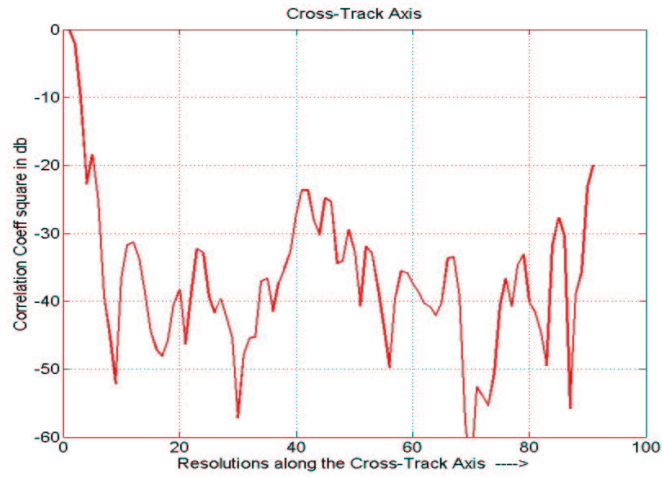


Fig 6.26: Total Ambiguity plot along the Cross Track using random code-1.

Fig 6.26 shows the total ambiguity using a Random Code 1. And the maximum Correlation = -20dB

6.3.3 Random Code-2

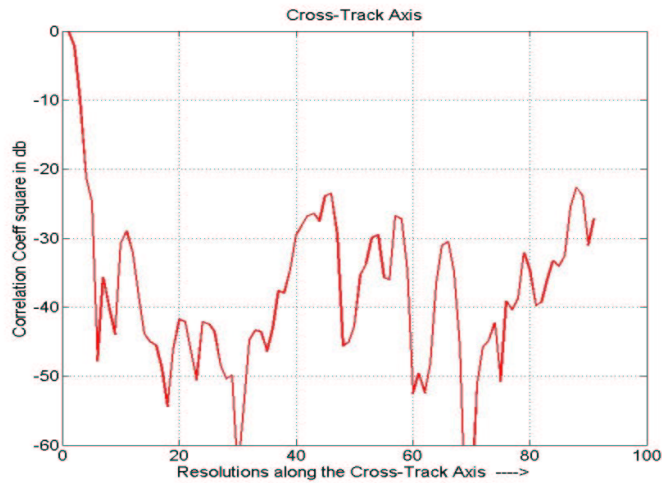


Fig 6.27: Total Ambiguity plot along the Cross Track using random code-2.

Fig 6.27 shows the total ambiguity using a Random Code 2. And the maximum Correlation = -23dB

6.3.4 Random Code - 3

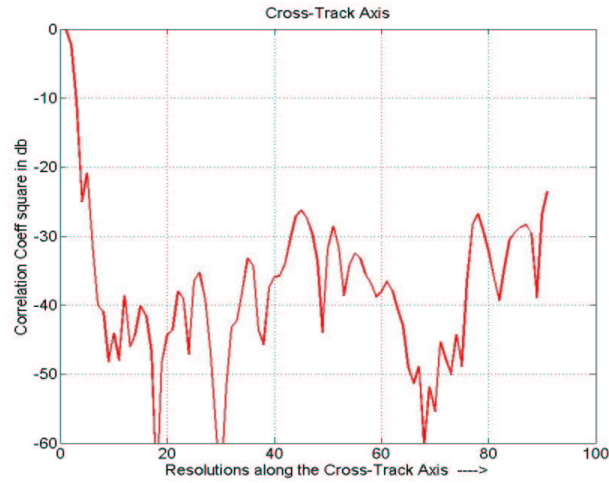


Fig 6.28: Total Ambiguity plot along the Cross Track using random code-2.

Fig 6.28 shows the total ambiguity using a Random Code 1. And the maximum Correlation = -23dB

6.3.5 Transmit Code given by the Algorithm

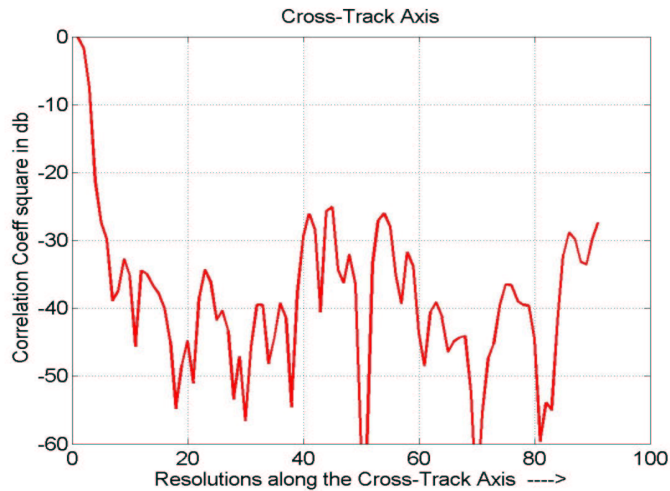


Fig 6.29: Total Ambiguity plot along the Cross Track using best transmit code.

Fig 6.29 shows the total ambiguity using a Random Code 1. And the maximum Correlation = -23dB

Hence from the results, it can be seen that the maximum correlation obtained by using the transmit code generated by the Algorithm is 19dB better than the standard transmit code, and is better by 8dB, 5dB and 5dB than Random code-1, Random code-2 and Random code-3 respectively.

6.4 Analysis of the Optimization Criterion χ with inputs from the Radar model.

It has already been shown that the optimization criterion is a justifiable criterion to derive a transmit signal that would minimize the maximum correlation between dissimilar targets. In this section a similar analysis is done with inputs from the radar model. The transmit signal that was obtained for $P=11$; $Q=11$ and $J=2$ case is used to compute the correlation coefficient values and $|1-\chi|$ values and the plot is as shown.

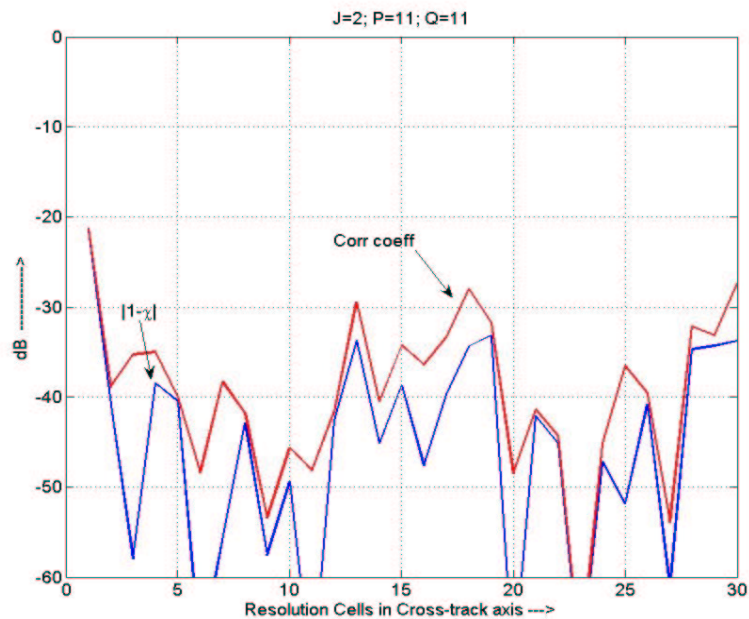


Fig 6.30: Plot showing the correlation coefficient curve and $|1-\chi|$ curve.

From Fig 6.30 it can be seen that even for the physical radar case, the optimization criterion is a good criterion that can be used to search for the best possible code.

6.5 Energy in the Response vector for $J=2$; $P=11$; $Q=11$ case

Fig 6.31 shows the energy in the response vector for every single target on the grid for two transmit element case with $P=11$ and $Q=11$.

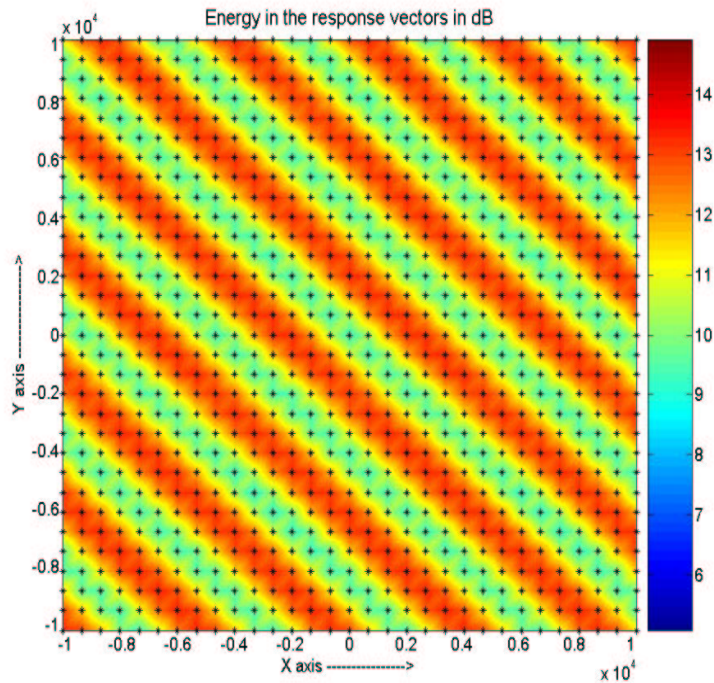


Fig 6.31: The energy in the response vector for every single target in the target grid shown in dB scale.

It is very important to learn about the energy in a response vector of a target as, there is a possibility of two vectors being totally uncorrelated to each other when one of the vectors has zero energy. A response vector with zero energy is not desired, as the main effort of this study is to make two vectors with finite energy, as orthogonal as possible to each other. The Fig 6.31 proves that no target has a response vector with

zero energy, confirming our efforts of minimizing the correlation of the response vectors were in the right direction. The reason for the diagonal pattern in the distribution of the energy in the target grid, is the position of the transmit elements. In this particular case, two transmit elements taken such that they are placed diagonally to the target area perpendicular to the energy diagonals as seen in the plot. This way of placing the transmit elements causes an energy pattern as shown in the figure.

6.6 Comparison of Convergence of χ bound for $J=1$; $J=2$ and different values of P and Q .

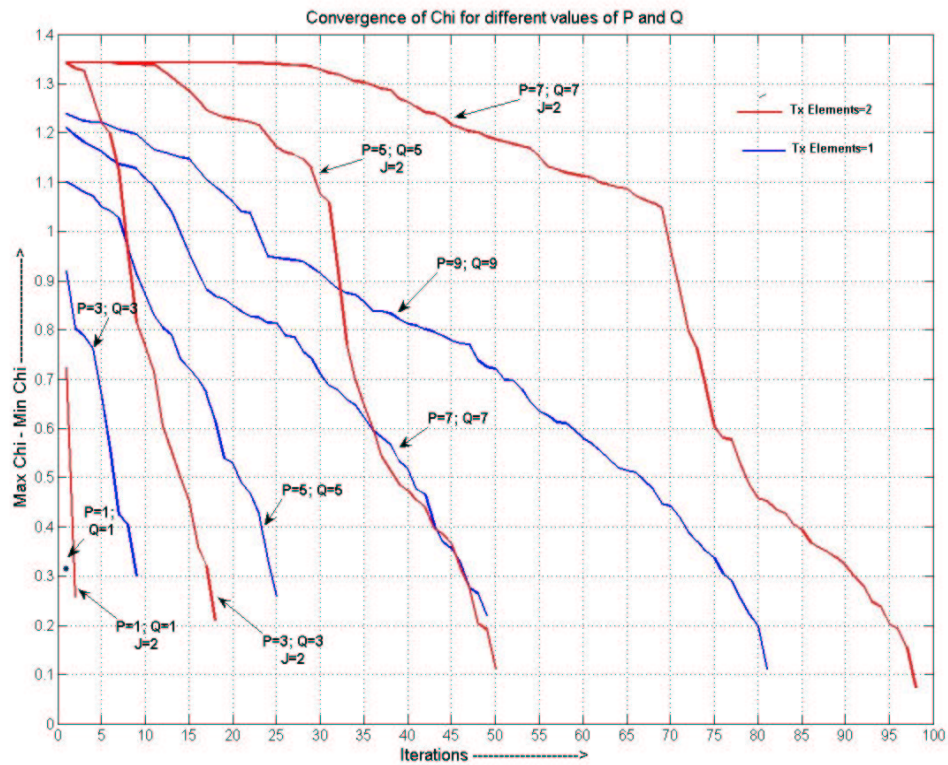


Fig 6.32: Plot showing the convergence of χ with for one and two transmit elements respectively.

In Fig 6.32, the blue curves represent the convergence corresponding to one transmit element and the red curves represent the convergence corresponding to two transmit elements. It is noticed that after every iteration, the χ bound is either equal to or lesser than the χ bound in the previous iteration. The functioning of the Algorithm for different values of P and Q can be seen clearly from Fig 6.31. Smaller the dimension of the transmit signal, lesser is the number of Stinker codes (Bad codes) and hence easier it is for the Algorithm to search for the best code as it does not have to eliminate too many stinker codes. Whereas, if the dimension of the transmit signal is very high, there will be higher number of stinker codes and hence the Algorithm needs to work hard to come up with the best code as it needs to eliminate a large number of stinker codes. This can be seen for the case of $P=7$; $Q=7$; and $J=2$. The red curve for $P=7$; $Q=7$; and $J=2$ is flat for about 30 iterations, which means that there are a lot of stinker codes that the Algorithm is trying to project orthogonal to. Hence, by increasing the dimension of the transmit signal, there is an increase not only in the possibility of coming up with the best code, but also the total number of stinker codes.

6.7 Comparison of Maximum Correlation Coefficient values for $J=1$; $J=2$ with respect to total Iteration Number.

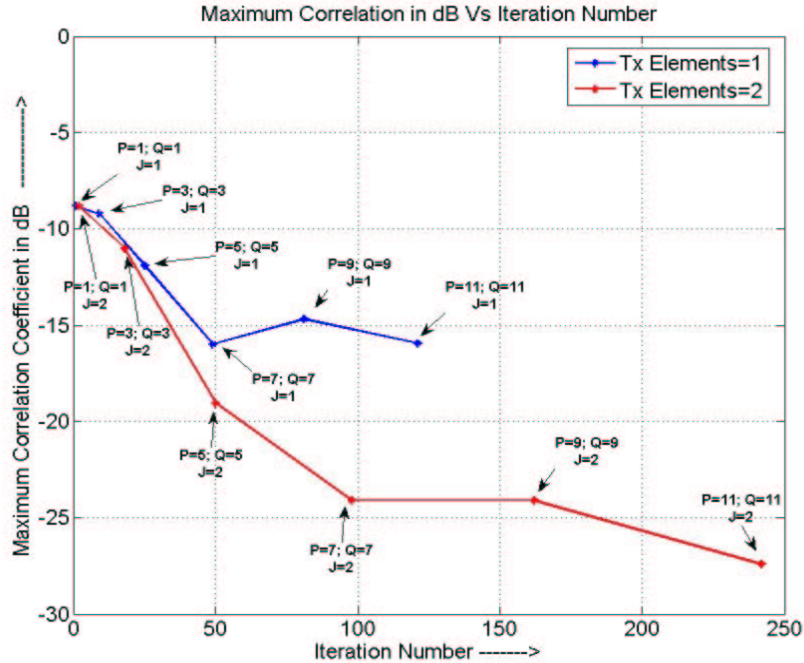


Fig 6.33: Plot showing the improvement of maximum correlation with increase in total number of basis functions.

From Fig 6.33, it is evident that, as the total number of basis functions is increased, that is, as the values of P and Q are increased, the maximum correlation between two targets is reduced relatively. As discussed before, this is explained as, by increasing the total number of basis functions, more flexibility is provided in the design of the transmit code which indirectly increases the subspace in which the Algorithm can search for the best code. By adding a transmit element to the radar system, a spatial dimension is introduced to the transmit signal thereby increasing the total subspace in which the Algorithm can search for a best code.

6.8 Relation between Rank of \mathbf{C} matrix (R_c) and the number of Transmit Elements (J)

It has been observed from the above cases that the rank of \mathbf{C} matrix is, in some way, related to the total number of transmit elements used in a radar system. It has been observed that the rank of the \mathbf{C} matrix is less than or equal to twice the total number of basis functions used. That is, rank of \mathbf{C} matrix, $R_c \leq 2PQ$ and the size of the \mathbf{C} matrix is given by $W \times W$ where, $W = PQ$

- For one transmit element, that is, $J=1$; the rank of the \mathbf{C} matrix is equal to PQ and it is a full ranked matrix as $R_c = W$, which means that there are no zero valued eigen values.
- For two transmit elements, that is $J=2$, the rank of the \mathbf{C} matrix is equal to $2PQ$, and again it is a full ranked matrix as $R_c = W$, which means that all the eigen values of the \mathbf{C} matrix are non-zero values.
- Now, for transmit elements greater than 2, that is, $J>2$, it has been observed that the rank of the \mathbf{C} matrix was $2PQ$ and it was not a full ranked matrix as $R_c \neq W$. That is, it has zero valued eigen values. This indicates that when the number of transmit elements are increased beyond 2; we have eigen vectors that put no energy on the targets of consideration.

Hence from the above observations, it is very clear that there is a relation between the rank of the \mathbf{C} matrix R_c and the total number of transmit elements used in the radar

system. Mathematical derivation of this relation is beyond the scope of this thesis and is left as a future work.

CHAPTER - 7

7.1 Conclusions

It has been proved by various experiments and cases conducted in this study that it is possible to come up with a space-time transmit signal that could reduce the maximum correlation between targets in a target grid. An Algorithm that works to come up with this kind of transmit signal has been developed and its performance has been analyzed numerically. A mathematical Synthetic Aperture Radar model has been developed and the performance of the Algorithm has also been analyzed under the simulated conditions of a physical radar model. It has been learnt from the numerical experiments that the performance of Algorithm-2 not only depends on the total number of independent measurements taken (M), the dimension of the transmit signal (N), but also depends on the structure of the H-matrices. Having developed Algorithm-2, we wanted to see the improvement of the new algorithm compared to Algorithm-1. It has been found that Algorithm-2 shows a considerable improvement when a certain kind of H-matrices (varying-H matrices) are used as inputs. The performance of both the Algorithms improve as the total number of measurements and the dimensions of the transmit signal are increased. In order to have a general idea about the efficacy of the transmit signal given by Algorithm-2, we compared its performance with a randomly generated code and a code given by the genetic algorithm. It has been found that the result of Algorithm-2 performs far better than a randomly generated code in terms of the standard deviation of the χ values and the mean of the correlation coefficient values, but the result given by the Genetic

algorithm performs slightly better than the code given by Algorithm-2. From this we can conclude that Algorithm-2 may not always give a best possible code for a given radar scenario.

Using the inputs to the Algorithm from the simulated radar model, it has been found that the performance of Algorithm-2 improves tremendously as the total number of basis functions is increased. This is because, as we increase the total number of basis function, more flexibility is provided to the algorithm to search for a better code. An upper limit on the total number of basis functions that can be used has also been derived in this study. The performance of Algorithm-2 has been analyzed by increasing the total number of transmit elements from 1 to 2. It has been found that the performance of the Algorithm improves considerably as we move from one transmit element to two transmit elements, but the ambiguity function seems to be invariant.

The ambiguity functions have been analyzed in detail for one transmit element case and a two transmit element case, and it has been concluded that when only one transmit element is used, the ambiguity function is totally invariant and it is rotationally symmetric. Where as, when two transmit elements are used, it has been found that the ambiguity function seems to be invariant, that is, it changes its pattern from one target to another. It still remains to be rotationally symmetric conforming to the symmetry property of the ambiguity function [2].

Hence, it has been shown in this study that a Space-time transmit signal can be developed for a multi-static radar system that exploits the spatial and temporal characteristics to reduce the maximum correlation between targets in a target area.

7.2 Suggested Future Work

Following are some of the suggestions for the future work on this topic.

- 1) All the experiments in this thesis have been performed on the cross-track axis. That is to say, the Algorithm works only on the cross track axis targets. The Algorithm needs to work on the along track axis targets also, in order to obtain a clear picture about the performance of the Algorithm in physical conditions.
- 2) As we increased the number of transmit elements from 2 to 3, it was observed that the C matrix does not continue to be a full ranked matrix. Hence this Algorithm needs to be modified suitably in order to handle a case of $J > 2$.
- 3) We observed a relation between the total number of transmit elements and the rank of the C matrix. A clear understanding of the performance of the radar model for $J > 2$ will be achieved if a mathematical relation can be derived between the total number of transmit elements and the rank of the C matrix.
- 4) As we observed that the ambiguity function for a radar scenario having two transmit elements, seems to be invariant, the transmit signal given by the Algorithm cannot be used in order to observe the entire target grid. Hence

the Algorithm needs to be modified accordingly in order to deal with such a scenario.

- 5) Finally, the Algorithm takes immense amount of time in order to come up with the best code for a target grid of 31 X 31. The Algorithm needs to be optimized with respect to the total processing time it takes to generate the code so that the Algorithm can used on much larger grids.

References

- [1] Microwave Remote Sensing Active and Passive Vol II – Radar Remote Sensing and Surface Scattering and Emission Theory by Fawaz T. Ulaby, Richard K. Moore, Adrian K. Fung -1982.
- [2] Introduction to Radar Systems – Third Edition by, Merrill I. Skolnik. Tata McGraw Hill - 2001
- [3] “SAR and MTI Processing of Sparse Satellite Clusters” by Nathan A. Goodman Doctoral Thesis, The University of Kansas.
- [4] “Design of Space-Time Transmit Codes for Optimizing Multistatic Radar Performance” by Sih Chung Lin. MS Thesis, The University of Kansas.
- [5] “Space-Time Radar Transmission, Target, and Measurement Model” – Rev. E, August 2004 by James Stiles.
- [6] “Transmit Signal Model” – – Rev. E, August 2004 by James Stiles.
- [7] Synthetic Aperture Radar – <http://www.sandia.gov/RADAR/whatis.html>
- [8] Spotlight Synthetic Aperture Radar –Signal Processing Algorithms by, Walter G. Carrara, Ron S. Goodman, Ronald M. Majweski
- [9] “Performance and Processing of SAR satellite Clusters” by Jim Stiles, Nathan Goodman and Sih Chung Lin, The University of Kansas, RSL.
- [10] “Resolution and Synthetic Aperture Characterization of Sparse Radar Arrays” by Nathan A. Goodman, James M. Stiles, The University of Kansas.

- [11] “Finding an Upper Bound for the Transmit Code Problem Using Genetic Algorithms” by Fernando Palacios Soto, MS Project, The University of Kansas.
- [12] “Space-Time Radar Transmission, Target, and Measurement Model” Jim Stiles, Rev E. – August 6, 2004
- [13] “Transmit Signal Model” Jim Stiles, Rev. E, August 2, 2004.
- [14] “Determination of Numerical Model Parameters” Jim Stiles, Rev A, July 8, 2004.